A thesis submitted to McGill University in partial fulfilment of the requirements of the degree of Master of Engineering

VALIDATION OF SEISMIC RESPONSE PREDICTION OF A GUYED TELECOMMUNICATION MAST WITH AMBIENT VIBRATION MEASUREMENTS

Mahtab Ghafari Osgoie

Supervisor:
Professor Ghyslaine McClure

Department of Civil Engineering and Applied Mechanics
McGill University
Montréal, QC, Canada, 2012
Master of Engineering Thesis

VALIDATION OF SEISMIC RESPONSE PREDICTION OF A GUYED TELECOMMUNICATION MAST WITH AMBIENT VIBRATION MEASUREMENTS

Mahtab Ghafari Osgoie

Department of Civil Engineering and Applied Mechanics
McGill University
Montréal, Québec, Canada, August 2012

Validation of seismic response prediction of a guyed telecommunication mast with ambient vibration measurements

Mahtab Ghafari Osgoie

Master of Engineering thesis

Department of Civil Engineering and Applied Mechanics
McGill University
Room 492, Macdonald Engineering Building, 817 Sherbrooke Street West
Montréal, Québec, H3A 0C3
Canada
Tel: 514-398-6860
Fax: 514-398-7361

Cover:
Hydro-Québec telecommunication mast located near Highway 20, in St. Hyacinthe, Québec, Canada.

DEDICATION

Dedicated to my family, beloved parents and brother, for all their pure and endless love.

"*Try not to become a man of success but rather to become a man of value*."

Albert Einstein

ACKNOWLEDGMENTS

This research is submitted in partial fulfilment of the requirements for the degree of Master of Engineering in Civil Engineering at McGill University.

First I would like to thank my advisor, Professor Ghyslaine McClure of the department of Civil Engineering and Applied Mechanics of McGill University for supporting me during these past two years. In addition to her supervision and invaluable suggestions, her kind, patient and amiable attitude during this time have created a strong sense of respect and friendship between us.

This research is supported jointly by Hydro-Québec's Research Institute (IREQ) and the Natural Sciences and Engineering Research Council of Canada (NSERC) through the University-Industry collaborative grant program (grant no. CDRPJ396079-09). I am grateful to Hydro-Québec, Dr. Xiao Hong Zhang (McGill postdoc) and Dr. Daniel Gagnon of IREQ for allowing and helping with the field tests at the St. Hyacinthe tower site.

My deepest appreciation goes to my family in particular to my beloved mother Hamideh for her pure and unconditional love, and to my kind and devoted father Mirghaffar who inspires me every day to strive for the best in my social and professional life. I appreciate immensely all of their support during my entire life in both Iran and Canada. In addition, I would also thank my brother, Ali, who has always supported me in all aspects of my life through his words of wisdom and great guidance.

Finally I would like to thank all of my close friends, in practical Saeedeh and Alireza, in Iran, and others in Canada who have made my life in Canada and Iran enjoyable and memorable.

TABLE OF CONTENTS

LIST OF TABLES

LIST OF FIGURES

ABSTRACT

Telecommunication structures are essential components of communication and post-disaster networks that must remain operational after a design-level of earthquake. Although many studies have been done to evaluate the response of these structures when subjected to wind and earthquakes, almost all of them are numerical simulations using finite element analysis models. In fact the most common way for predicting the dynamic characteristics of these towers is using nonlinear dynamic analysis models, and there is a lack of experiments in this field. In other words, despite of all the numerical studies which have been done with care and expert knowledge, little validation with physical tests or measurements has been reported to evaluate the level of accuracy of these computational studies. Hence the degree of uncertainty of these modeling predictions has not been determined up to now even in controlled laboratory conditions. The research presents full-scale investigations of the dynamic characteristics of a real 111.2 m tall guyed telecommunication tower owned by Hydro Québec and located in St. Hyacinthe, Québec. Ambient Vibration Measurements (AVM) were carried out on the tower mast and supporting guy cables to determine dominant natural frequencies, mode shapes and damping properties. A comparison of the results extracted from the AVM records and those predicted by detailed finite element models indicates the level of accuracy of the models and future dynamic analysis. Acceleration measurements on the guy wires provide the database for calculating the cable tensions. The importance of considering accurate cable tensions for the study of the dynamic characteristics of the tower was demonstrated by the comparison between the numerical eigenvalue analyses of detailed finite element tower models with various adjustments in cable tensions. This was further emphasized in a series of earthquake simulations under three classical earthquakes records. A final series of numerical simulations were done under two different gravity loading cases, namely with and without consideration of tower attachments such as antennas, transmission lines, and other appurtenances such as ladder, resting platforms, etc., which contribute additional weight and inertia. These simulations were done using a range of guy wire tensions varying between 8% and 15% of the cables rated breaking

strength and under four earthquake records, adding an artificial Montreal record to the three previous classical ones. In conclusion, considering that the actual cable tension may vary in the studied range of values has provided a good agreement between the experimental dynamic characteristics of the tower and non-linear finite element models results. On that basis, the accuracy of the seismic analysis results is validated.

SOMMAIRE

Les structures de télécommunication sont des éléments essentiels des réseaux de télécommunication d'urgence qui doivent rester fonctionnels en cas de séismes. Bien que l'étude du comportement de ces structures sous l'effet du vent ou des séismes ait fait l'objet de plusieurs études numériques utilisant la méthode des éléments finis, très peu de ces études ont été validées à l'échelle réelle par des mesures expérimentales dans la littérature scientifique.

Cette recherche présente une étude expérimentale détaillée des caractéristiques dynamiques d'une tour de télécommunication haubanée de 111.2 m de hauteur, propriété d'Hydro Québec et située à Saint-Hyacinthe, Québec. Cette étude procède par mesures de vibrations ambiantes (ou bruit ambiant) le long du mât et des câbles de haubans. Ces enregistrements ont ensuite été analysés pour en extraire les caractéristiques dynamiques telles les fréquences naturelles dominantes et les modes de vibration associés ainsi que leur taux d'amortissement. Ces résultats expérimentaux ont ensuite été comparés aux prédictions numériques par éléments finis afin de déterminer la précision des modèles. Les mesures d'accélération prises sur les câbles de haubans ont été utilisées pour calculer les tensions mécaniques dans les différents groupes de haubans. L'importance d'utiliser des valeurs précises des tensions dans les haubans pour obtenir des prédictions numériques réalistes est démontrée dans les analyses aux valeurs propres (fréquences et modes naturels dominants) et confirmée par une série d'analyses sismiques non linéaires utilisant trois exemples classiques de tremblements de terre.

Une dernière série d'analyses sismiques a considéré deux conditions de charges de gravité, soit le pylône sans masses additionnelles et le pylône chargé de tous ses composants fonctionnels - antennes, lignes de communication et accessoires tels les échelles, plates-formes de repos, etc., lesquels contribuent poids et inertie. Ces simulations numériques ont également considéré une variation des tractions initiales d'installation des câbles de haubans entre 8% et 15% de leur capacité ultime, et quatre cas de séismes, ajoutant un séisme artificiel pour Montréal aux trois cas classiques utilisés précédemment. En conclusion, les caractéristiques dynamiques du pylône obtenues par simulation se sont avérées en accord avec les mesures pour cet intervalle de

tractions des haubans, ce qui laisse présager une précision réaliste des simulations sismiques quand la variabilité des tractions des haubans est prise en compte.

Chapter 1 INTRODUCTION AND LITRETURE REVIEW

1.1 Introduction

Access to telecommunication and broadcasting services is the main purpose of using telecommunication masts, especially in difficult times such as after a severe earthquake. By taking into consideration this important role that telecommunication infrastructure play as critical links of communication, especially in post-disaster situations, one can easily see the value of their preservation and even necessity in the earthquake prone regions of the world. These towers are typically tall structures designed to support elevated antennas for radio and television broadcasting, telecommunication, two-way radio (emergency response systems such as police and fire), mobile phone base stations, and single channel connections such as microwave links that support air services, power networks, and railways. The properties of being light-weight, and easy to fabricate, assemble and install are all important considerations for telecommunication tower design. The Burj Khalifa (828 m) in Dubai, which was completed in 2010, is the tallest tower in the world. Before it, the Warsaw radio mast (645.4 m) in Poland has been the tallest structure ever built, although it collapsed on August 8, 1991 because of a human error during a maintenance procedure. Between the collapse of the Warsaw radio mast in 1991 and the completion of the Burj Khalifa in 2010, the KVLY/KTHI-TV mast (628.8 m) in the United States was the tallest telecommunication tower in the world: all three are shown in figure 1-1.

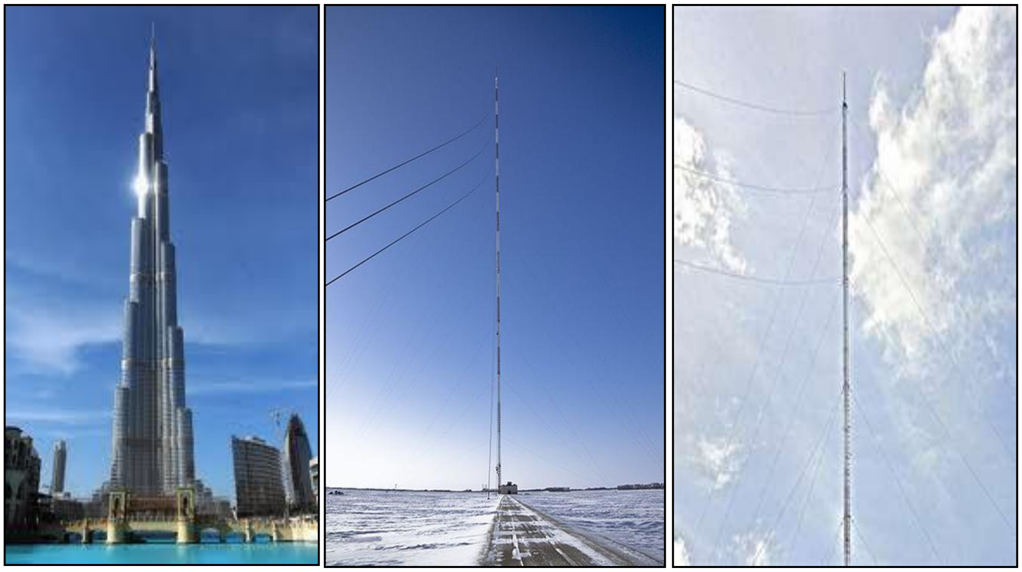

Burj Khalifa *Warsaw radio mast* *KVLY/KTHI-TV*

Figure 1-1 The world's three tallest towers (http://www.e-architect.co.uk, http://www.steelguru.com, http://en.wikipedia.org)

Although it is common to use the terms "tower" and "mast" interchangeably, we must recognize that there is a difference between the two. According to a structural engineering definition, a tower is a self-supporting, or cantilevered structure. On the other hand, a broadcast engineering definition of a tower is very general: an antenna structure supported on the ground. Likewise, the term "mast" has at least two definitions. In structural engineering a mast (or guyed mast) can be defined as being held up by stays or guys, whereas in broadcast engineering a mast is a vertical antenna support mounted on some other structure (which may be a tower, a building, or even a vehicle). In considering the structural engineering definition of these terms, due to the requirement to have an extended ground area for accommodating the guy wires in masts, it is more economical to build towers than masts for moderate or low heights (say up to about 80-100 m). Hence, in cities where unoccupied land is scarcer than in open terrain areas, towers are constructed more often than masts.

In general, there are two main groups of telecommunication towers: Self-supporting towers (see Figure 1-2 a), which include monopoles, and guyed towers (see Figure 1-2 b and cover page photo). The main construction material for guyed towers is high-strength steel for the guy cables and normal structural steel for the mast members. Tall masts are generally of lattice construction, as are self-supporting towers.

The lateral support for guyed towers comes from their guying system. The most common usage of the mast is for radio broadcasting, which may be employed using a variety of methods such as attaching aerials along the mast or using the mast structure itself as an antenna. The guy wires are attached to the mast at their top end and to the ground at the lower end. All of them are pre-tensioned during construction, typically with an initial tension in the order of 8% to 15% of their tensile breaking strength at a reference temperature of 10°C. The global torsional stability of the structure can also be improved by connecting the guy wires to stabilizers or outriggers at different levels on the mast. Tubular masts (See Figure 1-2 b), as opposed to lattice structures, become economical in short structures exposed to heavy icing where lattice sections would ice up completely. An advantage of guyed towers compared to self-supporting towers is that they tend to be more light-weight (hence economical); however a larger footprint area is needed to anchor the guy wires to the ground.

(a)

(b)

Figure 1-2 Examples of telecommunication structures (a) Self-supporting steel lattice tower, (b) Mühlacker transmitting tower (tubular steel guyed mast) (http://en.wikipedia.org)

Generally, the range of heights for a broadcast tower is between 120 m and 600 m, however those over 180 m are typically guyed towers. In other words, towers with a height of less than 180 m can be classified either as self-supporting or guyed towers based on the builder's preferences, budget, and location. It should be mentioned that most microwave and cellular towers are rather short and typically do not go beyond 90 m in height.

What make guyed masts particularly interesting in terms of dynamic response in general are the influence of geometric nonlinearities due to the sagging effects in guy cables and the relatively high slenderness of tall masts. The problem is analogous to studying a very flexible and slender beam-column on flexible intermediate supports. Accurate response prediction of tall guyed masts is therefore more difficult than most other conventional structures. In particular, the variability in cable tensions has a direct and important influence on the predicted response of the whole structure, in both static and dynamic regime.

1.2 Scope of Research

There are several published studies examining the influence of the combination of the wind and ice on the stability, strength, and serviceability of telecommunication towers in both a quantitative and qualitative way. Also, several reports on structural tower failures due to extreme wind and/or ice have been made; while there have been only isolated reports and research done in connection with earthquake-related damage. In addition, most of the published research involved numerical modeling studies without including any experimental validation. In fact, since it is difficult to obtain experimental results on the response of these structures when subjected to wind and earthquake loads, numerical simulations based on detailed finite element models are the most common way to predict their dynamic response. Many such studies have been published, which in spite of having been conducted with care and expert knowledge, have not been validated with on-site experiments. The degree of uncertainty in modeling complex structures is difficult to assess. Tall guyed masts exhibit nonlinear geometric response that is difficult to replicate in reduced-size laboratory models, and thus full-scale investigations are preferred in order to obtain accurate results.

The most recent related study conducted at McGill University was a doctoral thesis published by Ghafari Oskoei in August 2010. He proposed a simplified seismic analysis method based on the evaluation of the equivalent horizontal dynamic stiffness of guy clusters supporting the mast. He used a combination of detailed computer simulations and analytical studies on nine existing guyed towers; one of these towers is the 111.2 m St. Hyacinthe mast used herein. Although a numerical validation of the proposed modeling approach was done, to date there are no specific experimental data available to quantify the variability to be expected of such predictive methods. The present study is intended to provide some level of experimental validation with the St. Hyacinthe tower, a 111.2 m (365 ft) guyed telecommunication mast owned and operated by Hydro Québec and located near Highway 20.

In situ measurements of ambient tower vibrations are used to determine the dominant natural frequencies and cable tensions for the tested structure. The analysis of these measurements is the focus of this thesis. The measurements were made using TROMINO ENGY PLUS^{TM} (www.tromino.eu) and GP1 Sensors (www.sensr.com) for recording the ambient vibrations of the mast and guy wires. The individual guy cable tensions and the dynamic properties of the guyed mast (natural frequencies, mode shapes and corresponding damping estimate) were extracted from these measurements. Results of the eigenvalue analysis of numerical models were compared to the natural frequencies and mode shapes extracted from the *in situ* measurements. The approach utilized was to first determine the guy wire tensions on the basis of the frequency content of the measurements and then compare the natural frequencies and mode shapes obtained from experimental analysis with those from the finite element models having properly adjusted cable tensions. The numerical model included two different gravity load cases: with consideration of the weight of the supported antennas and transmission lines, and without.

As the next step, the results from detailed numerical simulations of seismic effects on tower models adjusted with realistic guy wire tensions were compared in order to assess the relative accuracy of the model.

1.3 Thesis Outline

This thesis comprises the following five chapters:

Chapter 1: **‘‘Introduction and Literature Review”** presents an introduction, the main objective and scope of research, the thesis outline, and literature review.

Chapter 2: **‘‘Detailed finite element modeling of guyed telecommunication towers for dynamic analysis”** presents the numerical considerations in making a numerical model: generalities, geometry and boundary conditions, material models, mass and damping modeling, loading and numerical methods.

Chapter 3: **“Ambient Vibration Measurements (AVM) on St. Hyacinthe guyed mast”** presents the general characteristics of the studied mast such as site details, tower function, and its history; and the extracted results of natural frequencies and cable tensions.

Chapter 4: **“Comparison between the seismic results of the numerical models and the tests”** compares the *in situ* measurements and the numerical results by considering the influence of cable tension accuracy.

Chapter 5: summarizes the main conclusions drawn from the current research and makes suggestions for future directions of study.

Appendix A: **“Complementary studies on seismic analysis of towers”** presents more detailed results on the influence of the variability of guy cable tensions on the predicted seismic response.

1.4 Literature review

1.4.1. A review of dynamic analysis models

1.4.1.1. McClure, Guevara, and Lin (1993-1994)

The first detailed finite element modeling study ever reported on the nonlinear seismic response of guyed telecommunication towers was published by Guevara and McClure (Guevara and McClure, 1993; McClure and Guevara 1994). Before this point there had been several others who attempted more numerical modeling of guyed towers (restricted to static loads) like Augusti (1986), and Ekhande and Madugula (1988). The problem though, was that their models contained several structural simplifications: a complete explanation and critical review of the simplifications made in their models can be found in Faridafshin (2006). It is fair to say that these simplifications did not have a significantly important role in predicting the static response of the structure, but they were nevertheless not appropriate for dynamic analysis.

According to the results of Guevara's study, the high frequency components of the excitation only affect the shortest towers. The equivalent beam-column approach was used to model the mast and one of the weak points of this approach was that the warping torsional behaviour of the mast could not reproduced. In conclusion, the detailed modeling of lattice masts was recommended. The main findings of the study related to dynamic interactions obtained between the mast and guy wires under the combination of horizontal and vertical ground accelerations.

1.4.1.2. Ghodrati Amiri (1997)

The goal of this study was to provide some general design guidelines for guyed masts based on series of numerical simulations on real structures. The guidelines were presented in the form of seismic sensitivity indicators which helped determine the importance of the seismic effects and whether or not detailed dynamic analysis of the structure is required for more in-depth assessment. Detailed nonlinear seismic analyses were performed on eight towers varying in height between 150 to 607 m. The masts were modeled as three-dimensional truss structures. Some details of this study can also be found in Faridafshin (2006).

Several tower response parameters were studied, such as base shear, axial force in the mast, shear force and bending moment along the mast, and guy wire tension. Simplified empirical equations related to tower height were suggested to predict the maximum tower base shear, the distribution of horizontal earthquake forces along the tower height, and the distribution of the maximum dynamic component of mast axial forces along the tower height.

1.4.1.3. Dietrich (1999)

The nonlinear analysis of the 150 m guyed mast which had been studied previously by Amiri (1997) was revisited in detail by Dietrich (1999) using real-time three-dimensional displacement-controlled ground motion (using the classical El Centro earthquake record) instead of ground accelerations. The study was focussed on the influence of vertical ground motion, the out-plane tower response to horizontal input motion, the effects of asynchronous ground motion and the presence of ancillary components on the predicted guy tower response.

For the particular case investigated, the results indicated that all three translational components of ground motion must be included in the seismic analysis in order to reflect the combined vertical and horizontal effects and the resulting non-uniform biaxial bending and shear in the mast.

1.4.1.4. Faridafshin (2006)

Once again, with a special consideration for the realistic modeling of ground motion at the tower supports, and taking into consideration the results obtained by Dietrich, Faridafshin investigated the seismic behaviour of three existing masts with varying heights (213 m, 313 m, and 607 m) using the modelling assumptions used by Dietrich instead of Amiri. The key objective of this study was to evaluate the accuracy of previous published studies and to identify whether wave propagation of the seismic waves at the tower ground supporting points had significant effect on the seismic response of the masts. The structures of different heights showed sensitivities that were dependent on the soil stiffness.

The peak response most often occurred in the very beginning of the ground shaking when one side of the tower was vibrating and the other parts had not yet been excited. The effect of considering or excluding damping and the vertical component of ground motion were separately investigated.

In conclusion, the importance of considering coherent three-dimensional ground motions, asynchronous shaking at multiple support points in tall masts and structural damping were confirmed.

1.4.1.5. Ghafari Oskoei (2010)

The goal of this study was to develop a simplified procedure for modeling the dynamic peak response of tall guyed telecommunication masts. The study focused on the dynamic behaviour of guy clusters, and lead to an approximate method to determine the equivalent horizontal static/dynamic stiffness of elastic guy cables, individually and in clusters. The study is based on numerical simulations on 57 guy cables from nine existing towers (all eight towers studied by Amiri and the St. Hyacinthe guyed mast used in the present study) with varying heights of 150 m to 607 m. A mathematical frequency domain procedure was developed to replace the nonlinear time-variant cable stiffness with an equivalent linear frequency-dependent spring/mass system, taking in to account the response spectrum of individual guy cables and the frequency content of the input seismic excitation. Then the guy cable clusters were substituted with their equivalent linearized springs and dynamic analysis results were compared. The simplified proposed method was based on a condensed model of the guyed mast where the individual horizontal stiffness elements were evaluated at each cluster level. Finally, generic structural mass/stiffness matrices were proposed for performing seismic analyses.

The procedure was tested numerically with the nine telecommunication masts subjected to five different seismic inputs. Also, further numerical validation of the proposed method was provided by studying the response of the 342 m and 607 m towers under the effects of eighty-one recorded California earthquakes.

1.4.2. A review of seismic design practice

The thesis is related to the experimental calibration of dynamic computational models of guyed masts in view of seismic analysis therefore wind-related studies are not covered in the review in the interest of space. The interested reader is referred to the work of the IASS (International Association for Shells and Spatial Structures) Working Group 4 on Masts and Towers and the monograph by Smith (2006) which summarizes the contributions of this group and lists several references.

Due to the dependency of communication networks on tall masts, some guidelines are needed for controlling their force and displacement response to earthquakes. Under very strong design-level ground motion it is possible that these tall masts would not maintain their serviceability; also, it is important that if minor damages occur, they should not cause any loss of functionality shortly after the earthquake.

Considering the importance of having news broadcasts to and from damaged areas after an earthquake, there is a good justification for ensuring telecommunication mast integrity during these times. In order to achieve this, structural engineers require specific seismic design guidelines.

1.4.2.1. IASS Guidelines (International Association for Shell and Spatial Structures)[1]

IASS-WG4 published its guidelines for the analysis and design of guyed masts in 1981. In fact, one of the objectives of this document was to provide design guidance for National and International Code drafting Committees, which explains why it has never been updated.

The seismic analysis recommendations for guyed masts now seem simplistic in view of current analysis tools, and essentially pertained to:

1. Simplified quasi-static analysis using a lateral load proportional to the tower weight (as suggested in most building codes at the time);

[1] The IASS (International Association for Shell and Spatial Structure) Working Group no. 4 was created in 1969 and is dedicated to structural design, construction and maintenance of Telecommunication Masts and Towers.

2. Linear analysis using modal superposition;
3. Representing the guy wires by linear springs;
4. Using lumped masses.

Since seismic design loads represent extreme events, only their combination with dead loads due to self weight was suggested (that is no ice) with the assumption that earthquakes occur in still air conditions.

1.4.2.2. Canadian Standard CSA-S37-01 (R2006)

In Canada, guidance on earthquake-resistant design and seismic analysis of communication structures is contained in Appendix M of Canadian standard CSA-S37-01(R2006).

The 1994 edition of this standard was the first to devote an appendix to seismic analysis of telecommunication towers. In January 1995, the devastating Kobe earthquake in Japan caused extensive damage to structures and led to increasing interest and motivation for establishing earthquake resistance guidelines with specific focus on telecommunication towers. The Federal Emergency Management Administration (FEMA, 1998 and 2000) of the United States increased the attention of the existing National Earthquake Hazard Reduction Program (NEHRP) to non-structural systems, non-building systems, and lifeline systems such as telecommunication towers. The results of these efforts accounted for the addition of the seismic regulation section to the ANSI/TIA 222-G Standard for the first time in 2006, which was done with the help of the American Electrical and Telecommunication Industries Association (TIA/EIA). In the meantime, the American Society of Civil Engineers (ASCE) had published its Guide for the Dynamic Response of Lattice Towers (Madugula, Ed. 2001) which comprises a special chapter related to seismic response.

Coming back to the Canadian Standard CSA-S37, it should be mentioned that a completely revised edition will be issued in 2012 and that seismic design checks will become mandatory for all post-critical towers playing a role in post-earthquake response and rescue. Three safety level categories are defined:

- **Prevention of injury or loss of life (Life Safety) - Performance Level 1 (PL1)**

  Preservation of life safety is the minimum requirement for all towers located in moderate to high seismicity zones.

- **Interrupted serviceability- Performance Level 2 (PL2)**

These towers may become unserviceable during the earthquake but should recover their functionality shortly after. Existing post-critical installation should meet this level of performance.

- **Continuous serviceability- Performance Level 3 (PL3)**

This applies to those towers that should maintain serviceability during and after an earthquake as they are essential structure in a telecommunication network or towers that are utilized in the control of electrical utility systems.

1.4.2.3. American Standard ANSI/TIA/EIA-222-G on Seismic design provisions

This standard is dedicated to mandatory minimum design requirements for all types of antenna-supporting structures. It lists four seismic analysis methods of increasing accuracy and complexity with limitations for their applicability to various tower types, geometry and height. The methods are: Equivalent static lateral force; Equivalent modal analysis; Classical modal superposition analysis; and Time history analysis.

Guyed masts are required to be modeled in three dimensions, as either an elastic truss model or a three-dimensional frame-truss model. Also the analysis must consider the geometrically non-linear P-Δ effects on the mast.

1.4.3. A review of communication tower failures in past earthquakes

Lessons can be learned from the performance of telecommunication infrastructure during past earthquakes. A summary of some of the most damaging earthquakes is presented next in chronological order.

1.4.3.1. 2001 Gujarat earthquake (India)

Earthquake at a glance:

An earthquake measuring 7.9 on the Richter scale (7.6 Moment Magnitude) hit the Kutch (also spelled as Kachchh) region, located in the northwest part of the State of Gujarat at

8:46 AM on January 26, 2001 (Ravi Mystry et al., 2001). It was felt in most parts of India and caused substantial loss of life and property.

Effects on telecommunication towers:

According to the damage reconnaissance reports, most of communication cables were damaged. Preliminary reconnaissance reports related to the amount of the damage did not agree with complementary observations. Poor quality of engineering and construction was identified as the main cause of the damages for all structures. Figure 1-3 presents a telecommunication tower which survived the earthquake at Kachchh District, Gandhidham.

Figure 1-3 Destruction outside the Communications Center for Kachchh District, Gandhidham, January 26, 2001, in which the tower remained standing (Ravi Mystry et al., 2001)

1.4.3.2. 2003 Bam earthquake (Iran)

Earthquake at a glance:

An earthquake with a moment magnitude of 6.6 Mw struck the city of Bam, located approximately 1000 km southeast of Tehran, at 5:26 AM local time on Friday the 26th of December 2003. There had been no record of any major earthquake in the area for at least the previous 2500 years.

Effects on telecommunication towers:

Reconnaissance reports on the 26 December 2003 Bam Earthquake listed only minor and non-structural damages to telecommunication central offices compared with other lifeline equipment. Although damage of some telecommunication towers on the building rooftops was observed (because of collapsing of roofs), the main towers mostly survived the earthquake intact. Figure 1-4 presents one telecommunication tower falling due to roof collapse.

Figure 1-4 Almost intact tower falling down due to roof collapse. (Masoud Moghtaderi-Zadeh et al., 2003)

1.4.3.3. 2004 Sumatra earthquake (Indonesia)

Earthquake at a glance:

Several earthquakes with magnitude of 9.3 Mw shook the northern part of Sumatra and the Andaman Sea at 7:59 AM on December 26th, 2004. This earthquake was the second-largest recorded by seismographs since 1900, a rare earthquake event in the history of the Indian Ocean.

Effects on telecommunication towers:

Poor performance of lifeline telecommunication systems was observed in the Andaman and Nicobar islands. Telecommunication structures experienced severe damage during the earthquake, especially at the fixed connection services, where 40% of the connections were reported broken. Figures 1-5 and 1-6 present one toppled telecommunication tower by tsunami.

Figure 1-5 One self-supported lattice communication tower in Hambantota (Indonesia) was toppled by the tsunami (Donald Ballantyne, 2004)

Figure 1-6 Collapsed telecommunication tower as a result of tsunami (Teddy Boen, 2004)

1.4.3.4. 2005 Kashmir earthquake (Pakistan)

Earthquake at a glance:

The 7.6 Mw October 8, 2005 Kashmir earthquake occurred at 8:50 AM about 10 km NE of Muzaffarabad and 105km NNE of Islamabad.

Effects on telecommunication towers:

Extensive structural damage to the telecommunications network was reported in the districts of Muzaffarabad, Rawalakot and Bagh. Figure 1-7 presents one damaged telecommunication tower because of lateral spreading at one hilltop. No specific failure of guyed masts is reported.

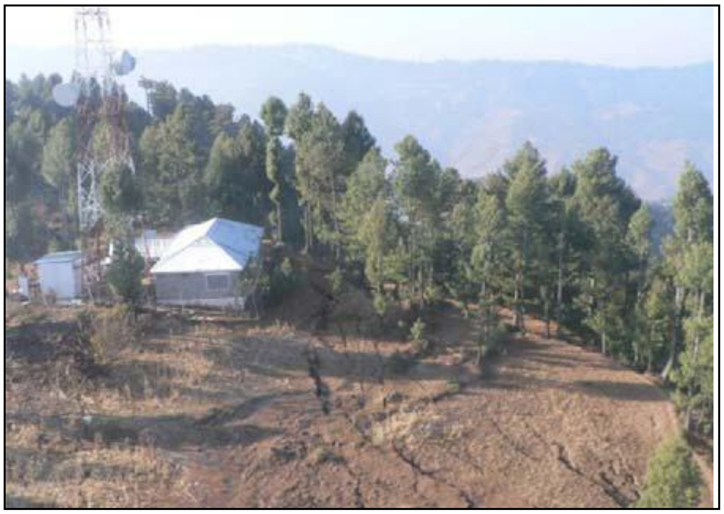

Figure 1-7 Lateral spreading at Dana hilltop in the vicinity of the SCO-Tower near Azad Jammu and Kashmir (Jean F. Schneider, 2008)

1.4.3.5. 2008 Sichuan earthquake (China)

Earthquake at a glance:

The 2008 Sichuan earthquake was a deadly earthquake of 8.0 Ms and 7.9 Mw that occurred at 2:28 PM on Monday, May 12th, 2008 in the Sichuan province of China, killing an estimated 68,000 people.

Effects on telecommunication towers:

Half of the wireless communication in Sichuan province was lost, and telecommunication service to and from Wenchuan and four nearby counties was cut off. “China Mobile” which is the largest telecommunications service provider in China experienced severe disturbances because of the dysfunction of nearly 2,300 base stations. The emergency response provided included some emergency telecommunication vehicles, many equipped with satellite communications facilities.

Government efforts during the first week following the earthquake restored electric power and telecommunication services in priority. Figure 1-8 presents one collapsed telecommunication system during the Sechuan earthquake.

Figure 1-8 Damaged telecommunication system in the Sechuan2008 earthquake (Aiping Tang et al., 2010)

1.4.3.6. 2010 Chile earthquake

Earthquake at a glance:

An 8.8 Richter scale earthquake lasting about 140 seconds hit the central part of Chile on Saturday February 27th, 2010 at 3:34 AM and affected the most populated area of the country. It was the fifth strongest earthquake ever recorded.

Effects on telecommunication towers:

Although telecommunication networks were not inspected to assess damage, the ASCE/TCLEE (Technical Council on lifetime Earthquake Engineering) reported severe disruption to all telecommunication services (both landline and wireless services) for different reasons: power outages, equipment failures, antennae damage, building collapses and loss of reserve power in most network facilities in the affected areas. Figures 1-9 and 1-10 present one collapsed transmission line due to foundation failure.

Figure 1-9 A Transelec transmission line structure collapsed due to a foundation failure (Hugh Rudnick, 2010)

Figure 1-10 Hualpen – Bocamina 154kV Transmission Line Collapsed Tower (Hugh Rudnick, 2010)

1.4.3.7. 2010 Haiti earthquake

Earthquake at a glance:

The catastrophic and deadly 2010 Haiti earthquake was of magnitude 7.0 Mw with its epicenter near the town of Léogâne, approximately 25 km west of capital city of Port-au-Prince. The earthquake occurred at 4:53 PM on Tuesday, January 12th, 2010.

Effects on telecommunication towers:

Digicel technical buildings were damaged, and so were their antennas or hosting buildings. There was no electricity, poor GSM (Global System for Mobile Communications, originally Groupe Spécial Mobile) connectivity and cellular systems were saturated; SMS (Short Message Service) messaging retained functionality but its reliability was uncertain. Data connectivity was available with the MINUSTAH (United Nations Stabilizing Mission in Haïti - task force deployed for post-disaster assistance). It took 6 days for the President to get internet access locally. Figures 1-11 presents the only undamaged telecommunication tower in Port-au-Prince after the earthquake. Figure 1-12 shows a collapsed tower.

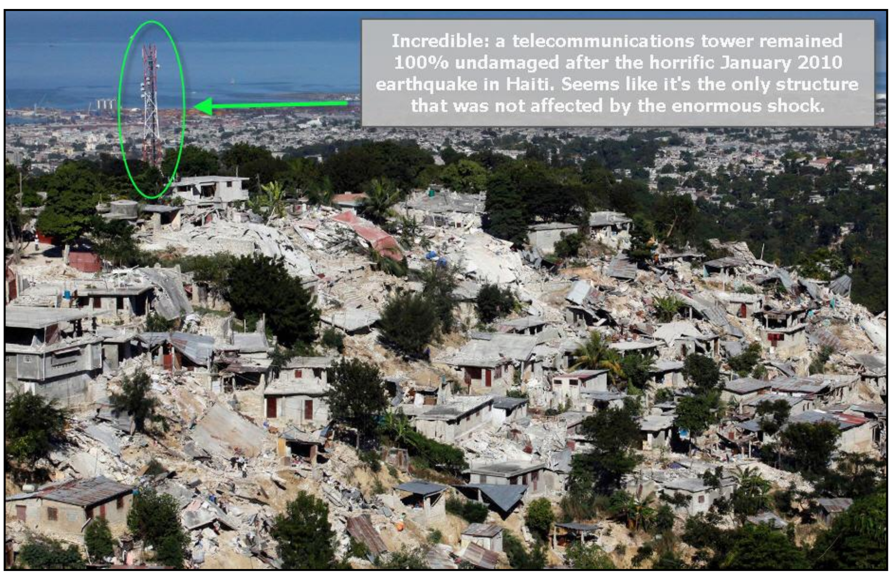

Figure 1-11 A telecommunications tower remained undamaged after the divesting January 2010 earthquake in Port-au-Prince, Haiti (Adele Waugaman et al., 2010)

Figure 1-12 collapsed antenna tower in Carrefour, Haiti (Adele Waugaman et al., 2010)

1.4.3.8. 2010 New Zealand earthquake

Earthquake at a glance:

On September 4th 2010 at 4.36 AM, a 7.1 Mw shook Christchurch and wider Canterbury. The earthquake was felt throughout the South Island and the lower North Island. The epicenter was located near Darfield, 40 km west of Christchurch City center at the shallow depth of 10 km.

Effects on telecommunication towers:

In New Zealand mobile telecommunication land sites are largely short steel towers between 15 m and 20 m high. Some rural sites use steel guyed masts to support antennas and these guyed supports remained intact after the earthquake. Observations afterwards indicated that the little damage present was related to the mast foundation as a result of soil liquefaction. Figure 1-13 presents one tilted cellular mast due to ground deformation.

Figure 1-13 Cellular mast out of plumb due to ground deformation (JM Eidinger, 2012)

A more comprehensive survey of earthquake –induced damages to telecommunication towers during the years from 1999 to 2011 is presented in the technical report STENG 2012-15 (Ghafari Osgoie, 2012). This survey is a complement to an earlier work covering the pre-1999 period by Schiff (1999).

It is noteworthy that no structural damages to telecommunications structures have ever been reported for earthquakes with peak ground acceleration less than about 0.7g. Towers mounted on rooftops have collapsed because of building damage, while towers on ground were most affected because of soil failures.

In conclusion to this earthquake-induced damage review segment, it is seen that ground-based telecommunication structures are typically robust under large earthquake loads and most service disruption relate to dysfunction of equipment rather than structural failure. However, details of structural failures or damage due to strong shaking are not typically available in reconnaissance reports.

1.4.4. A review of structural identification techniques

Structural identification (SI) as a subset of system identification is a process which determines the relationship between response parameters from two sources. One of these sources is derived from the results of a mathematical model, and the other is extracted from experimental measurements. The purpose of system identification is to predict the behaviour of the system by experimental estimation of system characteristics.

Structural identification is used in different applications such as:

1. Model validation and updating: By increasing the ability to predict the behavioural response of structures, the ability to control the structure, and to validate the level of accuracy that the finite element model can provide.
2. Structural Condition Assessment and Monitoring: New developments in computers, signal processing and instrumentation technology have enabled the assessment and monitoring of structural integrity and performance.
3. Earthquake engineering: Access to data showing the correct seismic characteristics of the structure is critical.
4. Soil-structure interaction: Study of the interaction between a structure and the surrounding soil medium is aided significantly with the use of structural identification techniques.

1.4.4.1. History

Since the 1970s structural dynamic monitoring, which makes use of structural identification techniques, has been used in different fields of engineering, such as mechanical and aeronautical, while in the field of civil engineering dynamic monitoring tests have been used only since the 1980s. The main usage of these instruments in civil engineering relates to Structural Health Monitoring- SHM of special structures such as important bridges and tall flexible buildings (Farrar and Worden, 2007).

1.4.4.2. Dynamic monitoring systems

Direct *in situ* system monitoring is the technique used in the process of damage detection which relies entirely on non-intrusive methods; as compared to the previous force vibration tests which can be considered more intrusive. It can be classified into two types: static and dynamic monitoring. Static monitoring is done during a short period of time, such as displacement variations during construction, the progression of a crack, or to monitor environmental conditions. However, dynamic monitoring seeks the identification of the response frequencies, damping and mode shapes of the system.

Dynamic monitoring systems have more function than the static ones and can be used in a variety of applications such as assessing the operational conditions of the structures, or providing quality data for rapid disaster management decisions following unexpected catastrophic events. Considering the importance of earthquake resistance of critical structures, and the difficulties to replicate their behaviour in laboratory experiments, dynamic monitoring can help in calibrating analytical models and in improved understanding of their dynamic response.

Some of these dynamic monitoring systems are as follows:

I. Wire-based monitoring systems (conventional systems)
II. Wireless based monitoring systems
III. Inclination sensors
IV. GPS sensors

GPS sensors used for monitoring the deformations in structures include geodetic sensors, motorized theodolites, accelerometers, extensometers, tiltmeters, inclinometers, and meteorological sensors such as temperature sensors (Rafael Aguilar Velez, 2010).

I. Wire-based monitoring system s (conventional systems)

Wire-based systems, also called conventional systems, are still widely used by the civil engineering community because they are available, low-cost and reliable (high sensitivity and resolution) and come with reliable commercial software packages.

The wire-based systems used for structural monitoring include three components:

1) Measurement sensors: Low cost and high sensitivity make accelerometers the most common equipment for measuring dynamic characteristics. It should be mentioned that these sensors are also used in combination with other transducers such as velocity meters or displacement meters.[2]

2) Data acquisition equipment: A Data Acquisition (DAQ) system is an electronic device designed to collect and store the information that is acquired by the measurement sensors.

Recorded data from the sensors need to be modified before dynamic extraction can proceed. Signal modification procedures are generally amplification, filtering and signal conversion like analog to digital, digital to analog or frequency to voltage. Signal amplification is the level of an electrical signal which is represented by variables such as voltage, current, and power. For preventing some errors which are caused by signal weakness, the signal level should always be larger than a specific limit for transmission. These errors which are caused as a result of signal weakness can be solved by amplifying the signals. Filtering improves the performance of vibration monitoring and analysis by eliminating some unwanted signals. These signals can be generally produced by some external disturbances, error components in excitations, and noise within system components. Analog-Digital Conversion is typical. Figure 1-14 presents a general layout of a wire-based monitoring system.

[2] Generally five main groups of accelerometers exist: piezoelectric, piezoresistive, capacitive, force balanced (also known as servo) and strain-gauge based.

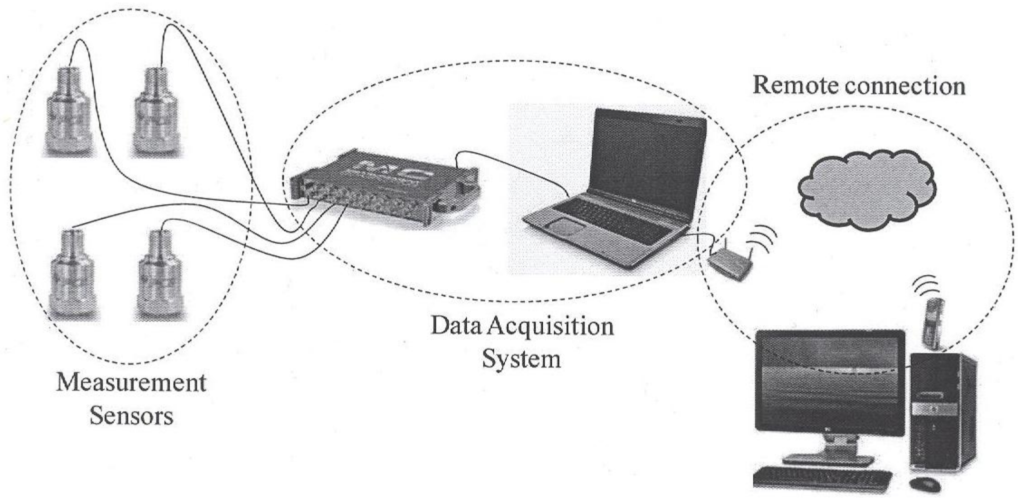

Figure 1-14 Monitoring system with wire based equipment. (Rafael Aguilar Velez, 2010)

3) Remote connection system: The measurement sensors are connected with cables to the data acquisition system that can be remotely connected to a central station.

It should be mentioned that structural monitoring can be continuous or portable testing. Continuous monitoring also called Structural Health Monitoring (SHM), is used in engineering structures. In this method the data are collected over an extended period of time (months, years or even permanently). On the other hand, portable testing is used in conditions where discrete measurements in time are required. Important items for structural monitoring can be classified as quick and easy setups, and connectivity with a laptop. Since a continuous monitoring system is generally used over long periods of time and without any opportunity for ongoing maintenance in remote locations, performance optimization is important: attention should be paid to reliability and remote operation, set up notifications during the performance of the work, and accessibility of the data for transferring and adjustment. The notifications may use as alarms to report the existence of possible damages or the achievement of a specified threshold level in measurements.

II. Wireless monitoring systems

The need to communicate with sensors in different fields such as microelectronics, physics, control, etc. was the motivation for creating small and easy to handle equipment. These sensing systems are called "motes" and generally have four functions: sensing, processing, communication and actuation.

Important characteristics of motes are their capacity to process and communicate wirelessly, their compact devices, and the most important is their ability to co-operate with other sensors in the wireless network.

The first commercial wireless mote was developed by the University of California-Berkeley (Lynch and Loh, 2006) and subsequently commercialized by Crossbow (2009) since 1999.

A wireless monitoring system includes three components:

1) Measurement units comprising autonomous sensors and DAQ platforms which are used for collecting data and sending them to a base station.

2) Base station, essentially coupling a DAQ platform with an interface board for data transferring to a local computer.

3) Remote connection system transferring data from the local computer to a central "brain" station for further signal processing. The Tromino sensors used in this research are examples of wireless sensors.

Figure 1-15 presents a general layout of wireless system.

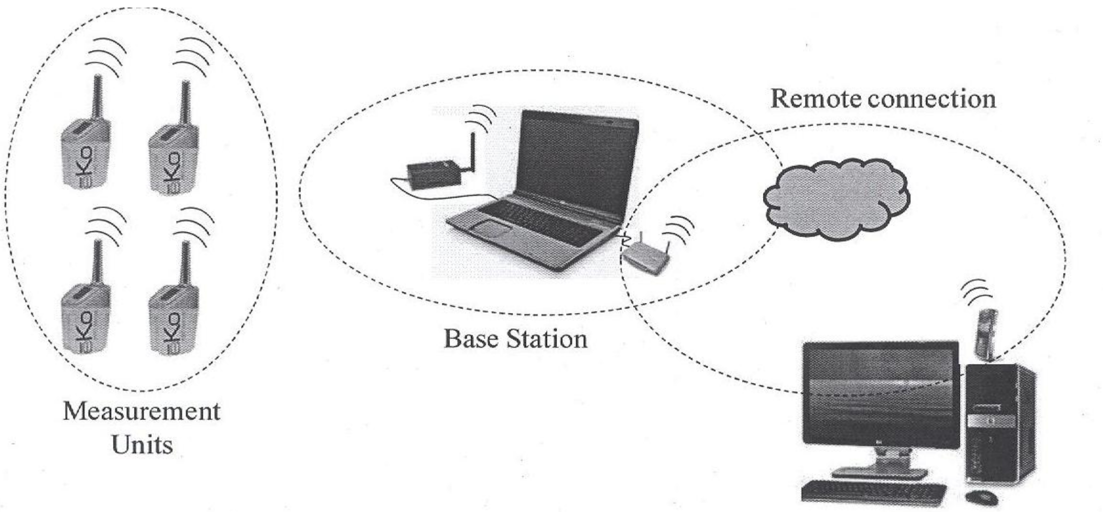

Figure 1-15 Monitoring system with wireless equipment (Rafael Aguilar Velez, 2010)

Comparison between wire-based and wireless systems

There are many restrictions in using wire-based systems in buildings or in the field. Some are architectural (deployment in buildings is, at times, difficult) and some economical due to the high cost of sensitive transducers and communication cables.

New transducers are now lightweight, small, wireless, and less expensive as well. Figure 1-16 presents comparative schematics of these two monitoring systems.

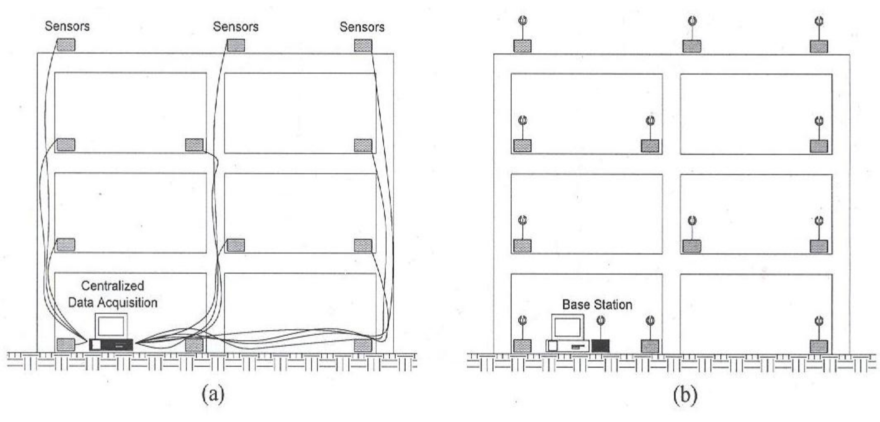

Figure 1-16 Structural monitoring system ;(a) wired-base system; and (b) wireless system (Rafael Aguilar Velez , 2010).

III. Inclination sensors

This type of sensor is generally used for identifying deformations in the structure's base by measuring changes in inclination.

The measurement principle is based on optoelectronics, measuring the angle between the horizon and the surface of an object. Figure 1-17 presents an example of inclination sensor.

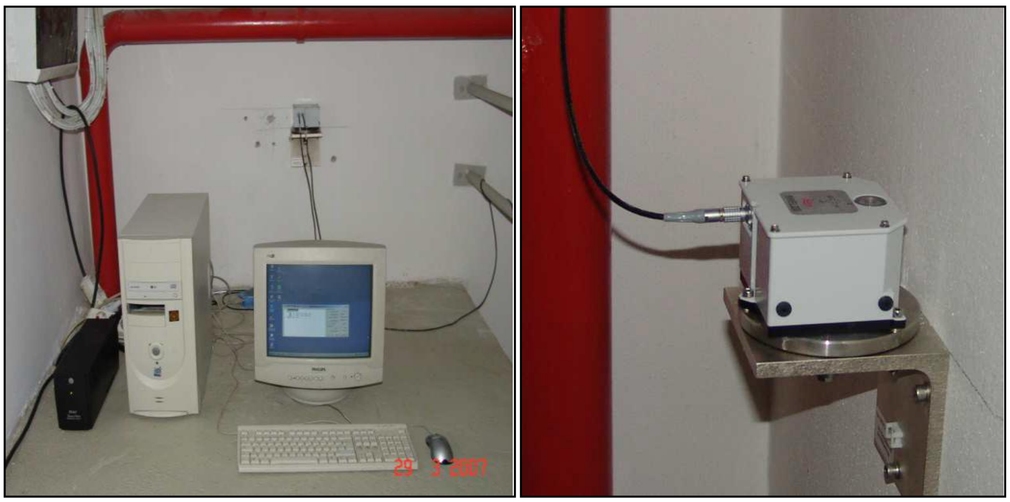

Figure 1-17 Installed inclination sensors and its monitoring system (Cemal Ozer YIGIT et al., 2008)

IV. GPS sensors

In the present study, GPS sensors are used to measure ambient accelerations of the guy cables; details about these sensors are provided in section 3.1.2. In general, the systems comprise two or more receivers, at least one of them serving as a base station, while the others are roving sensors. An example is shown in Figure 1-18 where the roving sensor is installed on a rooftop (Figure 1-18 (a)) while the base station is fixed on a concrete post (Figure 1-18 (b)).

(a) *(b)*

Figure 1-18 (a) Rover station, (b) Base station (Cemal Ozer YIGIT et al., 2008)

1.4.5. Data processing techniques for Ambient Vibration records

Dynamic tests on structures may be classified by the nature of the excitation as either forced vibration or ambient vibration tests. Forced vibrations refer to any motion in the structure which is induced artificially above the ambient level.
Methods of inducing motion in structures include: mechanical shakers (electro- magnetic, eccentric mass, hydraulic, including large shaking tables in laboratories); transient loads (Pull back and release, initial displacement, impact initial velocity); man-excited motions; and induced ground motions (nuclear blasts, conventional explosions).

Another method for determining the dynamic behavior of a structure is to record its response to seismic events (seismic monitoring). Although it is not entirely suitable to consider this a “test”, this monitoring is the most accurate way for testing critical structures in seismically active zones where weak and moderate earthquakes are frequent.

Ambient vibration tests have gained popularity for measuring and extracting the vibration properties of structures such as natural frequencies, mode shapes and damping ratios. Ambient vibrations are the low-amplitude motion due to different sources such as wind, earthquakes or micro-tremors, or operational loads and occupancy. The process is also called operational modal analysis. It should be mentioned that, in this method, the input forces are not measured and they are assumed to be broadband and stationary (Clough and Penzien, 2003).

Through this method, the results of the measured response, which are typically translational acceleration, velocity and displacement time histories, are processed using either frequency domain decomposition techniques (the most common, as used in this research) or nonlinear time-domain stochastic techniques (several are in use). Prior to specific property extraction, the ambient vibration records need to be pre-processed as follows: 1) Removal of outliers, 2) Scaling, 3) Mean removal, 4) Tapering and stacking, 5) Digital filtering item decimation, and 6) Data quality judgment. See Structural Vibration Solution A/S (2010a and b) for definitions and description of procedures).

Properties such as ease of set up and low cost, in addition to the ability to acquire the dynamic properties under the actual operating conditions, define the principal advantages of applied modal identification from ambient vibration tests.

Operational modal analysis can be achieved by using portable equipment in only a few hours to determine the dynamic properties of complex structures such as dams, bridges, offshore oil platforms, power plant boiler structures, turbine foundations, office buildings, stacks, historical office structures and nuclear power plant containment buildings (Trifunac, 2007).

In the test, no measurement of input forces is required. In addition to civil engineering applications, the test is currently used in mechanical engineering applications such as rotating machinery, and on-road and in-flight testing of vehicles and aircrafts (Ventura, 2012)

There are some important differences between ambient excitation and forced excitation. As one of these important differences, ambient excitation operates in natural and operational conditions from many independent sources that excite many global modes); however forced excitation excites the low frequency global modes for large structures with difficulty as it is difficult to enforce large amplitude excitation, especially if testing does not allow service disruptions. Generally ambient vibration measurements require highly sensitive equipment because of the low amplitude response levels, while forced excitation testing requires large amplitude artificial excitation. On the other hand, forced excitation has the property of dissipating the energy locally, which is good for local mode excitation of a sub-structure. In addition to all, it should be mentioned that forced excitation can improve signal to noise by having response levels over the natural (ambient) level and also it may be affected by geometric nonlinearities.

Chapter 2 FINITE ELEMENT MODELING OF A GUYED TELECOMMUNICATION TOWER FOR DYNAMIC ANALYSIS

2.1 Generalities

As it was mentioned in the first chapter, the dynamic behavior of the 111.2 m guyed telecommunication mast owned by Hydro Québec and located in St. Hyacinthe, Québec has been previously modeled in detail by Ghafari Oskoei (2010) using ADINA3, version 8.2. This same tower has been used for field validation measurements carried out in 2012.

2.2 Tower geometry and boundary conditions

The latticed steel mast is prismatic and triangular in cross section with panel dimensions of 1.116 m (3’-8”) m in width and 1.02 m (3’-4”) in height. It is supported laterally at six stay levels arranged at two ground anchor groups at distances 39.6 m (130 ft) and 83.8 m (275 ft) from the mast axis. Two outrigger structures are also provided to increase its torsional stiffness, at the top first and third clusters. The tower supports several communication antennas attached at different elevations and transmission lines that carry the antenna signal to the telecommunication base station located in the equipment shelter adjacent to the tower. The structure is modeled as pinned at the base of the mast. This pinned connection provides translational restraints (three degrees of freedom), while it allows rotations. In seismic analyses, the earthquake records have been modeled as synchronous accelerograms at every ground support points, with only translational accelerations that are consistent in both horizontal and vertical directions.

The following sub-sections summarize the salient features of the numerical models in general terms only and the interested reader is referred to the work of Faridafshin (2006) and Ghafari Oskoei (2010) for details: It is recalled that the present study used the tower models created by the latter doctoral study. It is also important to understand that the detailed geometry and tower design cannot be reproduced in the thesis because they constitute confidential information. Any researcher interested in using this case study for further validation is invited to contact the thesis supervisor or the author who will subsequently seek permission from the tower owner to divulge the detailed information.

2.3 Finite element modeling

The finite element model was built using commercial nonlinear finite element analysis ADINA software (ADINA R&D, Inc. (2004)).

The mast is modeled as a three-dimensional truss with elastic isotropic mild steel having a Young's modulus E= 2.0e11 Pa, Poisson ratio ν =0.3, and density ρ =7850 kg/m^3.
The guy wires are modeled using a nonlinear elastic material model, and 3-node truss elements along their profile. Based on previous convergence studies by Guevara and McClure (1993) and Gantes et al. (1993), 10 tension-only elements are used to mesh each guy cable. This mesh provides a good level of accuracy and can represent the first five transverse cable modes. Applying cable pre-stress through defining initial strain is essential to define a non-singular initial stiffness matrix of the system. Tension-only behaviour is assumed for the cables, and a bi-linear elastic-plastic material model is used (Young's modulus E= 1.72e11 Pa, Poisson ratio ν =0.3, and density ρ =7850 kg/m^3). The initial pre-tension is prescribed for each cable element as indicated in section 2.4.
A large kinematic formulation is used for the structure to account for potentially large displacements and rotations.
For modeling structural damping, an equivalent translational viscous damper with a value of 2% of critical viscous damping was used for all elements (mast and cables). All cable elements are used with a parallel dashpot. The earthquake loads are assumed to occur under still air conditions and aerodynamic damping is neglected. Note that it is possible to model aerodynamic damping in ADINA but this is beyond the scope of the project. These damping values, as used in previous studies, are assumed with a view of further validation with the extraction of AVM records presented in Chapter 3.

2.4 Loading

2.4.1. Static loading

The self-weight of the structure, including the weight of the mast and cable elements, was considered in all analyses.

As it was mentioned earlier, the model was studied under two conditions. In the first one the added weight of the antennas, platforms, ladders, and other ancillary components was assumed to be negligible in the global response of the tower and was not modeled; however, for the second condition, the weight and inertia of the antennas and transmissions lines were included in the model.

In North-American tower engineering practice, the guy cables are initially pre-tensioned to approximately 10% of their ultimate strength at a reference temperature: in Canada the reference is 10ºC (CAN/CSA S37). This cable pre-tension was modeled as the corresponding initial strain in each cable element. In fact, the self-weight of the cables makes them deflect downward and the cable pretension moderates this effect by tightening the sagging cables. Cable pre-tension is a crucial parameter to determine the horizontal stiffness of the guyed tower.

2.4.2. Seismic loading

The finite element models were analyzed under three classical Californian ground acceleration records: El Centro, Park field and Taft. Table 2-1 lists the information concerning the selected earthquakes.

To keep the numerical simulations as realistic as possible, all three orthogonal components of real earthquakes were considered. It should be mentioned that the orientation of the prescribed ground accelerations is selected to cause maximum response in the structure. For achieving this purpose the main horizontal component (labeled as the X direction) was aligned with a principal direction (that is along a plane containing a full set of guy cables) and the other orthogonal horizontal component was considered as the Y direction. Also the vertical component was labeled as the Z direction.

Table 2-1 Selected classical earthquakes[3]

Earthquake	Date	Magnitude (Mw)	Peak ground acceleration (g)	
			horizontal	vertical
El Centro	5/19/1940	7.0	0.313	0.215
Taft	7/21/1952	7.4	0.178	0.159
Parkfield	6/28/1966	6.1	0.442	0.367

2.5 Numerical considerations

To obtain the nonlinear dynamic response of the structure, direct time-step numerical integration of the differential equations of motion has been implemented in the model. Among the explicit and implicit methods for nonlinear analysis available in ADINA, the Newmark method was selected; the constant-average-acceleration method (with parameters $\gamma = 0.5$ and $\beta = 0.25$), also called trapezoidal rule, was used in this study. The integration time step was selected based on accuracy considerations only since the method is unconditionally stable. By considering a cut-off frequency of 30 Hz as an assumption in the current work (which largely exceeds the frequency content of the expected response, typically below 10 Hz) the time step was calculated as:

$$\Delta T = \frac{0.2}{\omega_{c0}} = \approx 0.001 \quad Sec \qquad (1)$$

where ω_{c0} is the highest frequency of interest in dynamic response (Faridafshin, 2006). The full Newton method was used for stiffness matrix updating at each time increment in the equilibrium iterations. More details about the numerical parameters used in the study can found in (Faridafshin, 2006).

3 The information about the selected earthquakes is from PEER (Pacific Earthquake Engineering Research Center) database.

Chapter 3 AMBIENT VIBRATION MEASUREMENTS ON THE ST. HYACINTHE GUYED MAST

3.1 Generalities

The AVM tests were conducted on 19 September 2011 by a team comprising an expert from IREQ Hydro Québec (Dr. Daniel Gagnon), a postdoctoral student from McGill University (Dr. Xiao Hong Zhang), the author, and three linemen from Hydro Québec.

This research part of the research project was summarized into a conference paper co-authored by Mahtab Ghafari Osgoie, Ghyslaine McClure, Xiao Hong Zhang, and Daniel Gagnon and titled "Validation of the accuracy of finite element analysis models of a guyed telecommunication mast with ambient vibration measurements", presented at and published in the proceedings of the 3rd International Structural Specialty Conference of the Canadian Society for Civil Engineering (CSCE), Edmonton, 6th -9th June 2012. The following section presents the manuscript of this conference paper with minor changes to fit into the general format of the thesis. According to CSCE's publication copyright policy, the author has permission to publish the manuscript as is in her thesis.
Figure 3-1 below shows the general layout of the tested structure while close-up details are shown in Figs. 3-2 and 3-3.

Figure 3-1 General view of the tested telecommunication tower

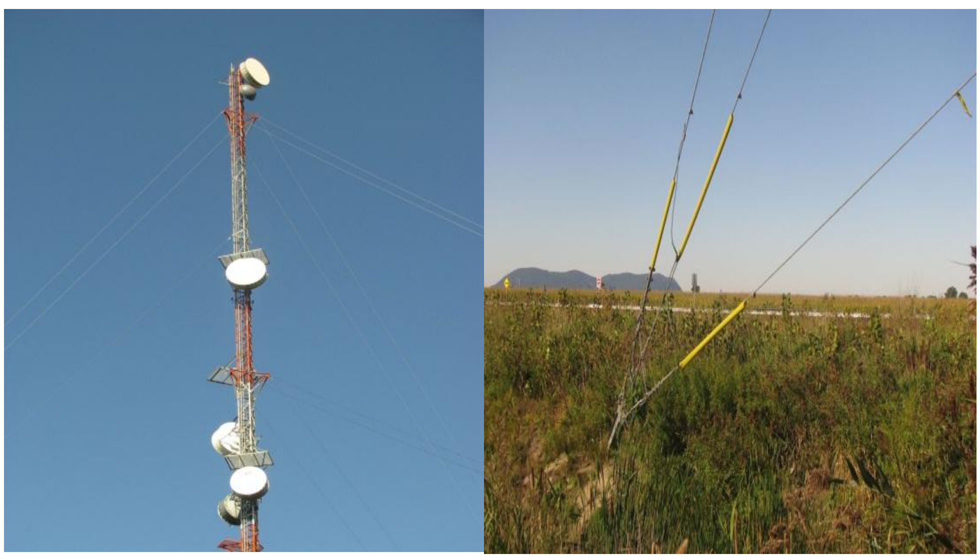

(a) Close-up of torsion outriggers, drum antennas and ice guards *(b) Ground anchor of lower guy clusters*

Figure 3-2 Details of the tested telecommunication tower

Figure 3-3 Foundation of the mast

It should be mentioned that a preliminary AVM test series had been conducted in 2010 on the mast only as the cable sensors proved defective. Hence the 19 September 2011 test series was more complete with velocity measurements at six elevations along the mast and acceleration measures on each typical guy wire of the mast (a series of 8 cables). Figure 3-4 shows the schematic location of the sensors for this September 2011 test. The tromographs are located at the elevation of each guying level. The GPS sensors are located as close to the anchor points as possible near the tower attachment point and near the anchor rods, and an additional sensor is placed about 1 m away from this lower sensor. All sensors are equipped with global positioning capabilities that provide their exact location.

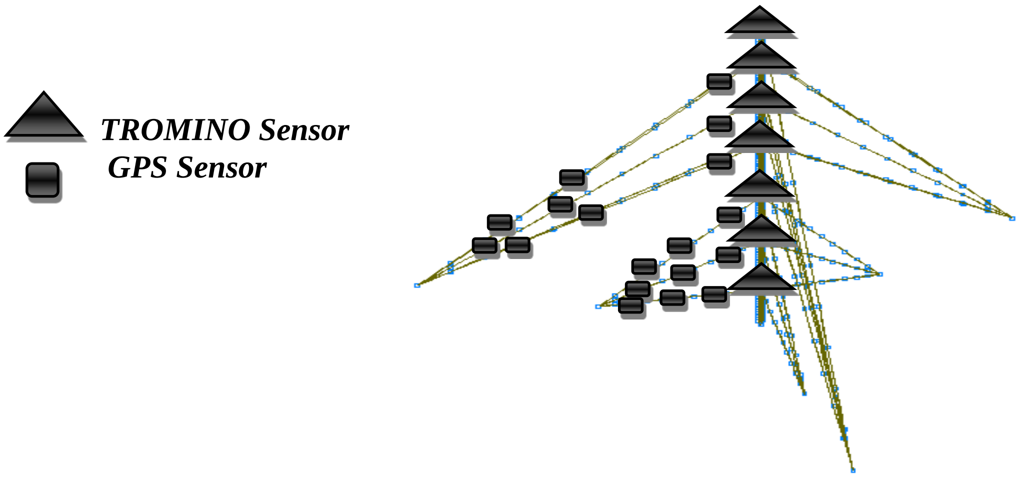

Figure 3-4 Location of the sensors

Two types of wireless AA battery-powered instruments were used for AVM data collection: tri-axial accelerations were measured on the guy cables using GP1 sensors, and velocities were recorded at seven selected elevations in the mast using TROMINO ENGYPLUS^{TM} sensors (tromographs). Both types of instruments were insensitive to electromagnetic fields.

A first series of measurements was taken in the morning where only the TROMINO sensors were installed at different elevations on the mast. Six different episodes were recorded, each of them lasting approximately 6 to 10 minutes to capture several hundreds of natural vibration cycles.

Figures 3-5 to 3-7 show some details of sensor installation by Hydro Québec linemen.

Figure 3-5 Work preparation by linemen

Figure 3-6 Installation of the sensors by linemen at different levels (inside red circles).

After this AVM test series on the mast, the TROMINO sensors were left in recording mode continuously while the three GP1 accelerometers were installed sequentially on six guy wires as shown in Figure 3-4. For each cable, a sensor was installed a few centimeters from the tower-cable attachment point, a second sensor near the ground anchor and the last one about 1 m higher: this is shown in Figures 3-7.

(a) Installation of GP1 Sensor near the anchor

(b) Installation of GP1 Sensor near the bottom sensor

(C) GP1 sensors at two levels near the ground anchor

Figure 3-7 Installation of the GP1 sensors on the guy cables at different levels

3.1.1. TROMINO Sensors

The TROMINO sensor (tromograph measuring micro-tremors) is a high-resolution wireless system used for vibration monitoring and seismic surveys. It is compact in size and lightweight: 10cm x 14 cm x 8 cm and approximately 1 kg (see Figure 3-8).

It is equipped with both velocity channels (with two resolution levels, ±1.5 mm/s for ambient vibrations and up to ±5 cm/s for stronger motion) and acceleration channels (for strong vibration monitoring). It comprises a built-in GPS receiver and an internal and/or external antenna for positioning and absolute timing/synchronization of different sensors. Each channel can have a frequency sampling rate of 0.1 to 1024 Hz. The sensor is controlled by the TROMINO MANAGER software for vibration monitoring and remote management of a single unit in a TROMINO network. It uses little power (75 mW) and can operate on 2 AA-batteries (1.5 V) for up to more than 100 hours continuously; it can also work on AC adapter for longer monitoring.

Data transfer from each sensor to a computer is done with a simple USB connection through a data transfer and pre-processing software called GRILLA which is supplied with the sensor (www.tromino.eu).

Figure 3-8 TROMINO Sensors (http://www.tromino.eu)

3.1.2. GP1 recording accelerometers

The SENSR GP1L is a compact and self-contained instrument that measures accelerations in three orthogonal dimensions. Its size is 10 cm*6.35 cm* 2.89 cm (3.94''*2.50''*1.14'') and its weight is 0.232 Kg (8.2 oz). It can work at the temperature range of -4°F to 176°F. Its measurement range is of ± 6g with a resolution of 0.001g, at a sampling rate of 10 Hz. (see Figure 3-9).

The sensor has the capacity of recording data up to 40 days. It comes with an internal signal processing module with the ability of calculating and recording automatically 16 different statistics related to peak and average response. Also the sensor can provide direct identification of the frequency content of the recorded signal through 3-axis waveforms. (http://www.sensr.com/)

Figure 3-9 GP1 Sensor used for guy cable measurements (http://www.sensr.com/)

The collected data from the Tromino sensors installed in the mast were a set of 21 synchronized velocity time histories: 7 sensors x 3 components of velocities. As mentioned above, six episodes were used for data analysis. GRILLA™ software (supplied with Tromino sensors) was used to transfer data from the sensors to a laptop computer and carry out data truncation and synchronization based on the time stamps in the individual data files (in .txt format). In total there were 12 setups in GRILLA, six of which were records taken on the mast itself and the rest related to cable measurements. It should be mentioned that during the measurements, one of sensors went out of order, so from the seven TROMINO sensors which we had at first, six of them remained operational for the AVM tests. Each cable measuring episode lasted between 4 to 6 minutes.

After pre-processing and labelling, the data were analyzed in detail using the ARTeMIS[TM] extractor (Structural Vibration Solutions A/S, 2010b) to identify the dynamic characteristics of the structure: its mode shapes and corresponding natural frequencies, and estimates of modal viscous damping ratios. The technique used for operational modal analysis in ARTeMIS is the Enhanced Frequency Domain Decomposition (EFDD) method. A brief summary of the data extraction procedure is presented here.

The first step for working with ARTeMIS extractor is to rearrange the data format and provide general information on each record obtained from the GRILLA software. The code contains the duration of the measurements and the geometry of the measurement layout by defining the points and lines through their coordinates. In this study, the base point of the mast was taken as the fixed reference point. Figure 3-10 shows an example of this code for Setup 1.

It should be mentioned that, based on the sensor's property, it gave all data in three directions, while in this research only two directions (one horizontal (X) and one vertical (Y)) were considered, the vertical motion being measured but not treated in the study.

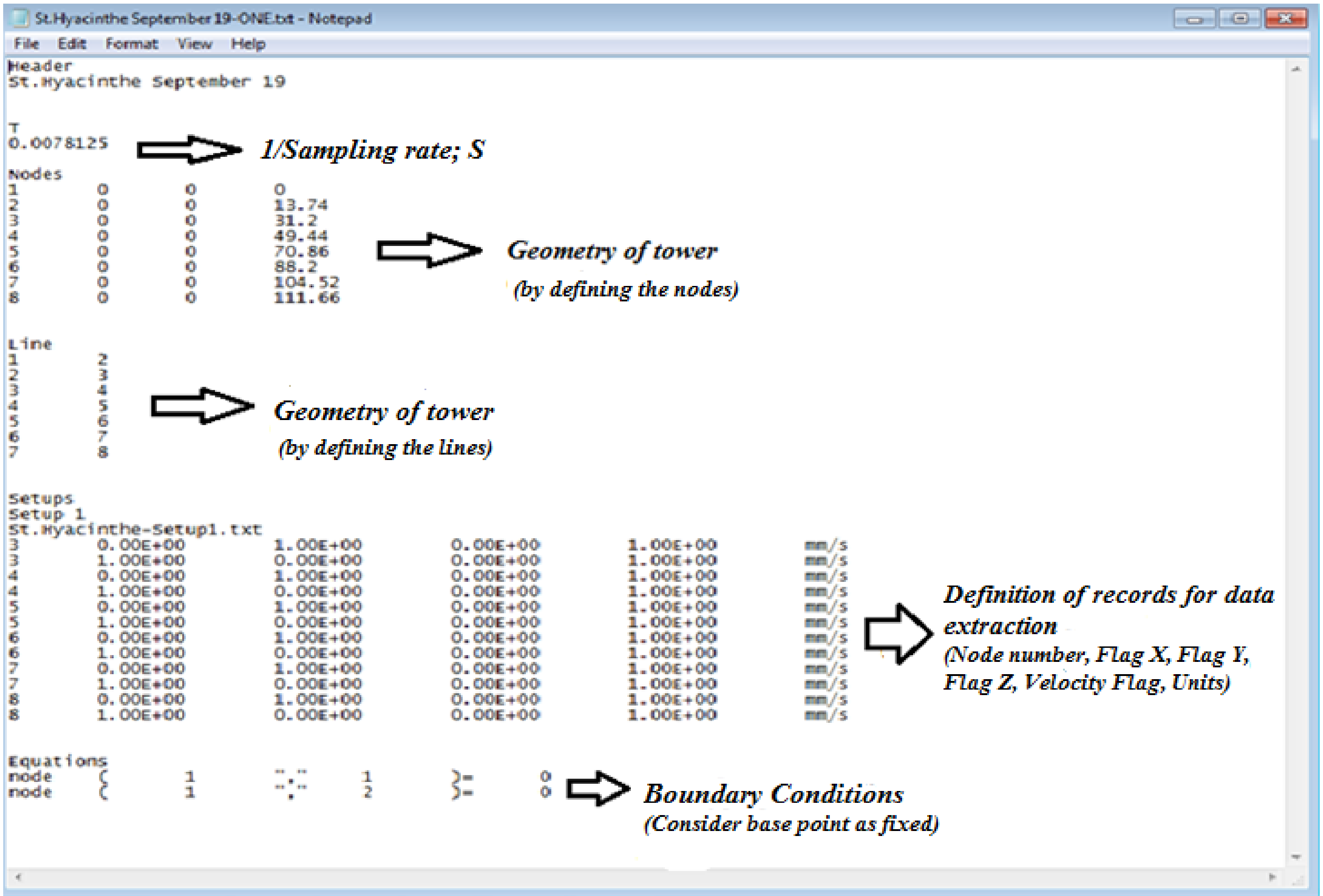

Figure 3-10 ARTeMIS setup code

Proper coding is important to accessing the data in ARTeMIS. Figure 3-11 shows one sample of the 12 different measurement setups represented in ARTeMIS. In the main window the power spectral density function shows the level of energy contained in the records as a function of frequency. The energy within the specific frequency range can be obtained by integrating the power spectral density at that specific frequency range.

One of the simplest methods for modal identification is the peak-picking method. The concept of this method is based on the fact that, generally, assuming white noise excitation, the spectral density function of the response reaches peak values at frequencies corresponding to the natural frequencies of the structure.

There are two methods for selecting the peak points on the frequency response functions: one is automatic (by software) and one is done by the user by moving the cursor on the curve and clicking. It should be mentioned that guyed masts have typically several closely-spaced modes and data must be analyzed with great care to select significant vibration modes; therefore, the second method was selected.

As it was shown in Figure 3-11 selecting each peak point gives the important information such as natural frequency and damping ratio for each mode. Based on the considered frequency range, the best frequency can be selected by the user, taking into account other indicators like the shift in phase angles and apparent damping levels.

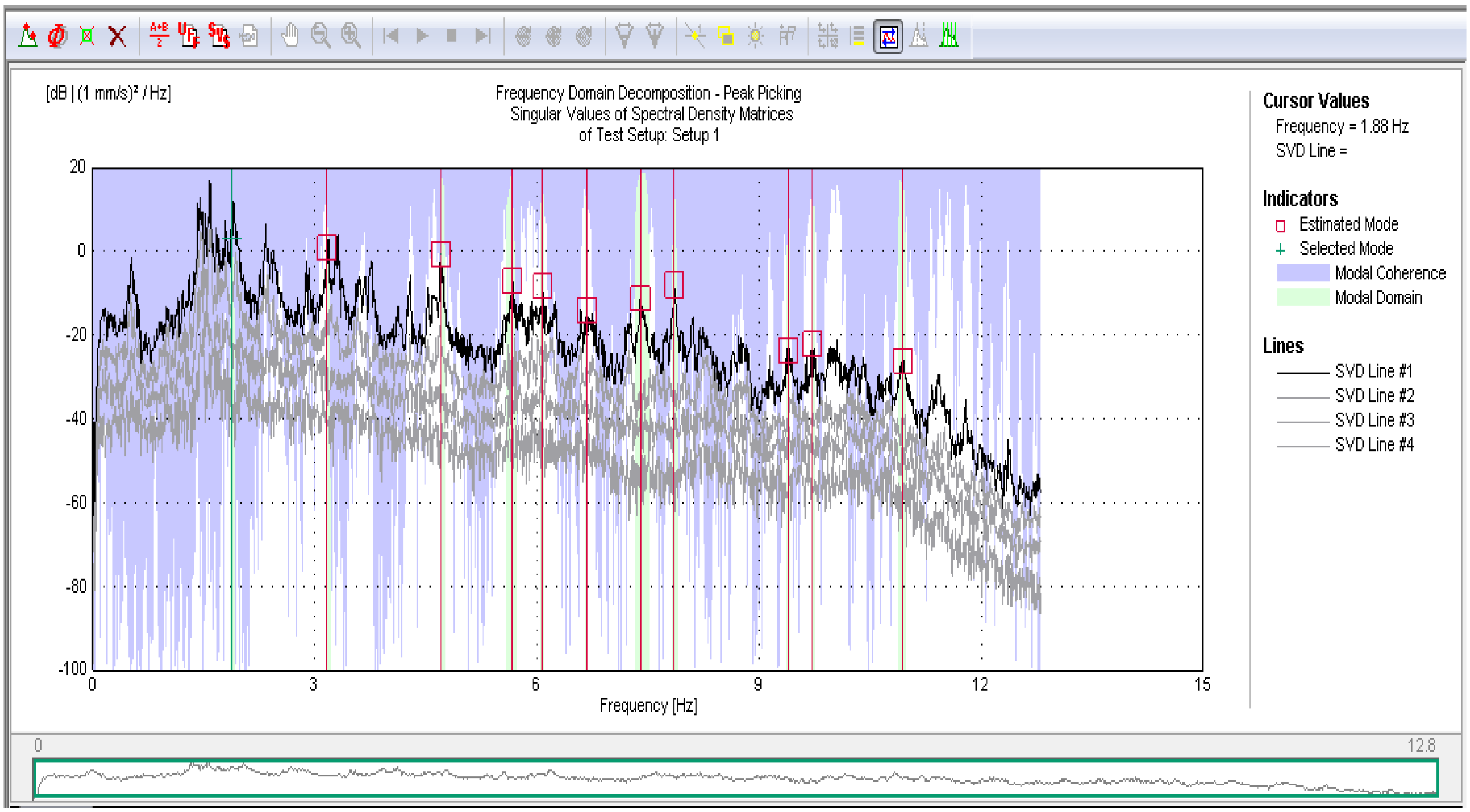

Figure 3-11 ARTeMIS extraction by frequency domain decomposition

After studying all 6 setups for the mast the best three lower frequency mode shapes of the mast were selected, as shown in figure 3-12.

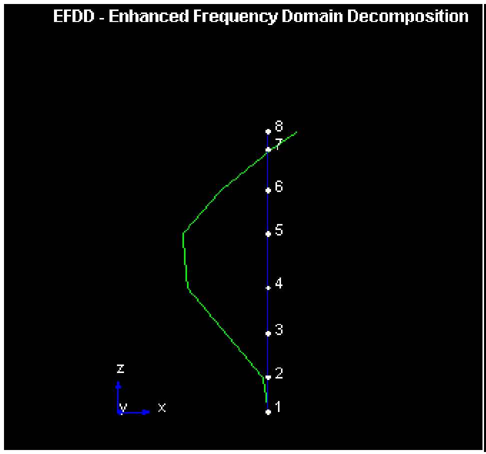

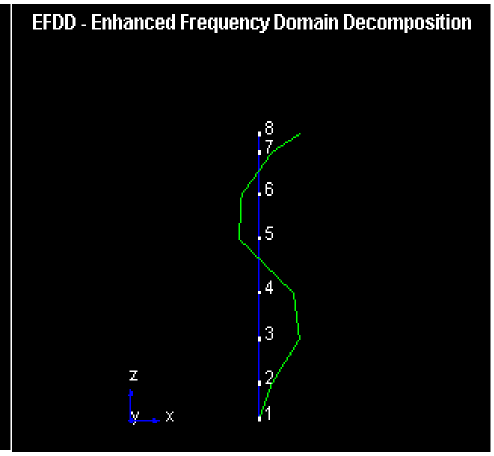

a) Mode shape 1 (f_1=1.5 Hz) *b) Mode shape 2 (f_2=1.9 Hz)*

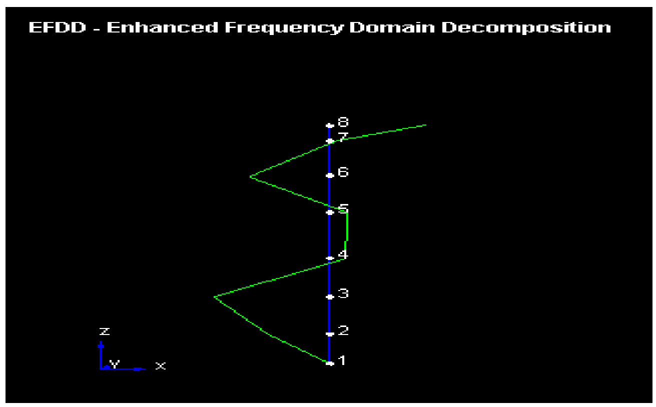

C) Mode shape 3 (f_3=2.4 Hz)

Figure 3-12 Three lowest-frequency mode shapes of the mast from the experiment extracted by ARTeMIS

The same tool was used for processing the acceleration time histories collected for the six individual cables. The results are discussed next.

3.2. Results

Considering the limited number of available sensors and their spatial distribution, it was possible to identify the first (lowest) three horizontal modes of the mast and the fundamental mode of each tested guy wire. The variability of the results reported in Table 3-1 stems from the averaging of the results obtained from the six different recording episodes analyzed. It is seen that the natural frequencies are reasonably consistent for the six episodes with a maximum coefficient of variation of about 5%. Damping estimates, however, are very inaccurate. The main conclusion here is that equivalent modal viscous damping is in the order of 0.5% for the three modes, considering that actual damping mechanisms in the structure are far from viscous, owing to friction in connections. Small aerodynamic damping is also a factor. Considering the low amplitude of ambient vibrations, these results appear reasonable and it is anticipated that damping levels under strong ground motion should be much larger (recall that 2% viscous damping has been used in the numerical models for seismic analysis).

The fundamental frequency of each cable was identified to determine an estimate of the guy wire tensions in view of updating the finite element model of the tower. Temperature was also recorded as this is an important parameter when calculating cable tensions. The damping value extracted by ARTeMIS is also indicated but these results are not deemed very accurate in the sense that their variability is large (50% to 100%) according to Table 3-1. The cables are numbered from top to base, with the longest cable having the lowest natural frequency. Cable 6 which represents the shortest set of cables has a relatively large pretension and it was not possible to identify clearly its natural frequency from the measured records, so experimental results are not available (NA).

Table 3-1 Mast natural frequencies and damping ratios

Mode	**Frequency from Experiment**	**Damping**	**Frequency from nominal FE model**
	Hz	**%**	**Hz**
1	1.5 ± 0.06	0.35 ± 0.17	1.8
2	1.9 ± 0.10	0.43 ± 0.26	2.1
3	2.4 ± 0.14	0.48 ± 0.50	2.5

Table 3-2 Cable frequencies and damping ratios

Nominal cable properties					Frequency from Experiment (Hz)	Damping ratio (% viscous)	Frequency from nominal FE model (Hz)	Taut string frequency (Hz)
#	Stay elevation (m)	L_c (m)	A (cm^2)	W (kg/m)				
1	104.14	133.68	1.22	0.98	0.51	1.1	0.538	0.55
2	87.88	119.11	2.18	1.76	0.57	0.05	0.534	0.54
3	65.13	109.57	1.51	1.22	0.67	0.9	0.596	0.58
4	49.28	63.21	2.55	2.07	0.87	0.7	0.95	1.02
5	32.00	50.93	1.51	1.22	1.08	0.29	1.22	1.23
6	13.72	41.94	1.22	0.98	NA	NA	1.54	1.75

Tables 3-1 and 3-2 also indicate numerical results for the natural frequencies obtained from a “nominal” finite element model of the mast in which the nominal design cable tensions were considered. The two last column of Table 3-2 indicates the theoretical taut string frequencies using the nominal cable properties but with a corrected length to account for elastic deformations. As expected, the natural frequencies of the cables obtained from the FE model are slightly smaller than the taut string frequencies (with differences in the order of 5% maximum), the latter serving as upper bound reference values. Normally, assuming that thermal effects are not significantly different in the cables, the experimental frequencies should be lower than the artificially constrained FE model frequencies. This is verified for cables #1, 4 and 5. However, the experimental frequencies obtained for cables #2 and 3 are not consistent with the other results. This is a clear indication that the cable tensions in these two cables are actually larger than the design values: it was verified with the tower owner that tensions were readjusted in those cable clusters following the severe January 1998 ice storm that had induced unserviceable twists in the tower top portion. However, the actual values of the adjusted tensions were not known when the model was created (the geometric adjustments were based on the overall deformation of the mast).

As the AVM tests were done during a sunny day from morning to afternoon, the ambient temperature varied significantly during the day. For the purpose of comparison of the experimental results with the numerical simulations, the ambient temperature was considered constant at 24°C. The nominal finite element model of the tower (created at 20°C) was therefore based on design cable tensions adjusted to 24°C. At this stage, the added lumped masses due to the presence of antennas and the continuous mass of the transmission lines running from the antennas to the ground telecommunication equipment shelter had not been included in the model, so it was anticipated that the measured natural frequencies would be overestimated by the numerical eigenvalue analysis.

Although the measured natural frequencies appear to agree reasonably well with the numerical results, especially for the guyed mast as a whole, the cable frequencies show more differences which indicate that the numerical model could be further adjusted by considering the cable tensions obtained from frequency extraction instead of the nominal tensions at 20°C. The average cable tensions (T_{av}) were approximately determined using the fundamental frequency equation of a taut string (out-of-plane symmetric mode):

$$T_{av} = 4mL_c^{\ 2} f^{\ 2} \qquad (2)$$

where m is the mass per unit length, L_c is the chord length and f the natural frequency. Three values were found for each cable since three sensors per cable were installed. There were some temperature differences between the top and bottom cable sensors and also during the measuring episodes so their average temperature was considered when calculating individual cable tensions. Table 3-3 indicates the calculated cable tensions and corresponding average temperatures. The last column in Table 3-3 gives the taut string tension value calculated with Equation (2) using the nominal model data at 20°C, for comparison it is seen again that the calculated tensions for cables #2 and 3 are significantly larger than the nominal values since these cables have been re-tensioned. The results in Table 3-3 indicate significant tension relaxation in the field (in the order of 10-25%) compared to nominal tensions used in the FE model based on design information except for cables 2 and 3.

Table 3-3 Calculated cable tensions for average temperature

Cable	**Average cable temperature**	**Calculated tension**	**Nominal tension at 20°C**
	(°C)	**(kips/kN)**	**(kips/kN)**
1	24	4.19/18.6	4.71/20.95
2	25	7.33/32.6	6.47/28.78
3	26.5	5.97/26.6	4.4/19.57
4	27	5.63/25	7.66/34.07
5	31	3.32/14.8	4.3/19.13
6	30	NA	4.75/21.13

At this stage, the FE model was updated with the calculated cable tensions based on field frequency measurements: since no reliable measure was available for cable #6, its nominal design value was unchanged in the model. A new eigenproblem was solved and the new natural frequencies for the first three mode shapes of the guyed mast and the fundamental mode of the cables are compared again with the experimental results in Tables 3-4 and 3-5.

It is seen in Table 3-4 that adjusting the cable tensions of the numerical model is very important to represent the realistic natural frequencies of the mast. The FE model is still expected to yield larger frequencies than those measured, considering the model simplifications (rigid base and cable tension estimates based on taut string theory, nominal properties for all components), and the variability of the order of 5% for the longest cable is deemed acceptable.

Table 3-5 indicates that the cable fundamental frequencies predicted numerically are improved by model updating but a significant difference is still found for the fundamental mode of the longest cable (Cable #1) and the numerical model underestimates the frequency. It should be emphasized that this cable is relatively slack compared to others and that its attachment point to the mast is actually more affected by the mast ambient motion than tauter and shorter cables. The top cluster is comprised of cable pairs (it is connected to an outrigger) so it is expected that the effects of nonlinear tension variations induced by temperature differences and geometric effects will be exacerbated when compared to single cables. Moreover, longer and slacker cables do not behave like the simplified elastic taut string model used to relate the cable tension to its fundamental frequency. Although analytical expressions exist to calculate natural frequencies of sagging elastic cables (Irvine, 1981), they have not been used here. Extraction of the fundamental frequency can also proceed with the comparison of higher mode frequencies, but this was outside the scope of our study. Overall, the accuracy range obtained with the simplified method was deemed sufficient (see Table 3-7).

Table 3-4 Comparison of the updated numerical model and the experiment for the guyed mast

Mode	Frequency Updated FE model (Hz)	Frequency Experiment (Hz)
1	1.59	1.5 ± 0.06
2	2.01	1.9 ± 0.10
3	2.46	2.4 ± 0.14

Table 3-5 Comparison of the updated numerical model and the experiment for the guy cables

Cable	Frequency Updated FE model (Hz)	Frequency Experiment (Hz)
1	0.40	0.52
2	0.56	0.57
3	0.67	0.67
4	0.82	0.87
5	1.06	1.08
6	1.51	NA

Figures 3-13 to 3-16 compare the three fundamental mode shapes of the mast and first fundamental mode shape of each cable from the experiment (as measured with the

Tromino and GP1 sensors and extracted by ARTeMIS) and those obtained from the modified finite element models using ADINA. ARTeMIS mode shapes look rather crude given the small number of data points available, contrary to finite element simulations. The importance of dynamic cable mast interactions is also visible on the calculated mode shapes.

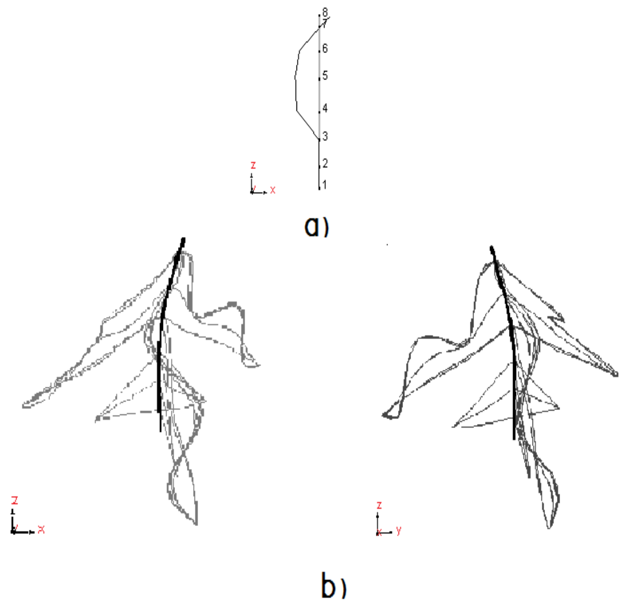

Figure 3-13 Comparison of mode shape 1 a) from ARTeMIS (experiment); b) from adjusted FE model.

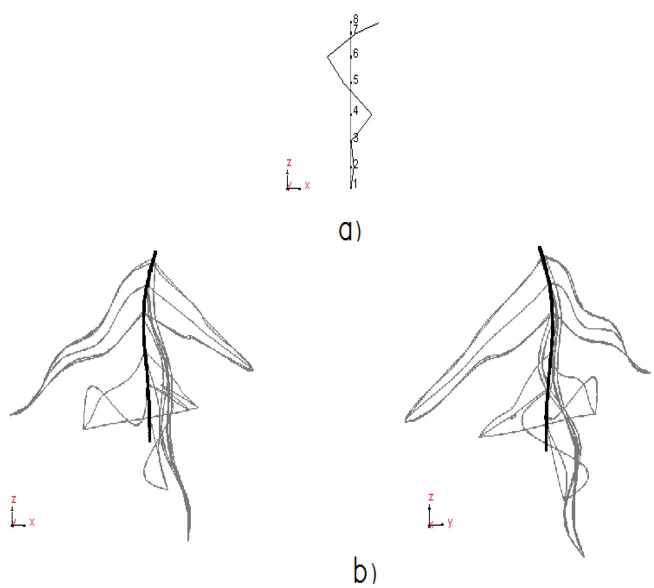

Figure 3-14 Comparison of mode shape 2 a) from ARTeMIS (experiment); b) from adjusted FE model.

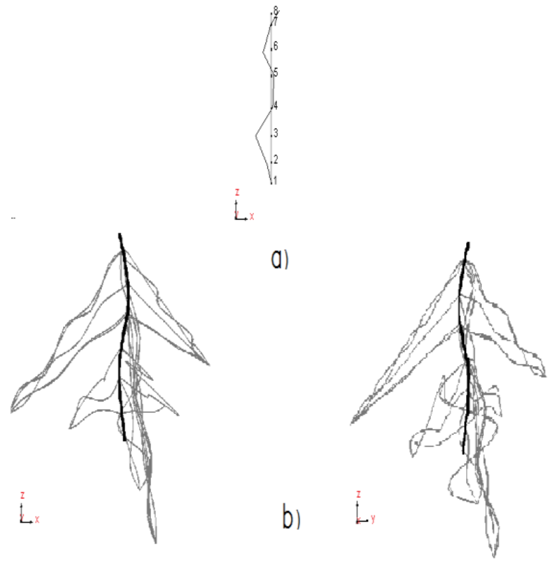

Figure 3-15 Comparison of mode shape 3 a) from ARTeMIS (experiment); b) from adjusted FE model.

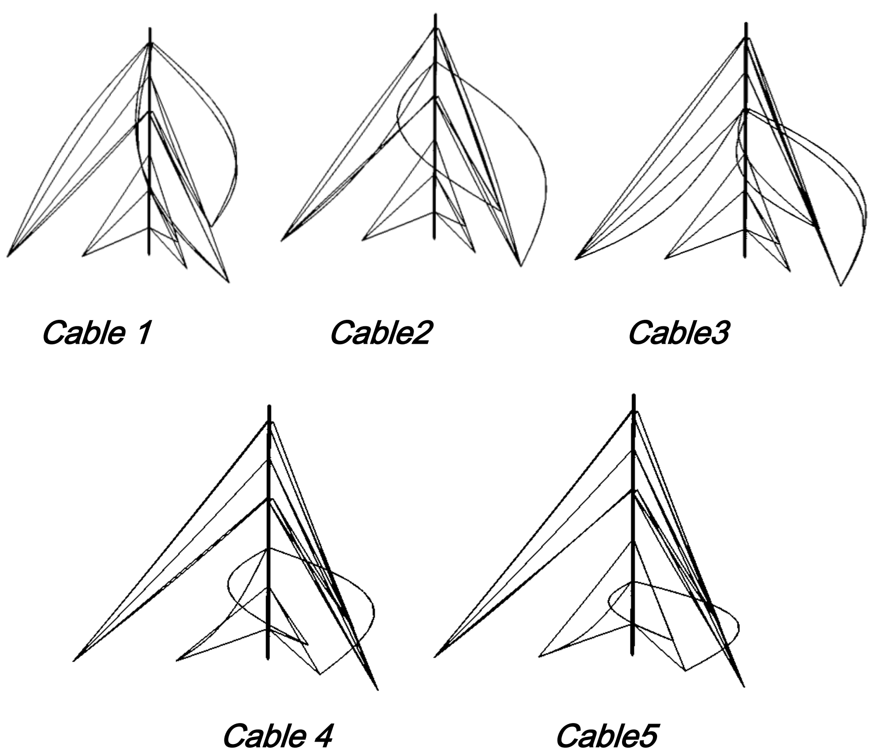

Figure 3-16 Fundamental mode shapes of the guy cables from numerical model

In the modified numerical model, different temperatures are considered for the different cables and the mast. In practice, temperature records would not be available at various positions in the mast and on each cable, so it is interesting to observe the variability in the calculated frequencies when a single value is selected as reference temperature, by considering the average temperature (between top and bottom sensing points) of each cable as a temperature of the whole of the structure. A range of natural frequency values is therefore obtained, as indicated in Tables 3-6 and 3-7. It is seen that this procedure yields results very similar to the "nominal" FE analysis model, which were presented in Tables 3-1 and 3-2. This further stresses the importance of accounting for the variability in temperature and cable tensions when predicting the natural frequencies of tall guyed masts.

Table 3-6 First three mode shapes of the guyed mast.

Mode	Frequency -Numerical model (Hz)	Frequency -Experiment (Hz)
1	1.80 - 1.83	1.5 ± 0.06
2	2.09 - 2.11	1.9 ± 0.10
3	2.40 - 2.52	2.4 ± 0.14

Table 3-7 Fundamental frequencies of the guyed cables

Cable	Frequency -Numerical model (Hz)	Frequency -Experiment (Hz)
1	0.40 - 0.54	0.52
2	0.53 - 0.56	0.57
3	0.58 - 0.68	0.67
4	0.81 - 0.96	0.87
5	1.06 - 1.22	1.08

According to the above results, it can be concluded that ambient vibration tests on the guyed mast have provided valuable data for the validation of the detailed finite element models used for nonlinear dynamic analysis. Fundamental frequencies of the cables are identified and average cable tensions are calculated on the basis of the extracted frequencies. The results indicate that detailed models provide reasonably accurate predictions of fundamental frequencies of the cables and excellent predictions for the three lowest frequency modes of the guyed mast. Also cable tensions are a very influent parameter on the global mast frequencies. The study underlines the importance of considering a range of realistic tension values in numerical models to obtain bounded values of natural frequencies and dynamic response.

All the numerical results presented up to now were obtained without considering the weight of the antenna and transmission lines. The eigenvalue analyses were then repeated with these additional lumped weights and masses and the results are compared in Tables 3-8 and 3-9.

Table 3-8 Comparison of mast natural frequencies with and without considering the weight of antennas and transmission lines

Vibration Mode	**Natural frequency (Hz)**			
	Experiment	**Nominal FE model at 20°C**	**Updated FE model (bare mast) at 24°C**	**Updated FE model (with equipment) at 24°C**
1	1.5 ± 0.06	1.80	1.59	1.57
2	1.9 ± 0.10	2.11	2.01	1.99
3	2.4 ± 0.14	2.52	2.46	2.46

Table 3-9 Comparison of guy cables natural frequencies with and without considering the weight of antennas and transmission lines

Nominal cable properties					**Fundamental frequency (Hz)**			
#	**Stay elevation (m)**	**L_c (m)**	**A (cm^2)**	**W (kg/m)**	**Experiment**	**Nominal FE model at 20°C**	**Updated FE model (bare mast) at 24°C**	**Updated FE model (with equipment) at 24°C**
1	104.14	133.68	1.22	0.98	0.51	0.538	0.407	0.547
2	87.88	119.11	2.18	1.76	0.57	0.534	0.561	0.567
3	65.13	109.57	1.51	1.22	0.67	0.596	0.672	0.672
4	49.28	63.21	2.55	2.07	0.87	0.95	0.825	0.866
5	32.00	50.93	1.51	1.22	1.08	1.22	1.066	1.07
6	13.72	41.94	1.22	0.98	NA	1.54	1.514	1.54

A comparison between the experimental and numerical results does not show any significant effect on the natural frequencies of the global structure (Table 3-8) but there is improved agreement for the cable frequencies when the weight and mass of the equipment is included in the FE models, especially for Cable #1 which is attached above the mast portion where there is a concentration of antenna drums (see Figure 3-2a).

It may seem counter-intuitive that the updated finite element model with added equipment shows cable frequencies higher than the bare mast model. In fact, Table 3-8 shows this trend is not observed for the whole mast, but only for individual guy cables (in Table 3-9). The explanation of higher cable natural frequencies lies in the fact that when initial cable tensions are adjusted in the mast models with additional equipment, the adjusted tensions are slightly higher to compensate for the added static deflection under weight.

Chapter 4 SEISMIC ANALYSIS OF THE TESTED GUYED MAST

As mentioned in chapter 1, several studies have been done to predict the seismic response of guyed telecommunication structures or to develop simplified analysis procedures more amenable to design practice. However, these studies were all based on nominal tower properties, taken from design drawings. There is a concern related to the variability in guy cable tensions in the field, compared to nominal design values specified at a reference temperature; this aspect is addressed here.

This part of the research was also summarized in a conference paper co-authored by Mahtab Ghafari Osgoie, Ghyslaine McClure, Xiao Hong Zhang, and Daniel Gagnon, and titled "Assessing the variability of seismic response analysis of a tall guyed telecommunication tower with ambient vibration measurements", to be presented in September 2012 at the 15th World Conference on Earthquake Engineering, in Lisbon, Portugal. The following presents the manuscript with minor changes to fit into the general format of the thesis. According to 15WCEE's publication copyright policy, the author has permission to publish the manuscript as is in her thesis.

Following the previous chapter, by calculating the cable tension and modifying the numerical model accordingly, the variability of the seismic response of the tower is examined by considering three different finite element models of the structure, namely: a FE model with nominal design properties at 20°C, and two FE models modified to a include realistic cable tensions based on the AVM test results, at 24°C. The difference between these two modified FE models lies in the addition of the weight of antennas (mostly located in the vicinity of Cluster #2) and transmission lines in the more accurate model while the other one represents the bare mast structure. As indicated in Table 4-1, the presence of mast attachments has little effect on reducing the initial cable tension, except in the longest cable (Cable #1) where the reduction is significant.

Although cable tension variability was not found to significantly affect the lower frequency modes of the mast (see chapter 3), it is expected to affect the mast quasi-static response.

Table 4-1 Initial cable tensions prescribed in the FE models for seismic analysis

Cable #	Initial cable tension(kN)		
	Nominal FE model at 20°C	**Updated FE model (bare mast) at 24°C**	**Updated FE model (with equipment) at 24 °C**
1	12.7	17.8	12.3
2	29.4	32.0	31.9
3	20.4	25.8	25.7
4	29.1	21.6	21.4
5	18.3	13.7	13.6
6	15.7	15.2	15.2

The seismic analysis proceeds with three classical earthquakes: Imperial Valley, El Centro, (1940), Park field (1966) and 1952 Kern County, Taft, (1952) as mentioned in chapter 3. The main horizontal component of the accelerogram is aligned in a principal direction of the mast (X direction, along one set of guy cables) and the corresponding vertical accelerogram (Z direction) is prescribed as well as the other horizontal component (Y direction). This input is assumed to be synchronous at each ground support point (i.e. at all cable ground anchor points and at the base of the mast), assuming all ground support points are pinned to the ground. Each earthquake record has peak horizontal and vertical ground acceleration (PGA), peak ground velocity (PGV) and peak ground displacement (PGD) as indicated in Table 4-2.

Table 4-2 El Centro, Parkfield, Taft earthquake components and peak values

Earthquake	Component	PGA(g)	PGV(cm/s)	PGD (cm)
El Centro	X	0.313	29.8	13.32
	Y	0.215	30.2	23.91
	Z	0.205	10.7	9.16
Parkfield	X	0.442	24.7	5.15
	Y	0.367	21.8	3.83
	Z	0.138	6.9	2.66
Taft	X	0.178	17.5	8.99
	Y	0.156	15.3	9.25
	Z	0.109	6.6	4.56

It should be mentioned that these three classical earthquakes were selected because of their characteristics. El Centro earthquake has a wide and rich range of frequencies and several episodes of strong ground motion. Parkfield earthquake presents a single strong pulse loading with dominant lower frequencies. Finally, Taft earthquake represents an earthquake with high frequency content and strong shaking with a relatively long duration. The computed time histories of the mast displacements at the elevation of the bottom cluster attachment point (13.72 m) and at the top cluster (103.94 m) were studied under all three earthquakes for three different FE models: the nominal FE model, the modified FE model with adjusted tension without attachments, and the modified FE model with antennas and transmission lines. Figures 4-1 and 4-2 present the displacement results due to the El Centro earthquake. The displacement reported in the Y direction simply corresponds to the transverse orthogonal direction to X (main input direction). As expected, the ground displacements are amplified at top cluster elevations compared to the bottom. In keeping with the natural frequency results reported earlier, it is seen that the response predicted with the added weight of antenna drums and transmission lines is actually closer to that predicted by the nominal model.

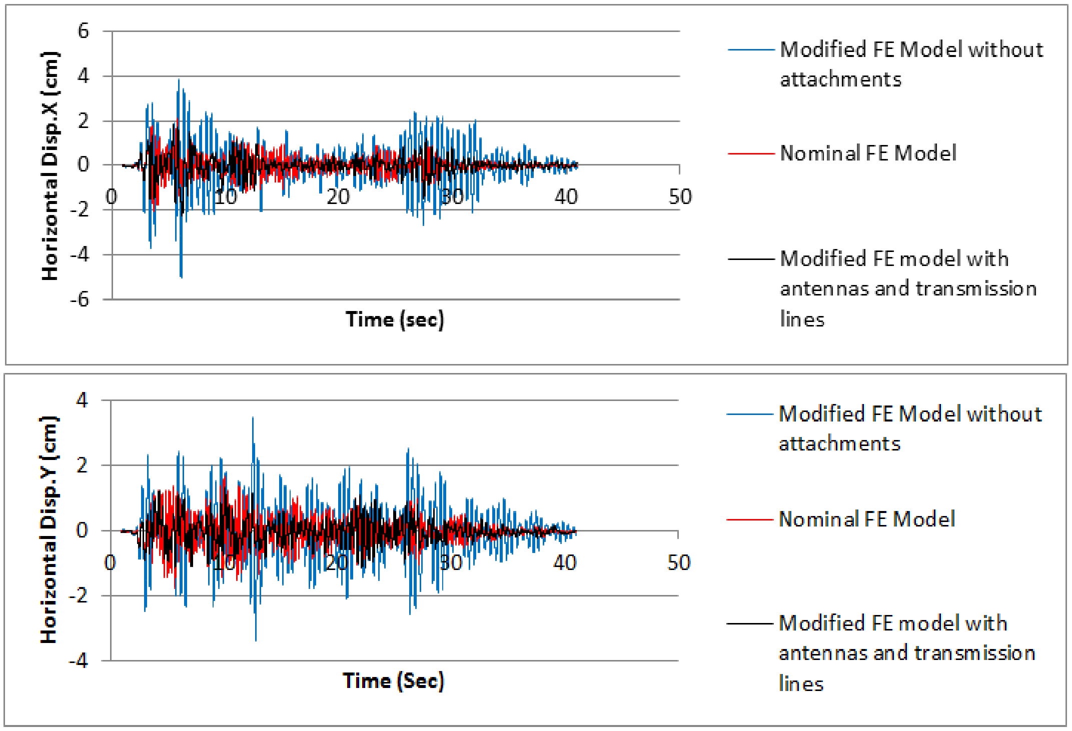

Figure 4-1 Numerical prediction of horizontal displacements of the mast at cable cluster elevation #6 (Bottom cluster) along X (along main input) and Y (transverse to main input)

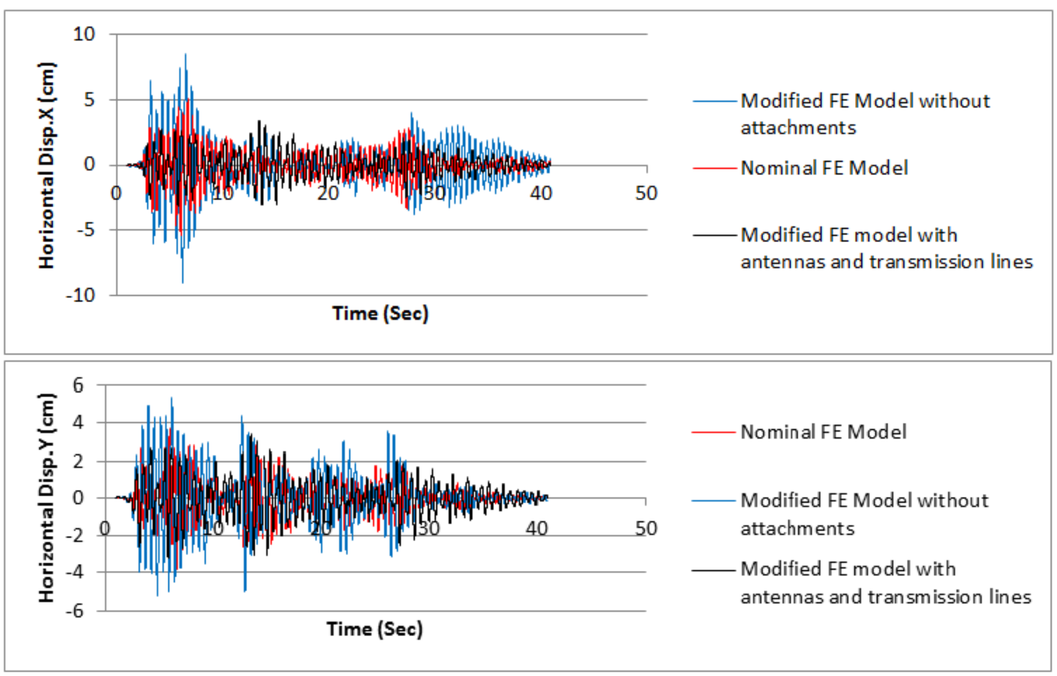

Figure 4-2 Numerical prediction of horizontal displacements of the mast at cable cluster elevation #1 (Top cluster) along X (along main input) and Y (transverse to main input)

Figure 4-3 shows the dynamic cable tension in the top cluster (Cable #1): in this case, the bare mast model is far from the measured frequency and its predictions are not expected to be accurate. In reality, the nominal design guy wire pretensions used in analysis are practically never achieved when the mast is constructed. This does not pose any practical problem as long as the overall structure stays within prescribed tolerances and fulfils its functionality requirements. As these structures are exposed to the natural environment, wire tensions will vary considerably with ambient temperature, direct exposure to sunlight, and ambient climatic loads (wind and ice) and the variation of the wire tensions will influence their seismic response.

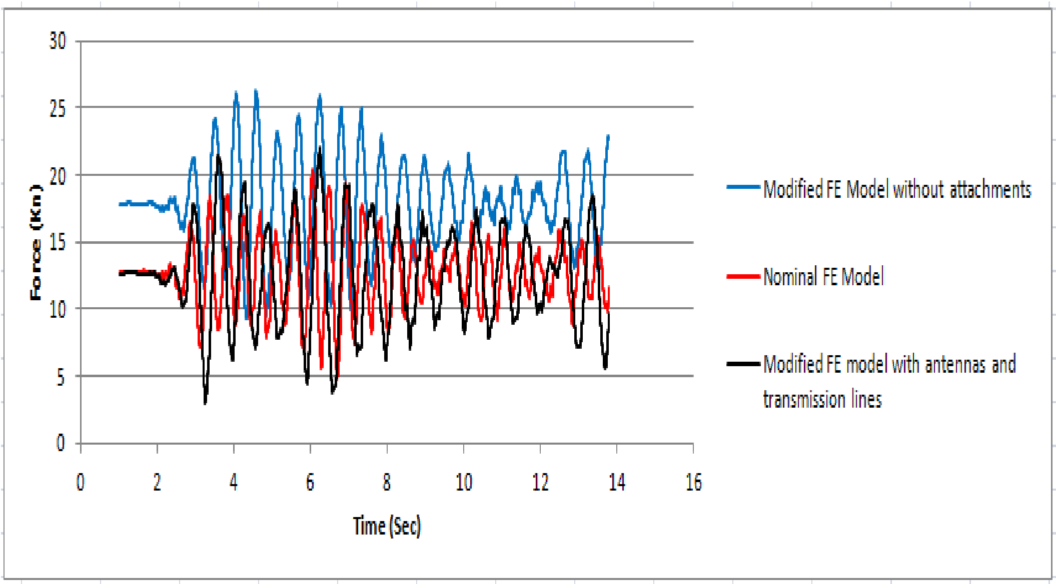

Figure4-3 Cable tension of Cable #1 aligned with the main input ground motion

The comparisons of the dynamic cable tensions for the other guy cables are also presented in Figures 4-4 to 4-8 below. These results emphasize the importance of considering the proper cable tensions (Nominal vs. Modified models) while there is little difference between the two adjusted models with and without attachments. It should be recalled that the antenna drums are more concentrated on the top part of the tower, between guy clusters #1 and #2, which explains their increased influence on the results for Cable #1.

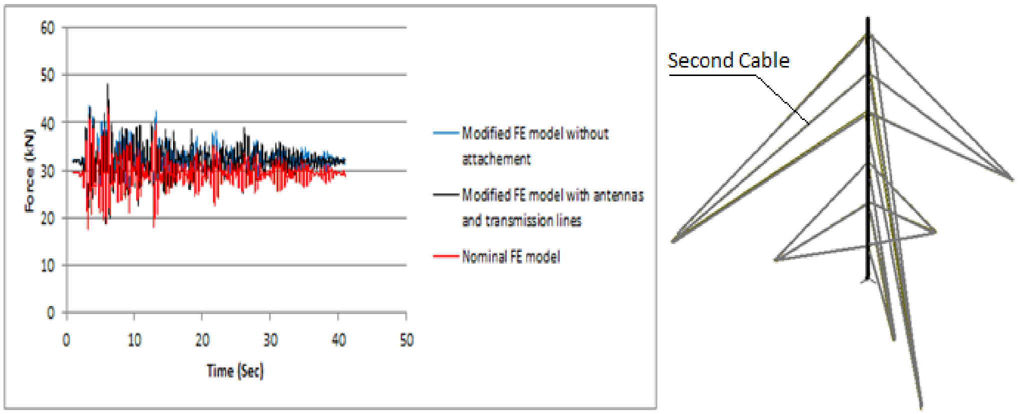

Figure 4-4 *Cable tension of Cable #2 aligned with the main input ground motion*

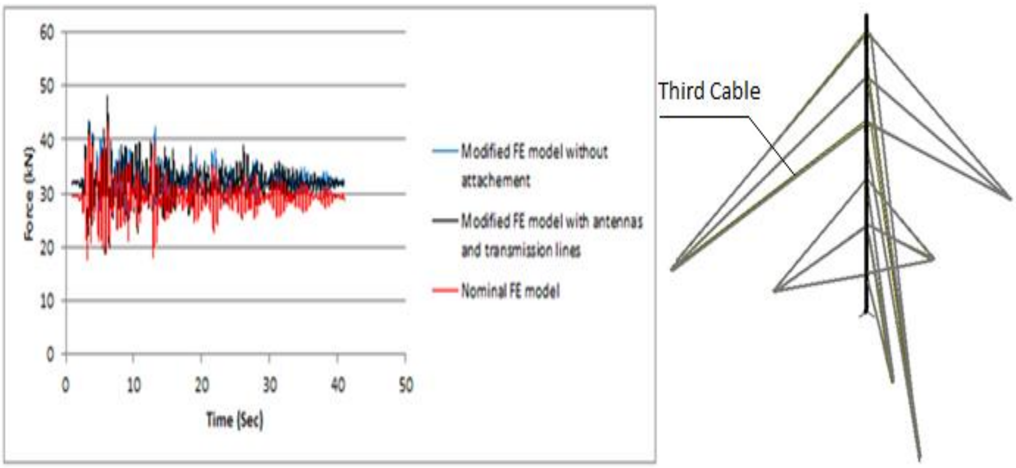

Figure 4-5 *Cable tension of Cable #3 aligned with the main input ground motion*

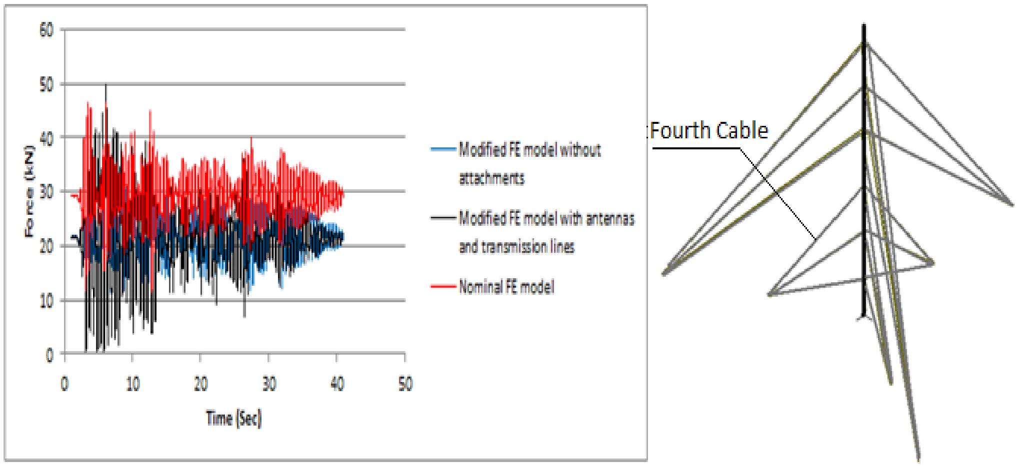

Figure 4-6 *Cable tension of Cable #4 aligned with the main input ground motion*

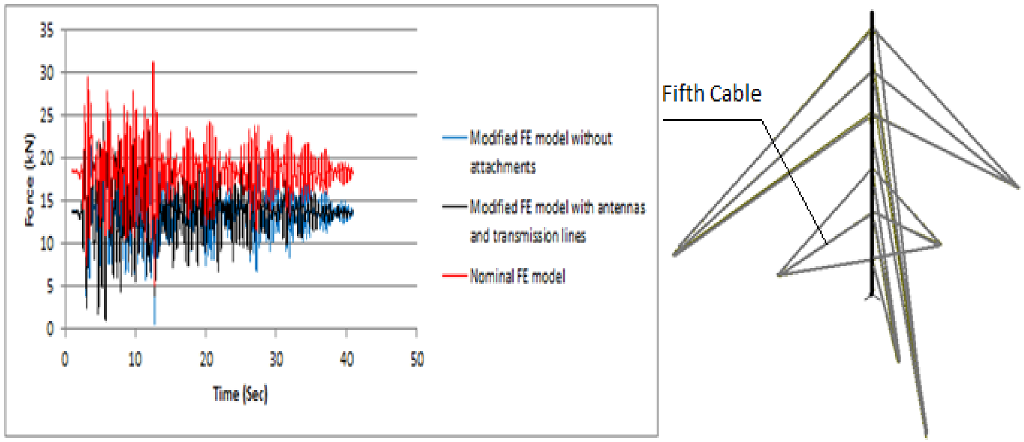

Figure 4-7 *Cable tension of Cable #5 aligned with the main input ground motion*

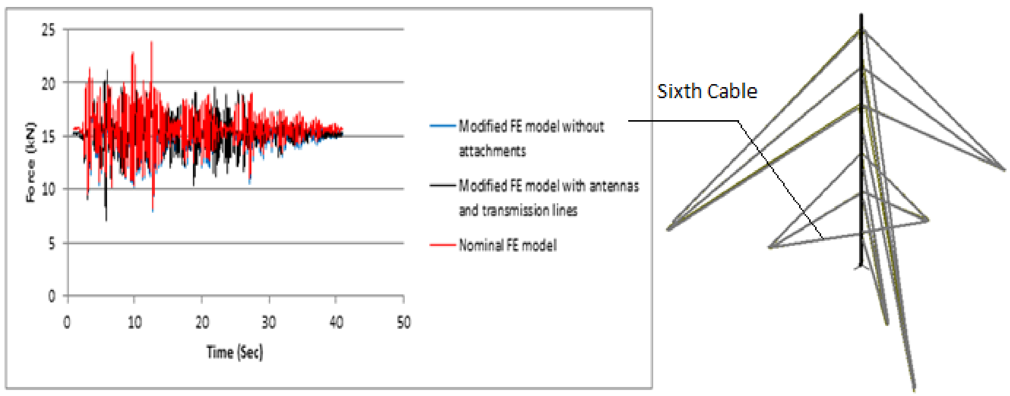

Figure 4-8 *Cable tension of Cable #6 aligned with the main input ground motion*

Figures 4-4 to 4-8 suggest that initial (static) cable tensions are a very influent parameter on the guyed mast seismic response. Predictive numerical models based on nominal parameters are deemed acceptable as long as a range of realistic tension values (within nominal tolerances) is considered. Frequency analysis of guyed masts including the uncertainty on the cable tensions will provide more realistic bounds of the structure's dominant natural frequencies and seismic response.

The results for the two other earthquakes show similar trends and confirm the strong influence of the initial cable tension. These results are presented in Appendix A for completeness.

Considering the importance of cable tension on the predicted seismic response, it was decided to study the influence of its variability from nominal design values. In CAN/CSA S37-2001(R06) (Canadian Standards Association, 2001), Section 5.1 Initial Conditions, it is mentioned that:

“*The initial condition of a structure for analysis shall be taken as that under the unfactored dead load, with the guys, if any, at their design initial tensions. In the absence of more specific information, a temperature of 10°C for sites south of latitude 55°N, and 0°C for sites north of latitude 55°N, may be used.”*

Later in clause 9.4.5:

“*Guy tension shall be measured at the anchorage. For the initial condition, as defined in Clause 5.1, guy tensions are normally set at 10% of the rated breaking strength of the strand or cable, and generally within limits of 8-15%. An initial tension tag shall be affixed to each guy assembly near the anchor where the tag can be easily observed and used by persons maintaining the guy tensions. In setting the initial guy tension, consideration shall be given to the response of the structure, including its dynamic behaviour and to variation in the guy initial tension.”*

Since the St. Hyacinthe tower is south of latitude 55°N, the temperature of 10°C is used as a reference for this part of the study. The limits of 8% and 15% of the breaking strength of each cable were considered to define the maximum range of the tension values. Also in this part of the study, a fourth earthquake record (synthetic) was added to provide an input with frequency content more realistic for the Montreal area.

Initial tension for each cable according to its rated breaking strength (RBS) was calculated for the limits of 8% and 15% at 10°C, and the nominal value was considered at 10%. Figures 4-9 to 4-14 show the calculated cable tensions for the six cables under the El Centro (1940) earthquake. It is seen that the strong influence of the initial tension is dominant for the longest cables (in the upper group) and that this influence is decreasing from Cable #1 to Cable #6. Also, the results for 8% and 10% RBS yield similar results for Cable #6. These results are confirmed by the simulations under the three other earthquakes (see Appendix A).

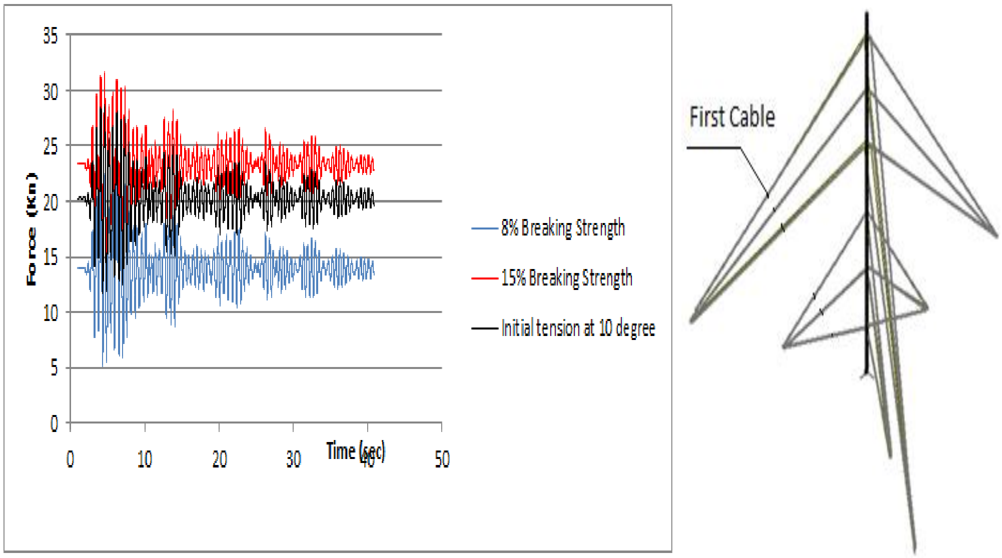

Figure 4-9   *Cable tension of Cable #1 under El Centro earthquake*

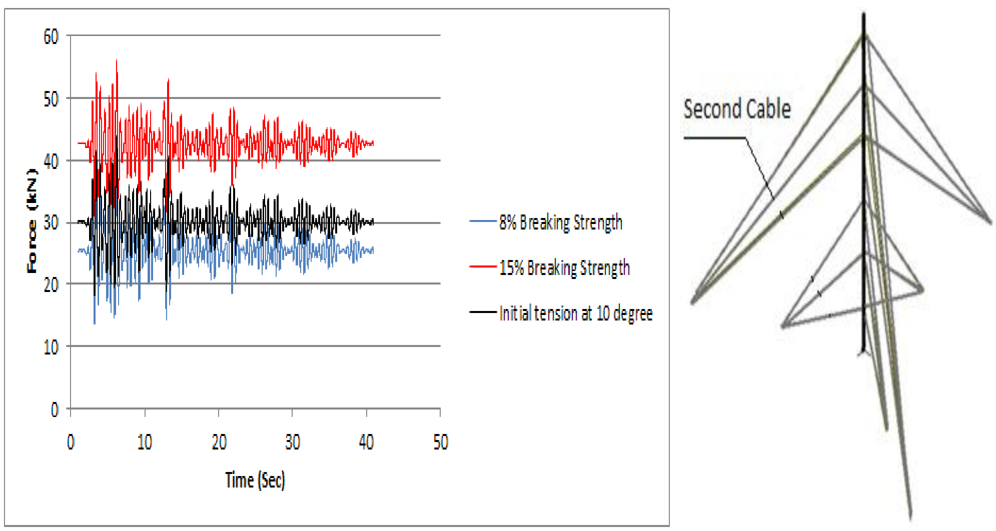

Figure 4-10   *Cable tension of Cable #2 under El Centro earthquake*

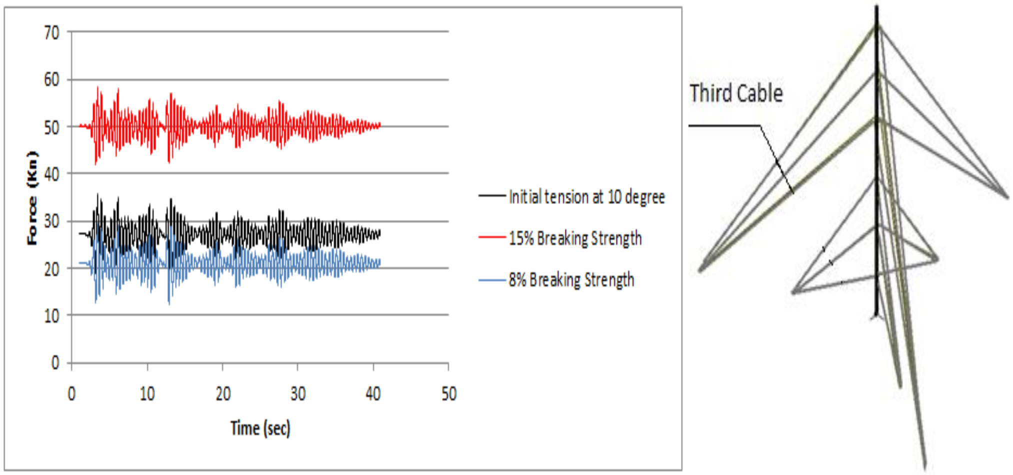

Figure 4-11 Cable tension of Cable #3 under El Centro earthquake

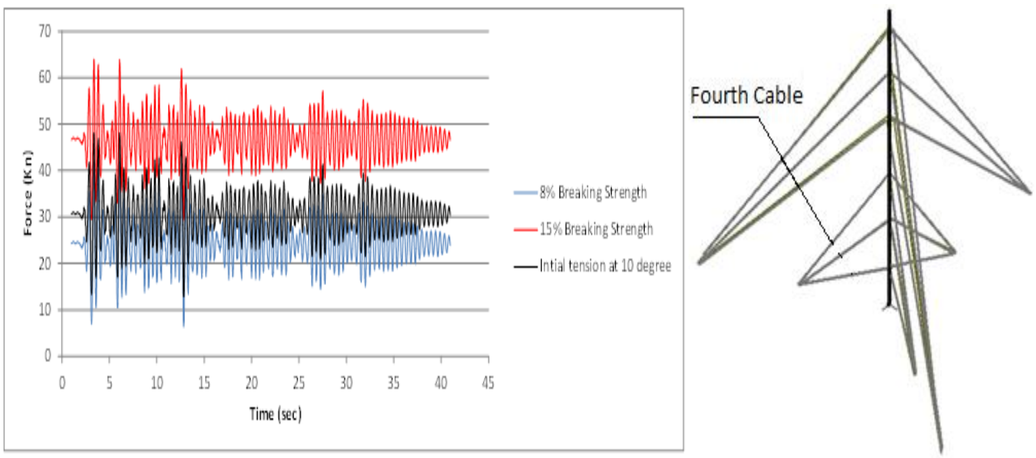

Figure 4-12 Cable tension of Cable #4 under El Centro earthquake

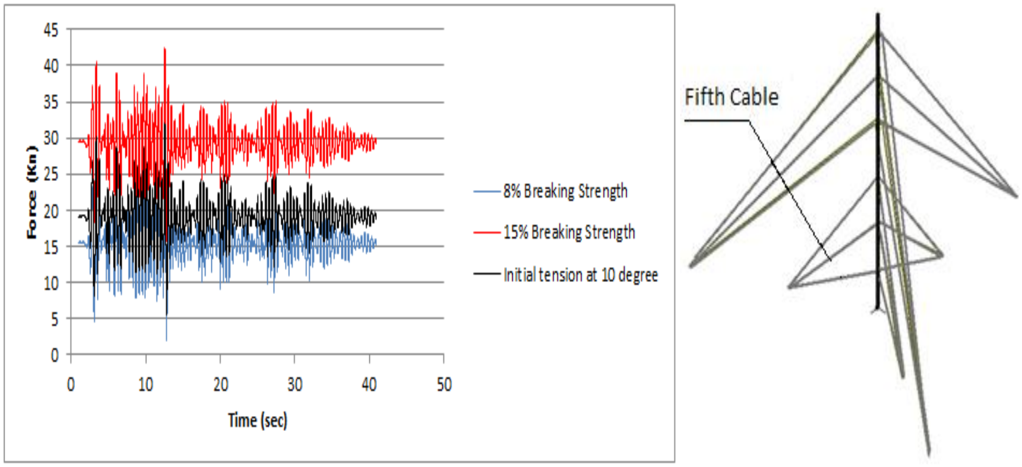

Figure 4-13 Cable tension of Cable #5 under El Centro earthquake

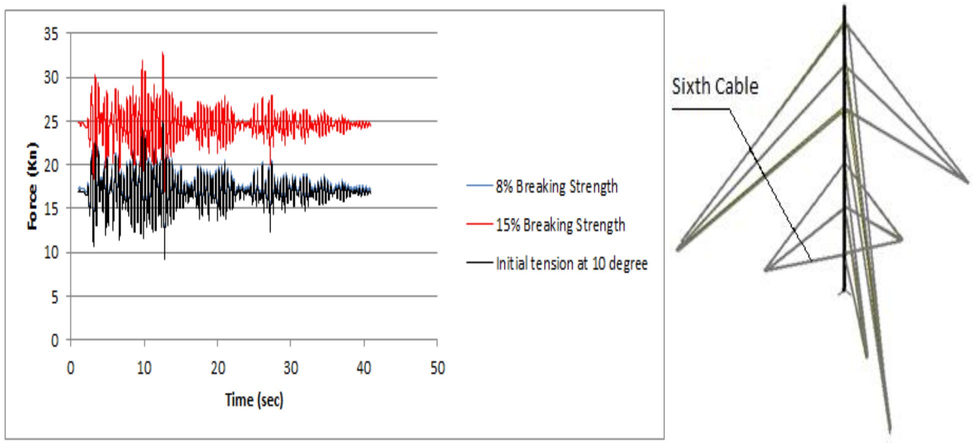

Figure 4-14　　Cable tension of Cable #6 under El Centro earthquake

The matrices below give the values of cable tension in each typical cable of a cluster when specific variations in cable tension are prescribed. In Figures 4-15 and 4-16 T_{ij} (i, j =1,2,...,6) is the tension in cable i when the tension in cable j is taken as 8% and 15% of RBS respectively. These values are obtained from static analysis on the nominal model at 10°C when the tension in cable j is prescribed at either 8% RBS, 10% or 15% of RBS. For instance in the matrix of Figure 4-15 T_{23} (21.4 kN) is the tension in Cable #2 when Cable #3 tension is prescribed at 8% RBS.

13.9	20.3	20.1	20.3	20.3	20.2
30.1	25.9	30.4	30.2	30.2	30.3
21.2	21.2	27.8	21.1	21.2	21.2
31.7	31.5	31.1	24.9	31.4	31.4
19.3	19.1	19.1	19.2	15.1	19.2
17.3	17.2	17.2	17.1	17.2	17.8

Figure 4-15　　T_{ij}: Initial cable tensions (kN) for 8% of RBS

$$\begin{bmatrix} 23.3 & 20.5 & 20.2 & 20.5 & 20.6 & 20.6 \\ 30.4 & 42.6 & 29.8 & 30.4 & 30.5 & 30.6 \\ 21.3 & 21.3 & 50.0 & 21.4 & 21.5 & 21.5 \\ 31.2 & 31.0 & 30.0 & 46.7 & 31.2 & 31.4 \\ 19.5 & 19.4 & 19.0 & 19.4 & 29.4 & 19.5 \\ 17.2 & 17.2 & 17.1 & 17.2 & 17.2 & 24.8 \end{bmatrix}$$

Figure 4-16 *T_{ij} : Initial cable tensions (kN) for 15% of RBS*

The results in Figures 4-15 and 4-16 indicate that cable tensions are not sensitive to changes in the prescribed tension in other cables tensions. There is little variability in the row entries except on the diagonal.

A similar notation is used to summarize the results of seismic analysis under the El Centro record. In figures 4-17 to 4-19 the matrices give the maximum dynamic cable tensions. In this case the 10% RBS case is also shown for completeness.

$$\begin{bmatrix} 22.8 & 29.1 & 28.2 & 29.1 & 29.0 & 28.4 \\ 44.3 & 39.3 & 44.2 & 44.2 & 43.8 & 44.1 \\ 30.1 & 29.3 & 35.5 & 30.1 & 30.1 & 30.1 \\ 49.2 & 48.4 & 48.5 & 42.8 & 47.4 & 48.2 \\ 32.2 & 32.1 & 32.4 & 32.2 & 28.9 & 32.5 \\ 25.1 & 25.0 & 25.1 & 25.4 & 25.4 & 25.9 \end{bmatrix}$$

Figure 4-17 *$T_{max\ ij}$: Maximum dynamic cable tensions (kN) for 8% of RBS under El Centro records*

31.6	28.8	28.5	28.9	29.0	29.0
44.2	56.1	43.3	44.3	44.3	44.4
29.9	29.8	58.3	30.0	30.1	30.1
48.6	48.5	47.7	64.0	48.8	48.9
32.4	32.4	32.1	32.2	42.4	32.5
25.4	25.4	25.3	25.3	32.5	32.8

Figure 4-18 $T_{max\ ij}$: Maximum dynamic cable tensions (kN) for 15% of RBS under El Centro records

22.5	29.1	28.9	29.0	29.0	29.0
44.8	39.4	44.3	44.6	44.5	44.4
30.1	30.0	35.5	30.5	30.1	30.1
49.4	48.9	49.6	42.8	48.8	48.8
32.8	33.0	32.8	32.9	28.4	32.5
25.5	25.5	25.6	25.5	25.4	25.4

Figure 4-19 $T_{max\ ij}$: Maximum dynamic cable tensions (kN) for 10% of RBS under El Centro records

With a view to better illustrate the effect of the variability of initial cable tensions on the peak dynamic tensions, Figures 4-20 and 4-21 give normalized peak tensions with respect to the 10% RBS reference under El Centro earthquake. Each value of the normalized matrix is obtained by dividing the elements of $T_{max\ ij}$ in Figures 4-17 and 4-18 by the corresponding elements of $T_{max\ ij}$ at 10% in Figure 4-19.

1.01	1.00	0.98	1.00	1.00	0.98
0.99	1.00	1.00	0.99	0.98	0.99
1.00	0.98	1.00	0.99	1.00	1.00
1.00	0.99	0.98	1.00	0.97	0.99
0.98	0.97	0.99	0.98	1.02	1.00
0.98	0.98	0.98	1.00	1.00	1.02

Figure 4-20 $T_{max\ ij}$: Normalized maximum dynamic cable tensions (kN) for 8% of RBS under El Centro records

1.40	0.99	0.99	1.00	1.00	1.00
0.99	1.42	0.98	0.99	1.00	1.00
0.99	0.99	1.64	0.98	1.00	1.00
0.98	0.99	0.96	1.50	1.00	1.00
0.99	0.98	0.98	0.98	1.49	1.00
1.00	1.00	0.99	0.99	1.28	1.29

Figure 4-21 $T_{max\ ij}$*: Normalized maximum dynamic cable tensions (kN) for 15% of RBS under El Centro records*

Figures 4-17 to 4-21 confirm that the individual cable dynamic peak tension is not sensitive to the variation of initial tensions in other cables except for cable #6 that is also influenced by variations in cable #5. Of course, this conclusion is specific to the case study at end: a relatively stiffer mast may distribute the influence of cable tension variations more evenly.

Table 4-3 compares the peak cable tensions under the El Centro record (Other results are in Appendix A) to their initial values (See figures 4-15 to 4-18) when tension in cable #1 is varied – DAF is the acronym for this dynamic amplification factor or ratio. Variations for other cables are not significantly different in trends but are less important in magnitude.

Table 4-3 Peak dynamic cable tensions under El Centro record for tension variations in Cable #1

Cable No.	Initial tension (kN)		Nominal peak tension (kN)	DAF 8%	DAF 15%	Nominal	8%/Nominal	15%/Nominal
	Static	% RBS						
1	20.2	8.08	28.6	1.64	1.36	1.41	1.16	0.96
2	30.0	10.22	43.9	1.52	1.32	1.46	1.04	0.9
3	21.0	10.13	29.6	1.28	1.17	1.41	0.91	0.83
4	30.6	8.86	48.1	1.72	1.37	1.57	1.09	0.87
5	19.1	9.21	32.1	1.91	1.44	1.68	1.14	0.86
6	16.9	10.32	25.1	1.46	1.32	1.48	0.98	0.89

These results show that the variations in peak cable tensions are in the order of ±16% compared to peak tensions for the nominal model. The results for the three other earthquake records are very similar (See Appendix A).

The effect of the variability of initial cable tensions on the horizontal displacement of the mast along the X and Y directions under the El Centro earthquake was also studied. The results are summarized in Figures 4-22 to 4-27 showing the range of displacements when the initial tension of one cable at a time is varied, while the other cables are at their nominal values.

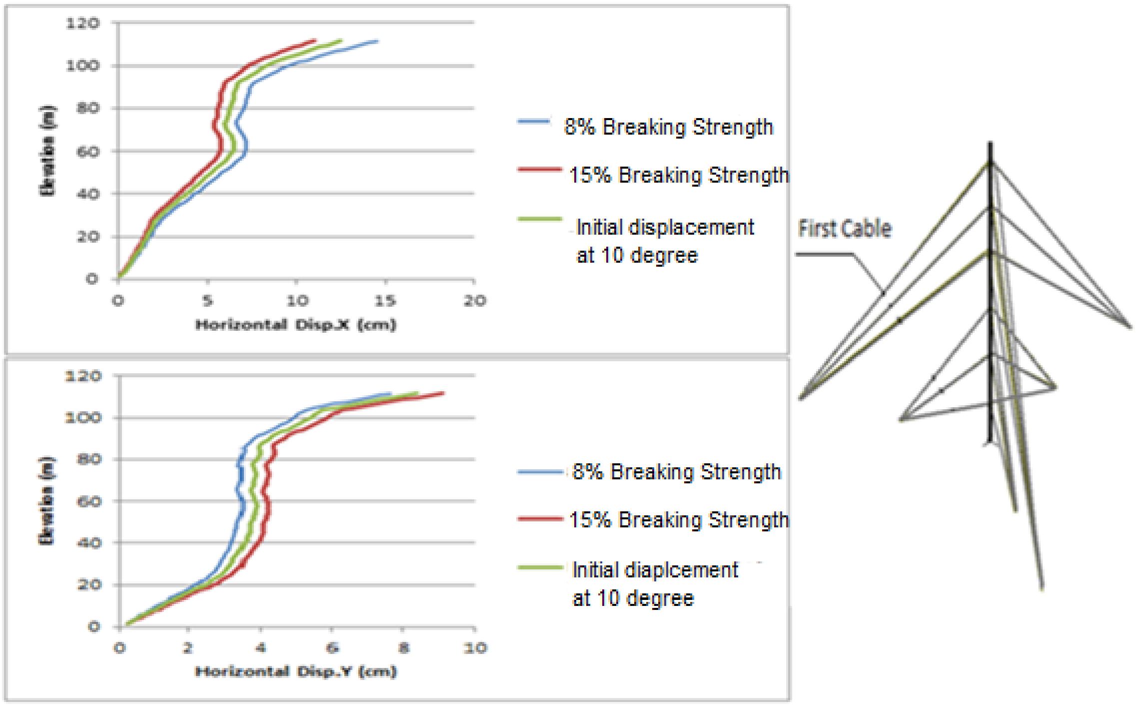

Figure 4-22 Variation of horizontal displacements of the mast for 8% of RBS and 15% of RBS of Cable #1 under El Centro earthquake

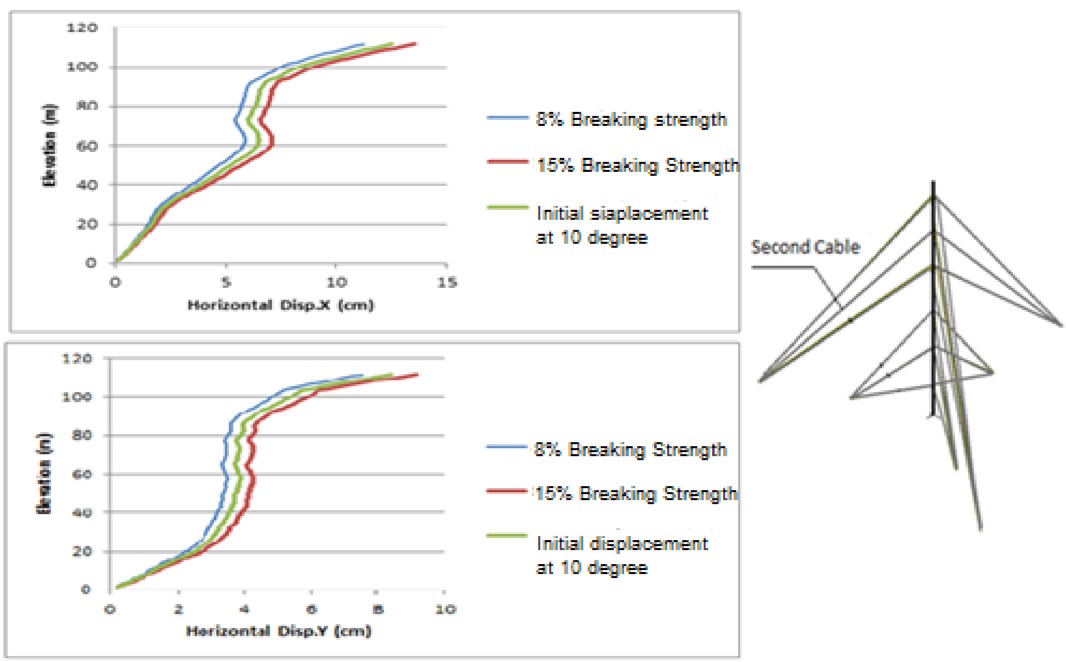

Figure 4-23 Variation of horizontal displacements of the mast for 8% of RBS and 15% of RBS of Cable #2 under El Centro earthquake

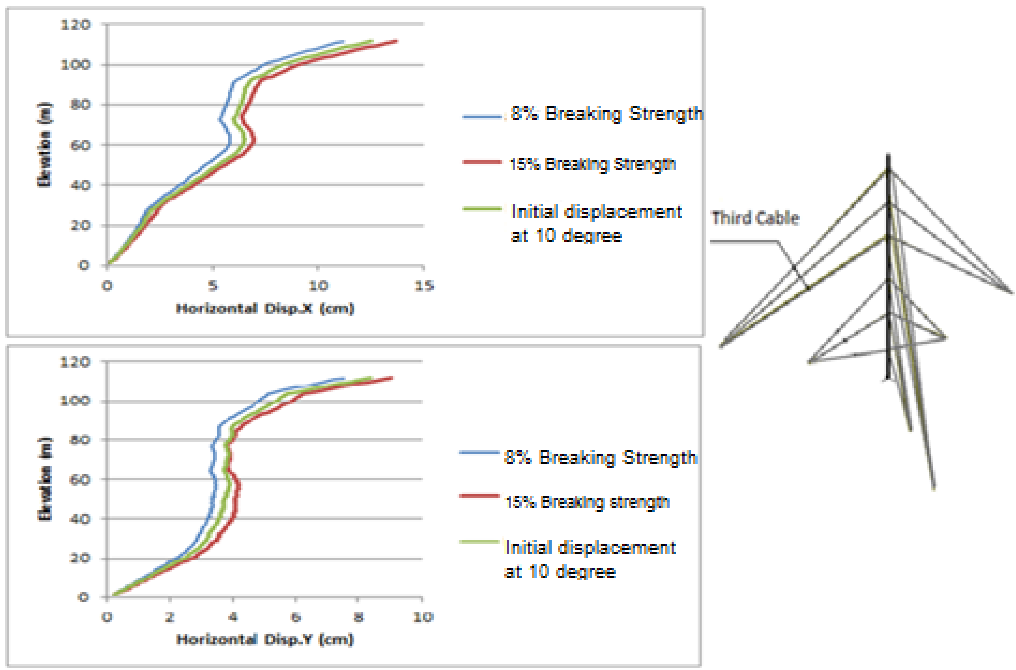

Figure 4-24 Variation of horizontal displacements of the mast for 8% of RBS and 15% of RBS of Cable #3 under El Centro earthquake

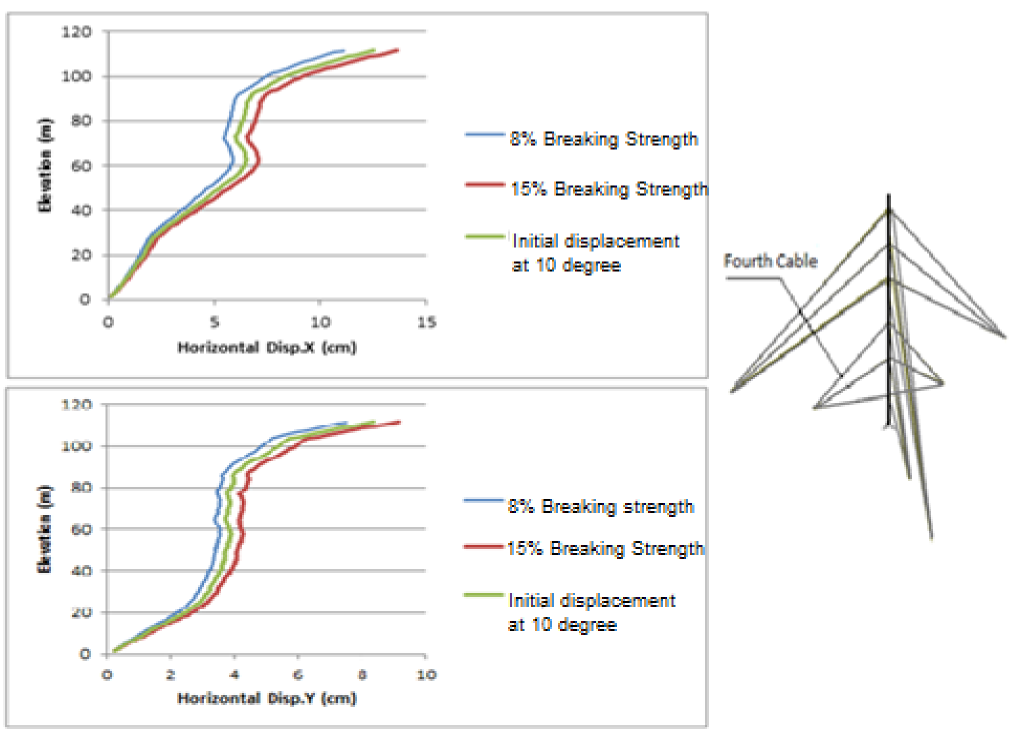

Figure 4-25 Variation of horizontal displacements of the mast for 8% of RBS and 15% of RBS of Cable #4 under El Centro earthquake

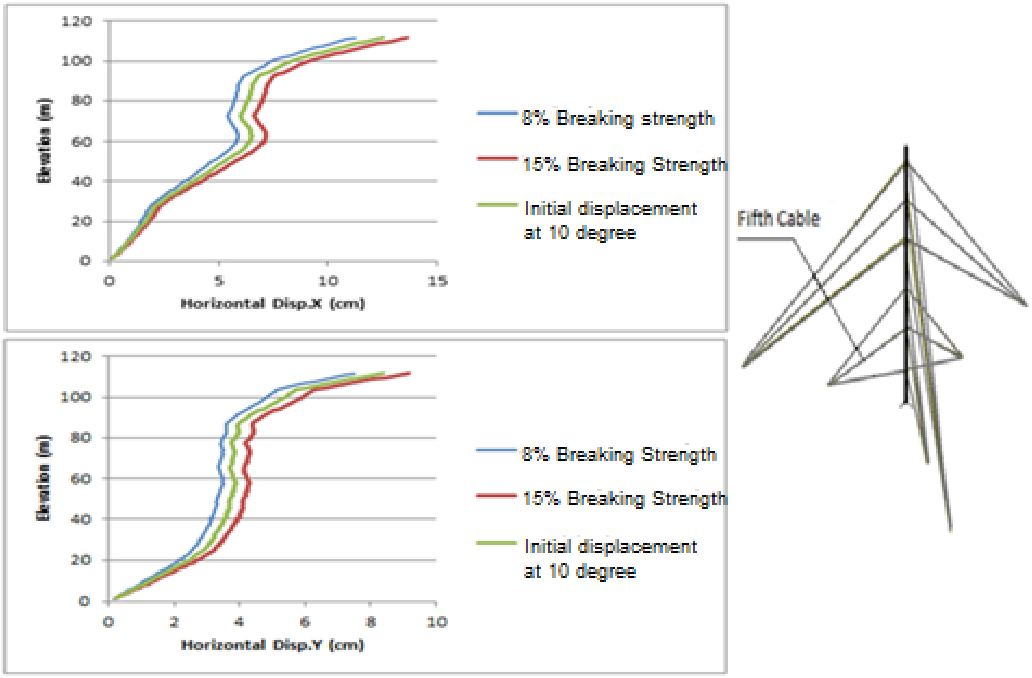

Figure 4-26 Variation of horizontal displacements of the mast for 8% of RBS and 15% of RBS of Cable #5 under El Centro earthquake

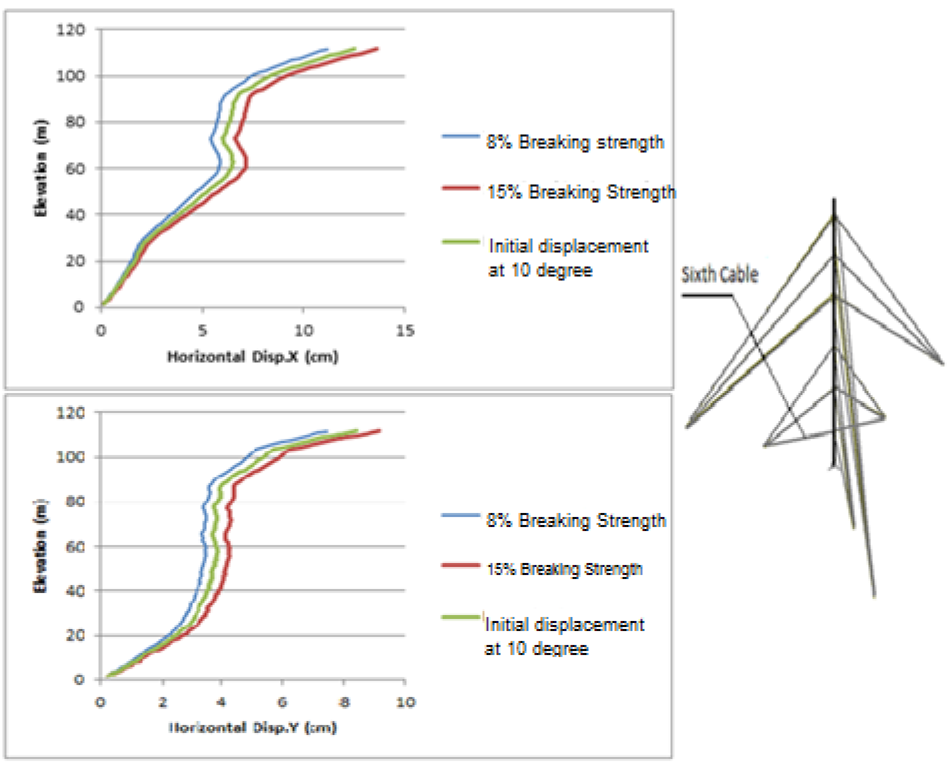

Figure 4-27 Variation of horizontal displacements of the mast for 8% of RBS and 15% of RBS of Cable #6 under El Centro earthquake

Figures 4-22 to 4-27 illustrate the range of mast displacements obtained when varying initial tensions within the tolerances of 8% to 15% RBS as stipulated in CAN/CSA S37. Tables 4-4 and 4-5 express the range of values obtained for the mast displacements at the top two guy cluster levels which are more likely affected by variations in initial tensions, as concluded earlier. The displacements reported are peak dynamic values along X and Y and the % values refer to the numerical predictions for the nominal 10% RBS case.

Table 4-4 Range of predicted displacements of the mast at first and second cluster elevations under varied initial tension in cluster #1.

Prescribed initial tension in cluster #1 as % of RBS		**Maximum X displacement**		**Maximum Y displacement**	
		Cluster #1	**Cluster #2**	**Cluster #1**	**Cluster #2**
8%	Disp. (cm)	9.98	7.26	6.17	4.45
	% change from reference	-15	-34	-10	-11
10% Reference	Disp. (cm)	8.70	5.42	5.61	4.02
15%	Disp. (cm)	6.79	4.58	4.23	3.69
	% change from reference	22	16	25	8

Table 4-5 Range of predicted horizontal displacements of the mast at first and second cluster elevations under varied initial tension in cluster #2.

Prescribed initial tension in cluster #2 as % RBS		**Maximum X displacement**		**Maximum Y displacement**	
		Cluster #1	**Cluster #2**	**Cluster #1**	**Cluster #2**
8%	Disp. (cm)	6.67	5.71	4.72	3.7
	% change from reference	-6.32	-4.99	-15.4	-8.4
10% Reference	Disp. (cm)	7.12	6.01	5.58	4.04
15%	Disp. (cm)	7.86	6.48	5.98	4.2
	% change from reference	10.4	7.82	7.17	3.96

As it was shown in Tables 4-3 and 4-4 the variability in cable tensions of clusters #1 and #2 has different effects on the horizontal mast displacements at high elevations, especially at the first and second cluster elevations. This was clearly shown by comparing the horizontal displacements of the mast under 8% of RBS (lower limit of cable tension) and 15% of RBS (upper limit of cable tension).Since Cable #1 has less lateral stiffness, decreasing the tension in this cable results in larger seismic displacements for the mast. There is a concentration of attachments like antennas, ladders and transmission lines above and around Cluster #2 which has a more important effect on the static tension of Cluster#1 than for Cluster #2. Therefore, decreasing the tension in Cable #2 causes less horizontal displacement of the mast compared to decreasing the tension in Cable #1.

Also in addition to above, it should be mentioned that large amount of lateral stiffness for Cable #2 limits the horizontal displacement for the mast around this guying level in both X and Y direction.

Also, although tension variations in all cables have some important effects on the seismic behaviour of the mast, the most substantial effect is obtained for fluctuations in tension of cable #1.

Chapter 5 CONCLUSIONS

5.1.Summary of main conclusions

The research presented in this thesis achieved its main goal which was to validate the range of accuracy of numerical predictions of the seismic response of a guyed telecommunication mast. The first level of validation was done by using ambient vibration measurements (AVM) on the structure to extract the main dynamic characteristics of the structure and adjust the finite element models accordingly. The second level of validation was essentially numerical again, but considering the influence of the variability of guy cable tensions on the predicted seismic response. The AVM test provided data for adjusting guy cable tensions. The first three mode shapes of the mast and the fundamental mode shape of each cable were used for this purpose and excellent agreement (with variations less than 5%) was found between the numerical model and the measured values after the guy cable tensions were properly adjusted. This validates the numerical procedure in the sense that reliable results are obtained with the assumptions made as long as realistic cable tensions are used in the models. It is emphasized that the test results represent very low amplitude response. Larger amplitudes expected during strong shaking may exacerbate the nonlinear character of the response but the most important effect of the higher amplitude response will likely be in the additional damping of the mast. In particular, the author notes that viscous damping in the order of 2% critical for seismic analysis represents about two to four times the measured damping at ambient levels.

Cable tension is the most important parameter affecting horizontal displacements of the mast. A realistic range of displacements can be obtained by numerical predictions if the variability of cable tensions is considered. This range of displacement is important especially for the upper portion of the mast near the top two guying levels. However, this effect is much less prominent for Cluster #2 compared to Cluster #1, since the mast has more lateral flexibility around Cluster #1 compared to around Cluster #2.

Generally cable tensions are a very influential parameter on the global mast frequencies. The study underlines the importance of considering a range of realistic tension values in numerical models to obtain bounded values of natural frequencies and dynamic response.

These results show that the variations in peak dynamic cable tensions for the four records considered in the study are in the order of ±15% compared to the peak tensions obtained from the nominal model, which is deemed acceptable for seismic analysis.

5.2.Limitations and recommendations for future studies

There are some limitations in the experimental field tests. One of them is related to the limited number of GP1 sensors (three per cable) which were used in the experiment. Ideally, synchronous measurements would have been made for all cables.

However, the most limiting assumption with respect to cable measurements relates to the way the cable tension is estimated using Equation (2). This equation is in fact valid only for a taut string and the longer cables experience geometric nonlinearities (sagging effects) that are not captured by the taut string assumption. Future work could examine how a more realistic cable tension value could be estimated by extracting the lowest two (or even three) natural frequencies of the guy cables. Analytical functions from Irvine (1981) could also be used, but the main goal is to seek to extract information from reliable measured data.

During the test the TROMINO sensors were set on small plates which were attached to the mast. Although setting the sensors on these plates provided easier access for linemen, the presence of the plates may have altered the recorded signal. Since this possible influence would normally show at higher frequencies than the ones of interest, it was not investigated further. In future tests, the author would recommend doing complementary measurements with the sensors directly resting on the tower platforms or members.

One of the assumptions in this study is related to neglecting the vertical component of measurements during analysing the data from sensors. Although the sensors measured in three directions, in this study only the horizontal response was examined. The author recommends that vertical response be also investigated in future studies.

Another source of uncertainty related to cable tensions is that they were not measured directly with tensiometers but were calculated based on extracted frequencies from AVM. Although the calculation provides nearly acceptable values for the tensions, direct measurements would have provided further validation.

In addition to all the above experimental limitations, there are some simplifications in the finite element models. In the study, the weight/mass of the transmission lines was lumped at tower nodes on one face of the tower and the weight/mass of antennas was lumped at one single node on the appropriate face. However, other appurtenances such as ladders, platforms and guiding rails have not been accounted for.

REFERENCES

ADINA R&D, Inc. (2004) Theory and modeling guide, Volume 1: ADINA. Report ARD 04-7, Watertown, MA.

Amiri, G.G., and McClure, G. (1996). “Simplified Model for Seismic Behaviour of Tall Guyed Communication Towers”. Proceedings of the Canadian Society for Civil Engineering. First Structural Specialty Conference. Alberta, Canada, 29 May-1 June. Vol. IIb, 823–834.

Amiri, G.G. (2002). “Seismic sensitivity indicators for tall guyed telecommunication towers”. Computers and Structures, 80:349-64.

ASCE (American Society of Civil Engineers). Ed. Murty K.S. Madugula. (2002). “Dynamic Response of Lattice Towers and Guyed Masts”. Task Committee on the Dynamic response of Lattice Towers. ASCE - Structural Engineering Institute, 266 p.

Ballantyne, D., (2006). “Sri Lanka Lifelines after the December 2004 Great Sumatra Earthquake and Tsunami”. Earthquake Spectra, Volume 22, No. S3, pages S545–S559, June 2006, Earthquake Engineering Research Institute, DOI: 10.1193/1.2211367

Boen, T., (2004). “Sumatra Earthquake 26 Dec 2004.” Available online at http://www.eeri.org/lfe/clearinghouse/sumatra_tsunami/reports/Boen_Sumatra%20Earthquake%2026%20Dec%202004.pdf

Brincker, R., L. Zhang, and P. Andersen, (2001). “Modal identification of output-only systems using frequency domain decomposition”. Smart Materials and Structures, 10: 441.

California Department of Water Recourses (CDWR) (2009): “The Strong Motion Program.” CDWR, Sacramento, Calif., < http://www.oandm.water.ca.gov/earthquake/> (Dec 2009).

California Geological Survey, formerly California Division of Mines & Geology (CDMG) (2009): "Center for Engineering Strong Motion." CESMD, Sacramento, Calif., <http://www.conservation.ca.gov/cgs/> (Dec 2009).

CAN/CSA S37, Canadian Standards Association. 2001(R06). "Antennas, Towers, and Antenna-Supporting Structures".

Clough, R. W., and Penzien, J. (2003). "Dynamics of structures". 2nd ed. (revised), Computers and Structures, Inc., Berkeley, CA

Eidinger, John M.; Tang, Alex K. (2012). "Christchurch, New Zealand earthquake sequence of Mw 7.1 September 04, 2010; Mw 6.3 February 22, 2011; Mw 6.0 June 13, 2011: lifeline performance". The Earthquake Engineering Online Archive, subsequently published as -- Technical Council on Lifeline Earthquake Engineering (TCLEE) Monograph No. 40; February 2012 - ASCE., authors retain copyright, 2012-02, PDF. Available online at

http://web.me.com/eidinger/GE/Home_files/TCLEE%20Monograph%20Rev%200%20lr.pdf

Evans, N.L., and McGhie, C., (2011). "The Performance of Lifeline Utilities following the 27th February 2010 Maule Earthquake Chile". Proceedings of the Ninth Pacific Conference on Earthquake Engineering Building an Earthquake-Resilient Society, Auckland, New Zealand. Paper No.036.

Faridafshin, F. (2006). "Seismic investigation of tall guyed telecommunication towers". Master's Thesis, Department of Applied Mechanics, Division of Dynamics, Chalmers University of Technology, Goteborg, Sweden.

Faridafshin, F., and McClure, G. 2008. Seismic response of tall guyed masts to asynchronous multiple-support and vertical ground motions. ASCE Journal of Structural Engineering, 134(8): 1374-1382.

Farrar, C. R., and James III, G. H. (1997). "System identification from ambient vibration measurements on a bridge." Journal of Sound and Vibration, 205(1): 1-18

Ghafari Osgoie, M., McClure, G., Hong Zhang, X, and Gagnon, D. (2012). “Validation of the accuracy of finite element analysis models of a guyed telecommunication mast with ambient vibration measurements”. Proceedings of the 3rd International Structural Specialty Conference (CSCE), Edmonton, Canada, June 6-9. Paper No. STR 1239.

Ghafari Osgoie, M., McClure, G., Hong Zhang, X, and Gagnon, D. (2012). “Assessing the variability of seismic response analysis of tall guyed telecommunication tower with ambient vibration measurement”. Proceedings of the 15th World Conference Earthquake Engineering (15WCEE), Lisbon, Portugal, September 24-28. Paper No. 0733.

Ghafari Oskoie, S.A. (2010). “Earthquake-resistant design procedures for tall guyed telecommunication masts”. Ph.D. Thesis, Department of Civil Engineering and Applied Mechanics, McGill University, Montreal, QC, Canada.

Ghafari Oskoei, S.A., and McClure, G. (2011). “A novel approach to evaluate the equivalent dynamic stiffness of guy clusters in telecommunication masts underground excitation”. Engineering Structures. 33: 1764-1772.

Ghafari Oskoei, S.A., and McClure, G. (2012). “A new robust linearized seismic analysis method for tall guyed telecommunication masts”. ASCE Journal of Structural Engineering, April 2012, 138(4): 502-513.

Gilles, D. (2011). “In situ dynamic properties of building in Montreal determined from ambient vibration records”. Ph.D. Thesis, Department of Civil Engineering and Applied Mechanics, McGill University, Montreal, QC, Canada.

Guevara, E.I., and McClure, G. (1993). “Nonlinear seismic response of antenna-supporting structures”. Computers & Structures, 47(4/5): 711-724.

Irivine, H.M. (1981). Cable Structures. MIT Press.

Kahla NB. (1994). “Dynamic analysis of guyed towers”. Engineering Structures. 16:293-301.

Madugula, M.K.S., Wahba, Y.M.F., and Monforton, G.R. (1998). “Dynamic response of guyed masts”. Engineering Structures, 20(12): 1097–1101.

Manafpour, A., (2004). “The Bam, Iran earthquake of 26 December 2003”. Field Investigation Report. Earthquake Engineering Field Engineering Team, (EEFIT); Halcrow Group Limited.

Meshmesha H, Sennah K, Kennedy JB. (2006). “Simple method for static and dynamic analyses of guyed towers”. Structural Engineering and Mechanics. 23:635-49.

Mistry, R., Dong, W., shah, I., (2001). “Interdisciplinary Observation on the January 2001, Bhuj, Gujarat Earthquake”. Sponsored by World Seismic Safety Initiative Earthquake and Megacities Initiative, April 2001.

Moghtaderi-Zadeh,M., Nadim, F., and Bolourchi. M., (2004). “Performance of Lifeline Systems in Bam Earthquake of 26 December 2003”. Journal of Seismology and Earthquake Engineering, 5(4) and 6(1), Winter and Spring 2004 Issue on Bam Earthquake.

Pacific Earthquake Research Center (PEER). “ PEER strong motion database.” PEER, Berkeley, Calif. ,http://peer.berekley.edu

Rudnick, H., (2010). “Lecciones del terremoto de Chile 2010 y su impacto en el suministro eléctrico”. Compotamiento del sector Electrico Chileno durante el Sismo del 27 de Febrero 2010. Experiencias y lec lecciones aprendidas, Santiago Auditorium. Available online at

http://www.cigre.cl/sem_19_oct_10/presentaciones/primer%20bloque/PUC_Rudnick.pdf

Schiff,A.J. (1999). Case Study of Earthquake Performance of Communication Towers. Prepared for the Electric Power and Communication Committee, Technical Council on Lifeline Earthquake Engineering (TCLEE). American Society of Civil Engineers.

Schneider, J.F., (2008). “Seismically reactivated Hattian slide in Kashmir,Northern Pakistan”. Journal of Seismology, 13:387–398.

Smith, B.W. (2006). Communication Structures. Thomas Telford, IASS. 338 p.

Structural Vibration Solution A/S (2010a). “ARTeMIS Extractor Handy (Version 5.0) [Software]”. http://www.svibs.com/products/ARTeMIS_Extractor.aspx

Structural Vibration Solution A/S (2010b). “User guide to ARTeMIS Extractor Handy (Version 5.0).” http://www.svibs.com/products/ARTeMIS_Extractor.aspx

Tang, A., Wang, L., and Zou G., (2010). “Earthquake Damage Characteristics and Assessment of Lifeline Systems on May 12th, 2008, Sichuan Earthquake.” Australian Earthquake Engineering Society 2010 Conference, Perth, Australia. Available online at http://www.aees.org.au/Proceedings/2010_Papers/49-Tang.pdf

Tang, A., Murugesh, G., Yashinsky, M., McLaughlin, J., Eskijian, M., Ames, D., Plant, G., and, Surampalli, R., (2005). “Earthquake and tsunami lifeline performance investigation India team.” Available online at

http://www.eeri.org/lfe/clearinghouse/sumatra_tsunami/reports/India%20_Alex%20Tang%20%20short%20report.pdf

TCLEE Technical Council on Lifeline Earthquake Engineering. (2010) “Preliminary Report on the 27 February 2010 Mw8.8 Offshore Maule, Chile Earthquake”.

Available online at

http://www.asce.org/uploadedFiles/Institutes/Technical_Activities_Committees_(TAC)/TCLEE%20Chile%20Web%20Report%207.10.pdf

Trifunac. M.D., (2007). “Comparisons between ambient and forced vibration experiments”, Earthquake Engineering & Structural Dynamics, 1(2): 133–150, 1972, DOI: 10.1002/eqe.4290010203.

Velez, R.A., (2010). “Dynamic Structural Identification using Wireless Sensor Networks”. PhD. Thesis in Civil Engineering at the Engineering School of the University of Minho, Portugal.

Ventura. C.E., (2012). “Application and use of operational modal analysis”. Presentation to the department of Civil Engineering and Applied Mechanics, McGill University, Montreal, QC, Canada, January 2012.

Waugaman, A., Senior Director United Nations Foundation and Vodafone Foundation Technology Partnership. (2010). “Haiti Earthquake: Telecoms Sans Frontières’ Emergency Response”. Presentation to the U.S. Department of State July 9, 2010. Available online at

http://www.unfoundation.org/assets/pdf/haiti-earthquake-tsf-emergency-response-1.pdf

YIGIT, C.O., INAL, C., and YETKIN, M., (2008). “Monitoring of tall building’s dynamic behaviour using precision inclination sensors” 13th FIG Symposium on Deformation Measurement and Analysis, 4 IAG Symposium on Geodesy for Geotechnical and Structural Engineering. LNEC, Lisbon, May 12-15.

Appendix A: COMPLEMENTARY STUDIES ON SEISMIC ANALYSIS OF THE ST. HYACINTHE GUYED TOWER

This appendix consists of two parts. The first part presents some detailed results of the maximum horizontal displacements of the mast at the top and bottom clusters and cable tension forces of all six cables, under the effects of the Parkfield (1966) and Taft (1952) earthquake records. Different approaches are compared throughout these graphs in order to evaluate the effect of the attachments and the accuracy of the nominal model.

The second part presents the detailed results of the study on the variability of the initial cable tension for the Parkfield and Taft records and for the additional synthetic record of Montreal (1732). The models are used where the initial cable tensions vary according to the scheme explained in Chapter 4, and the results are presented in matrix form for the maximum cable tensions of each cable under these selected earthquake Records. The initial tension values have already been reported in Chapter 4.

1. Evaluating the effect of tower attachments and accuracy of the nominal FE model

1.1 Park field earthquake (1966)

1.1.1 Cable tensions

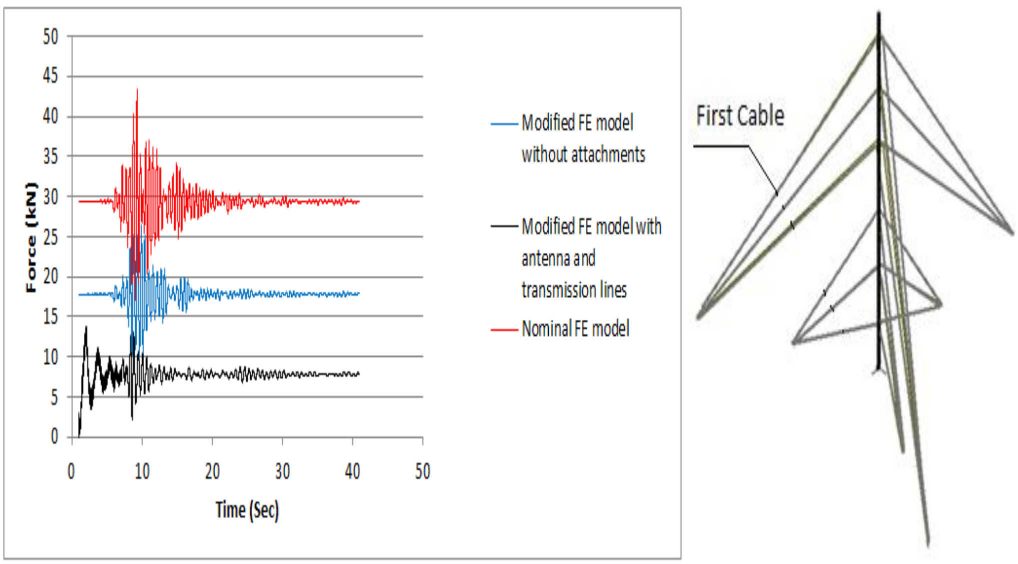

Figure A-1 Cable tension of Cable #1 aligned with the input ground motion

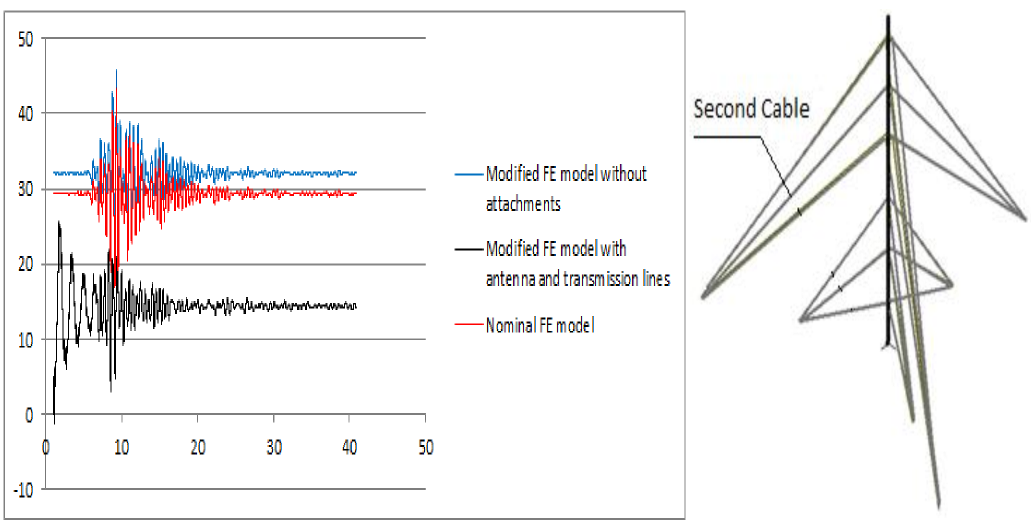

Figure A-2 Cable tension of Cable #2 aligned with the input ground motion

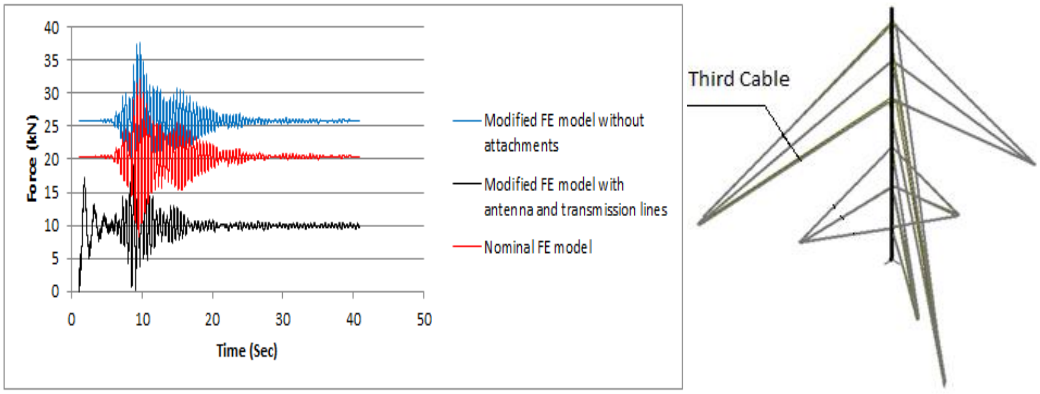

Figure A-3 Cable tension of Cable #3 aligned with the input ground motion

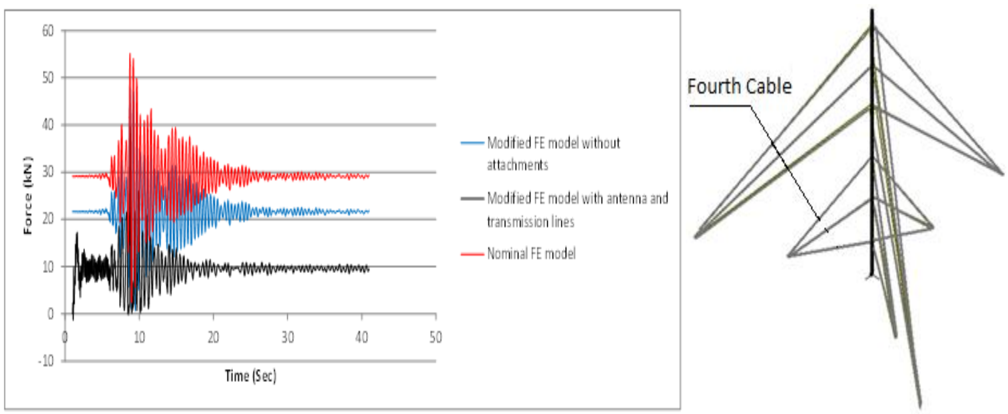

Figure A-4 Cable tension of Cable #4 aligned with the input ground motion

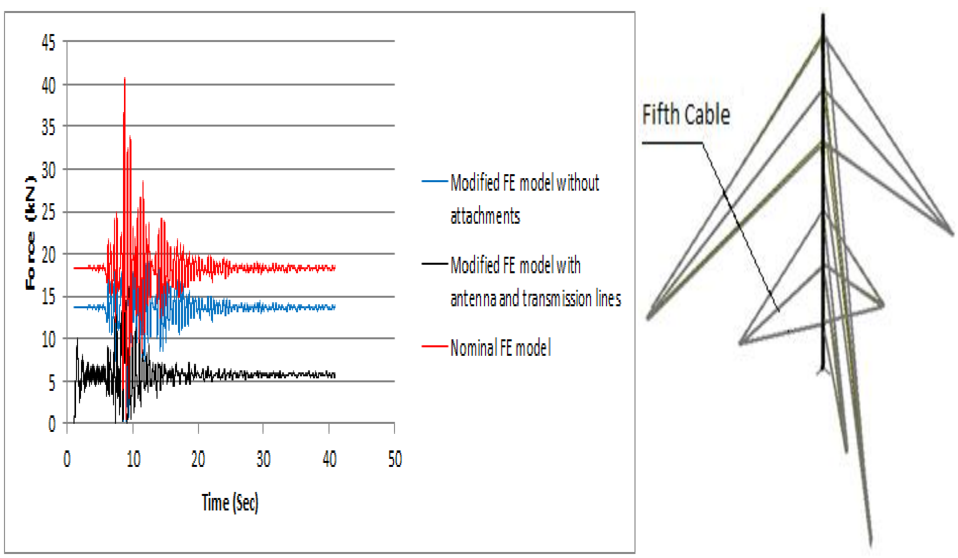

Figure A-5 Cable tension of Cable #5 aligned with the input ground motion

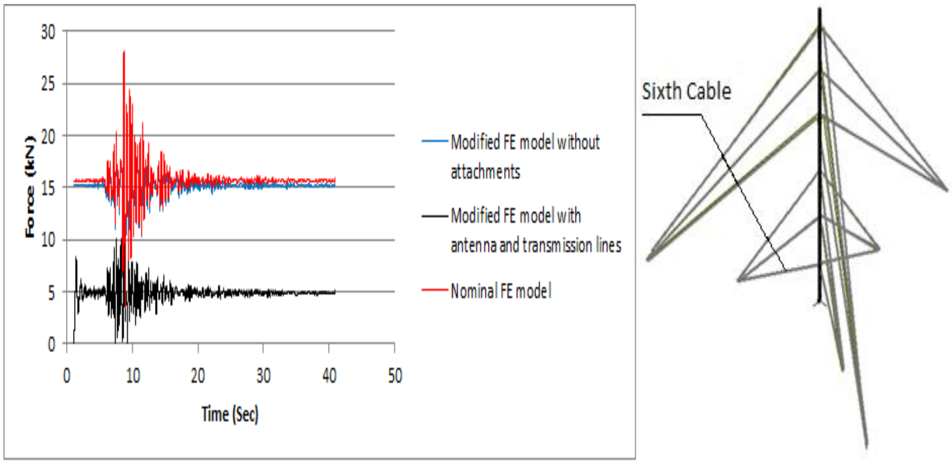

Figure A-6 Cable tension of Cable #6 aligned with the input ground motion

1.1.2 Horizontal displacements

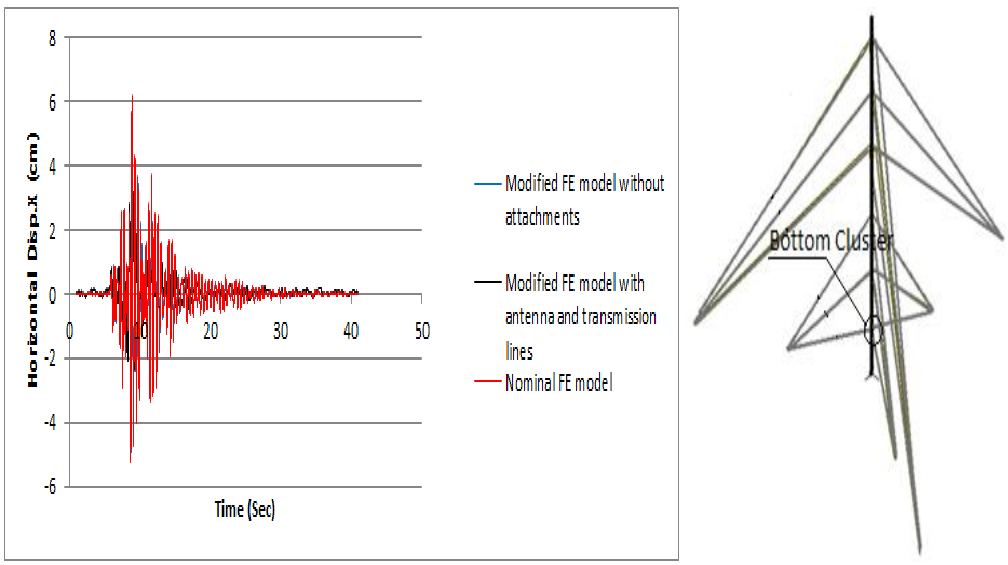

Figure A-7 Horizontal displacements of the mast at cable cluster elevation #6 (Bottom cluster) along X (along input)

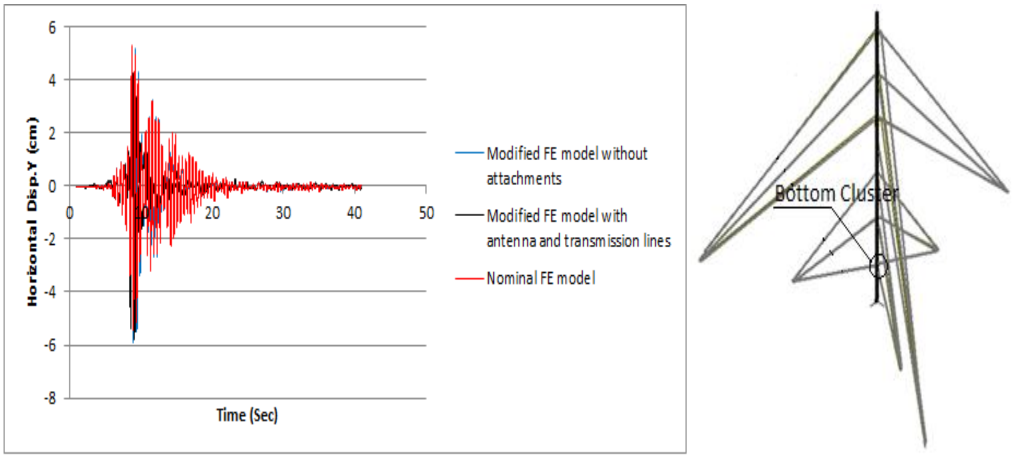

Figure A-8 Horizontal displacements of the mast at cable cluster elevation #6 (Bottom cluster) along Y (transverse to input)

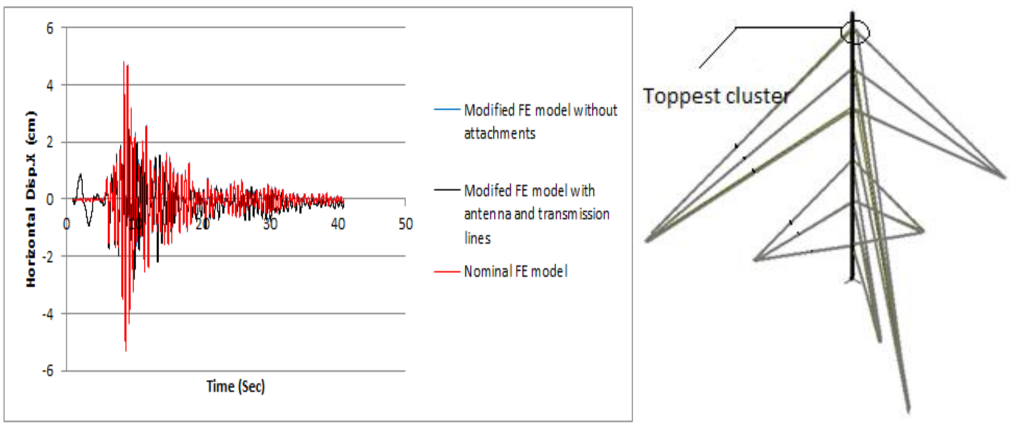

Figure A-9 Horizontal displacements of the mast at cable cluster elevation #1 (Top cluster) along X (along input)

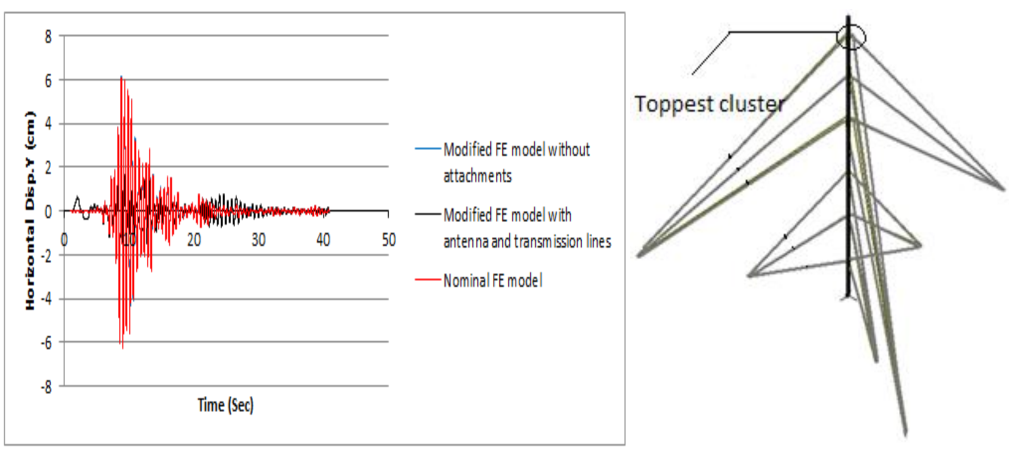

Figure A-10 Horizontal displacements of the mast at cable cluster elevation #1 (Top cluster) along Y (transverse to input)

1.2 Taft earthquake (1952)

1.2.1 Cable tensions

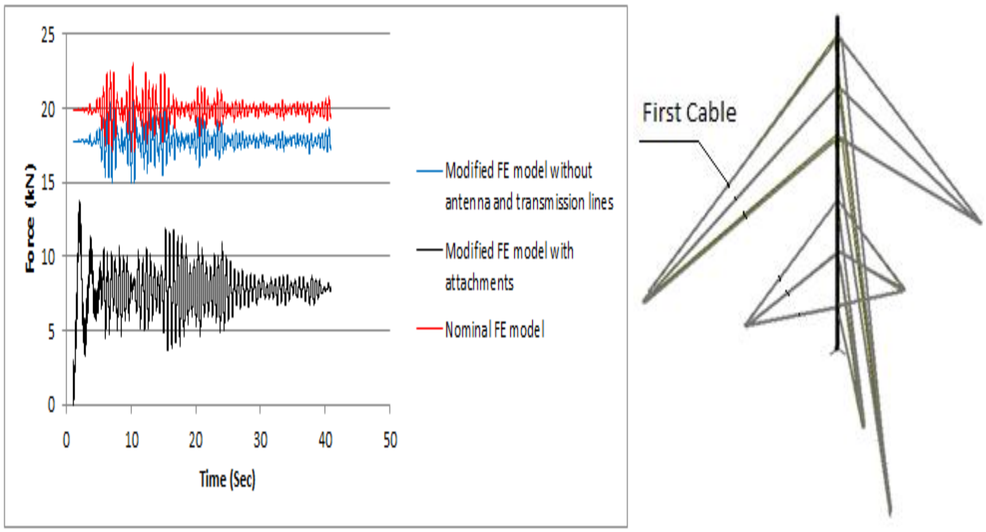

Figure A-11 Cable tension of Cable #1 aligned with the input ground motion

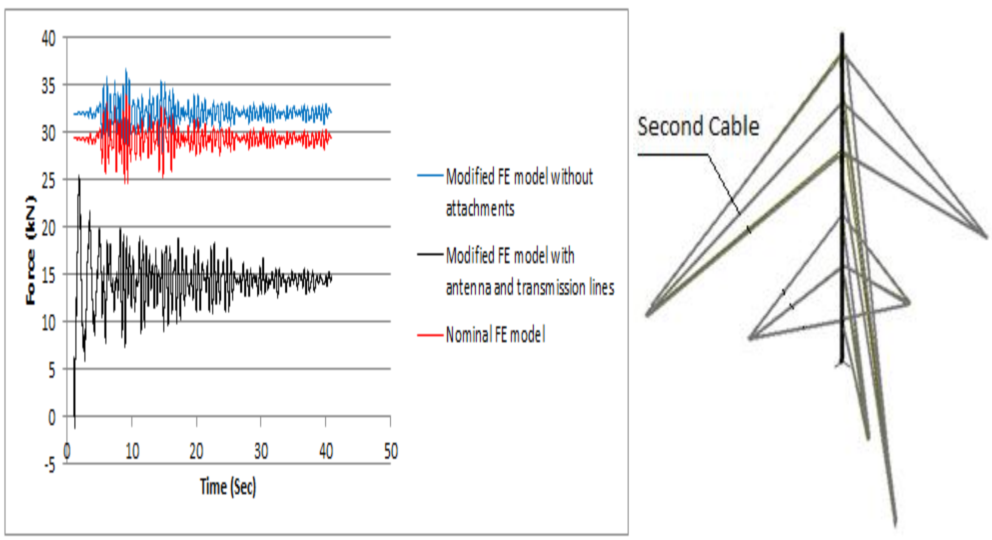

Figure A-12 Cable tension of Cable #2 aligned with the input ground motion

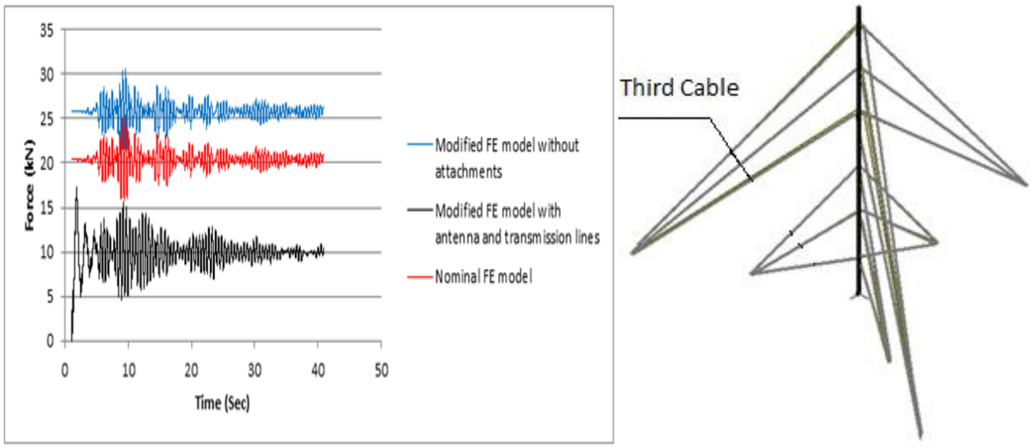

Figure A-13 Cable tension of Cable #3 aligned with the input ground motion

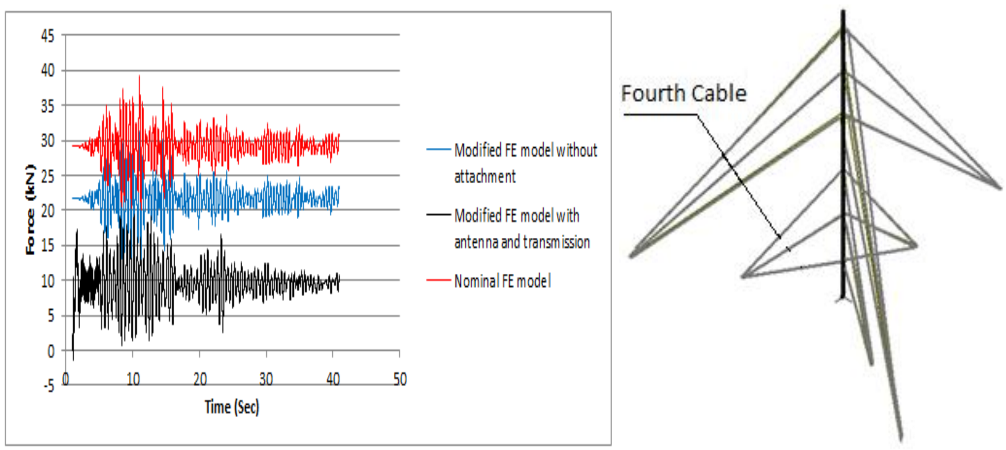

Figure A-14 Cable tension of Cable #4 aligned with the input ground motion

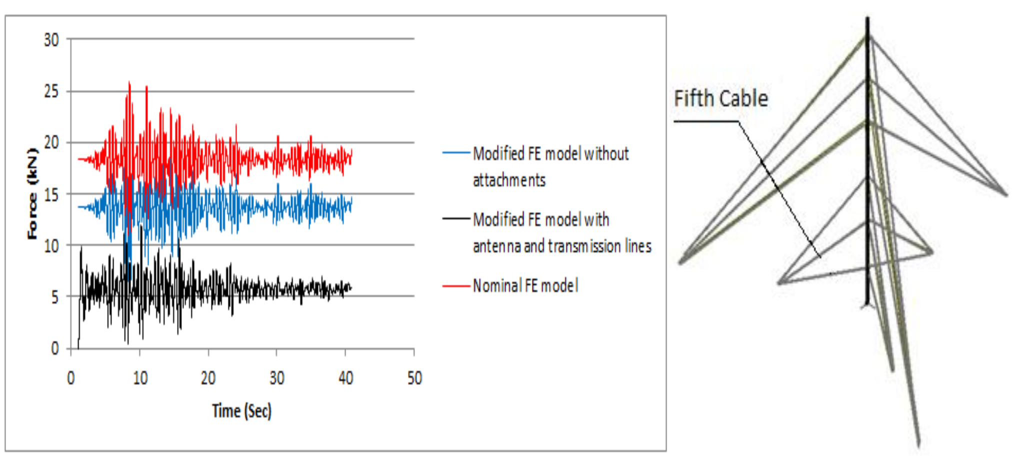

Figure A-15 Cable tension of Cable #5 aligned with the input ground motion

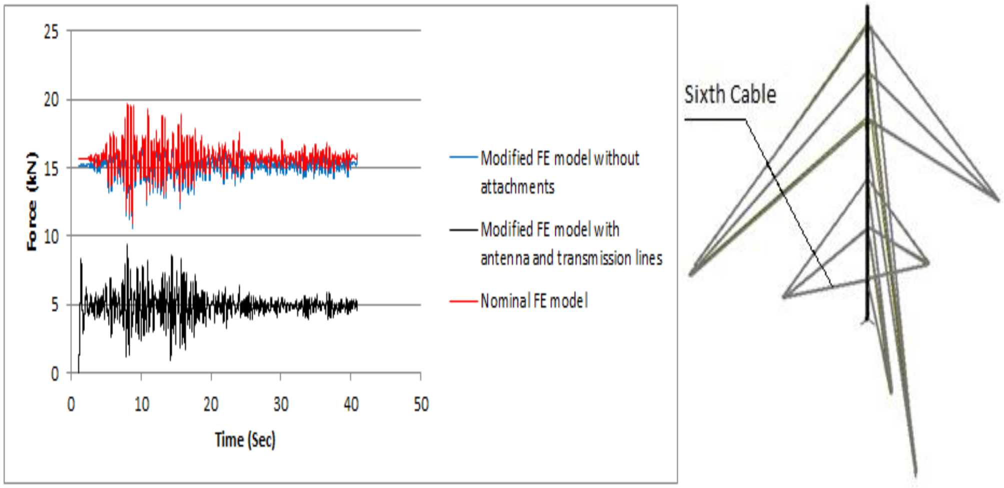

Figure A-16 Cable tension of Cable #6 aligned with the input ground motion

1.2.2 Horizontal displacement

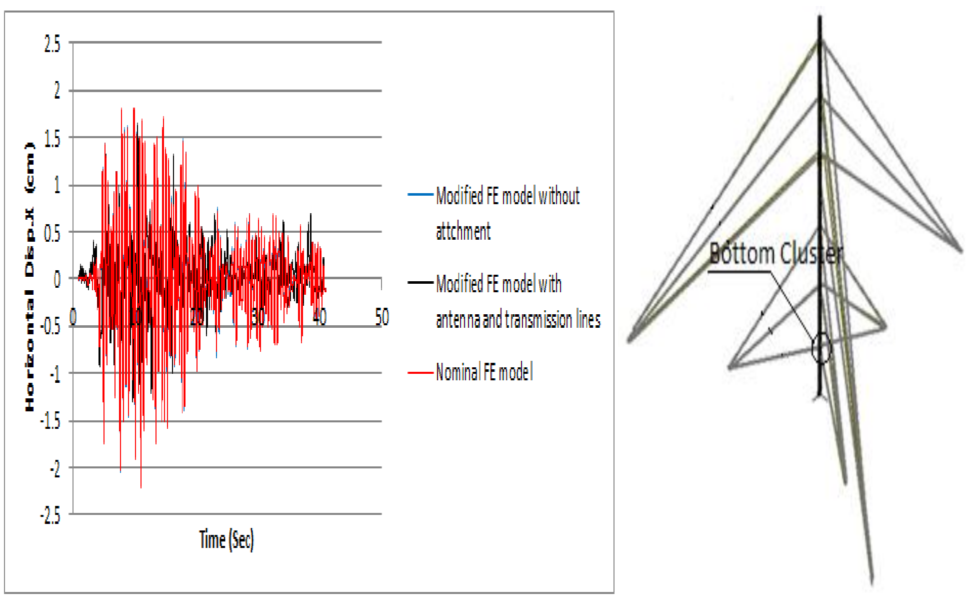

Figure A-17 Horizontal displacements of the mast at cable cluster elevation #6 (Bottom cluster) along X (along input)

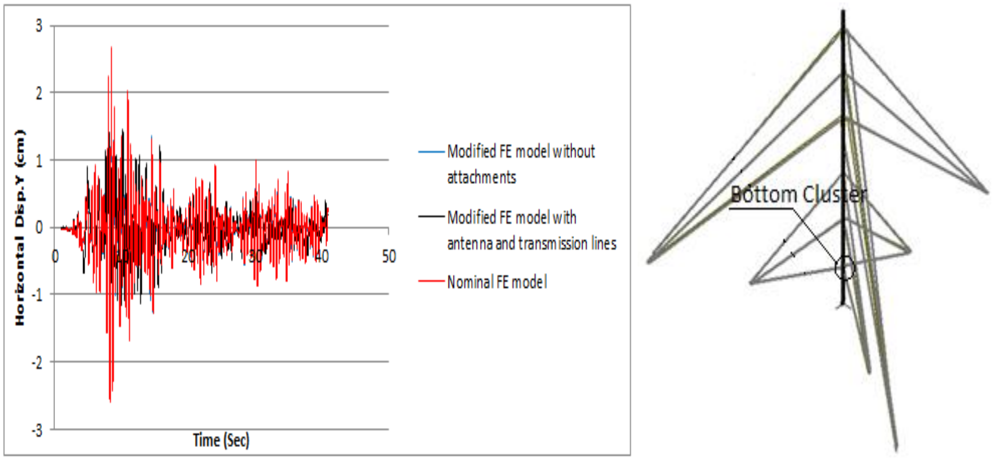

Figure A-18 Horizontal displacements of the mast at cable cluster elevation #6 (Bottom cluster) along Y (transverse to input)

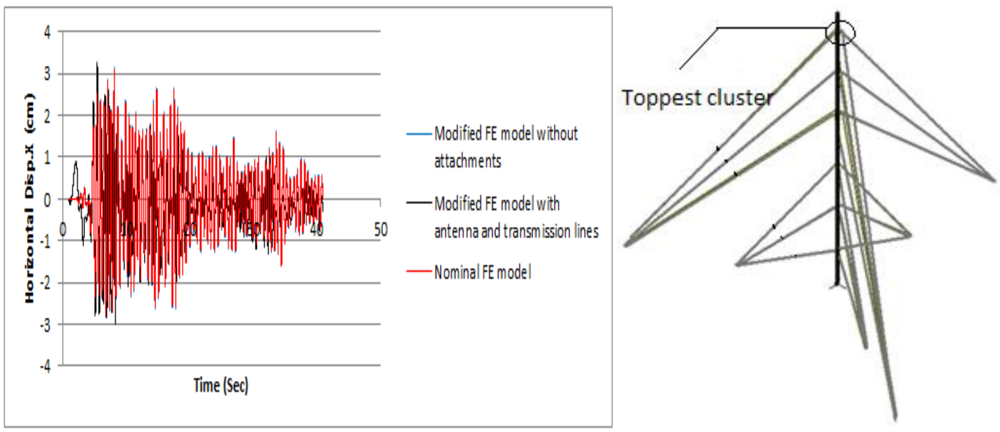

Figure A-19 Horizontal displacements of the mast at cable cluster elevation #1 (Top cluster) along X (along the input)

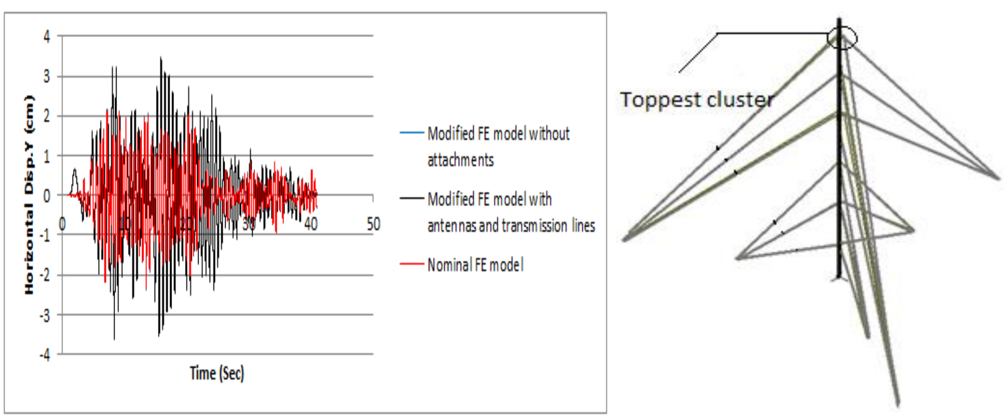

Figure A-20 Horizontal displacements of the mast at cable cluster elevation #1 (Top cluster) along Y (transverse to input)

2. **Influence of the variability of initial cable tensions at 10°C with limits of 8% and 15% of the rated breaking strength.**

   2.1 Park field earthquake (1966)

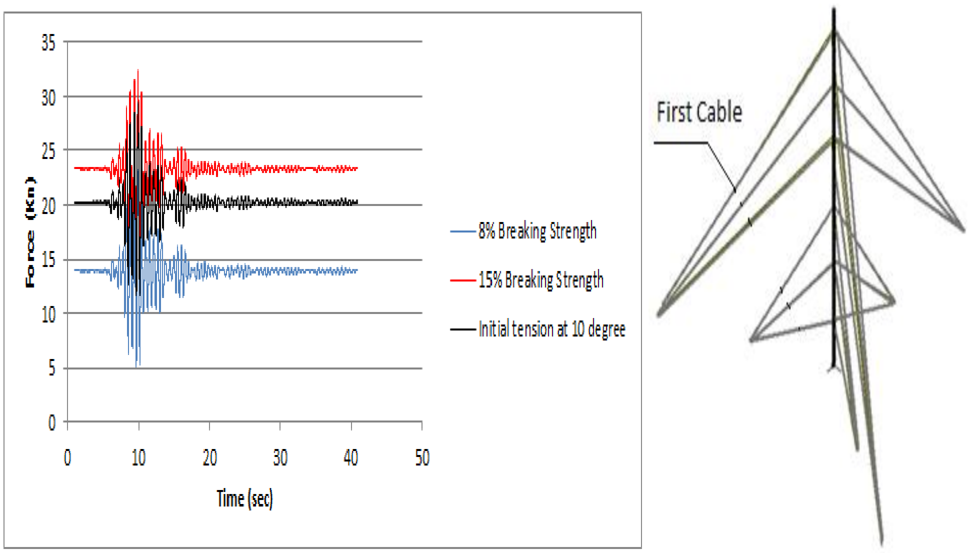

Figure A-21 Tension in Cable #1 under Park field earthquake

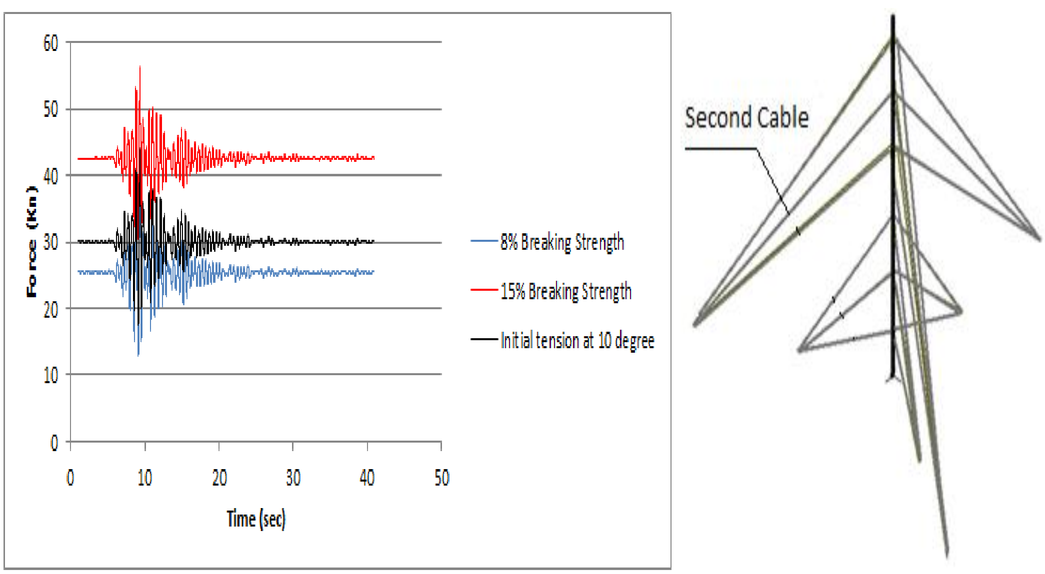

Figure A-22 Tension in Cable #2 under Park field earthquake

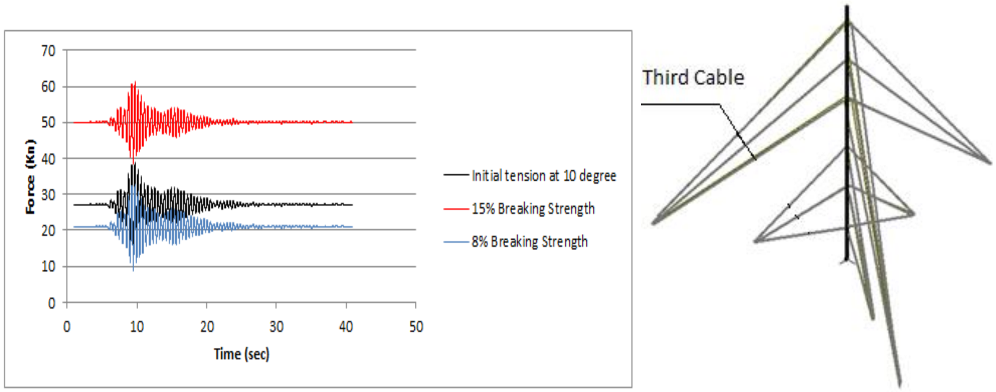

Figure A-23 *Tension in Cable #3 under Park field earthquake*

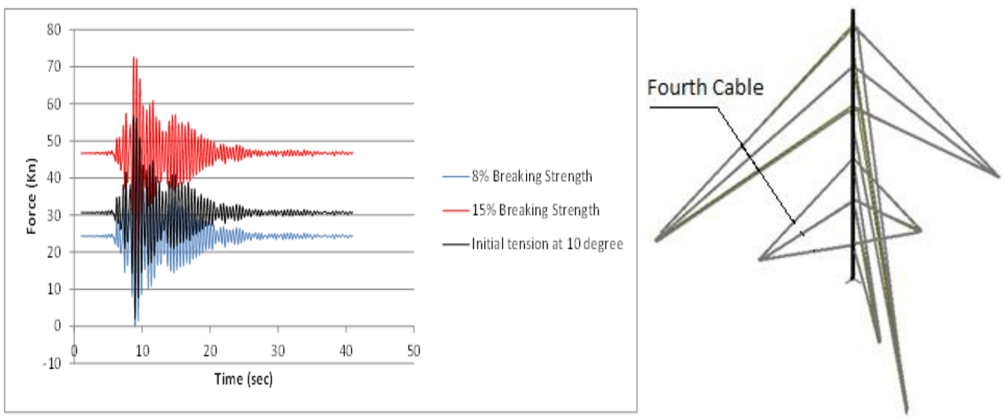

Figure A-24 *Tension in Cable #4 under Park field earthquake*

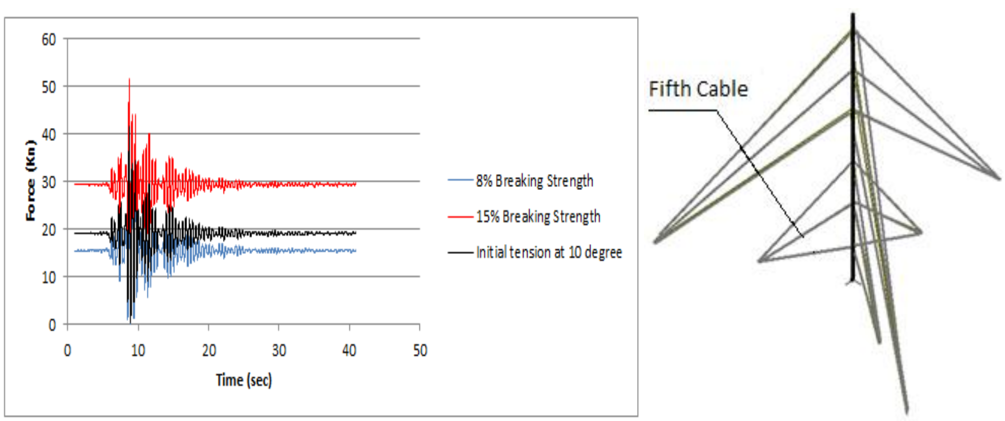

Figure A-25 *Tension in Cable #5 under Park field earthquake*

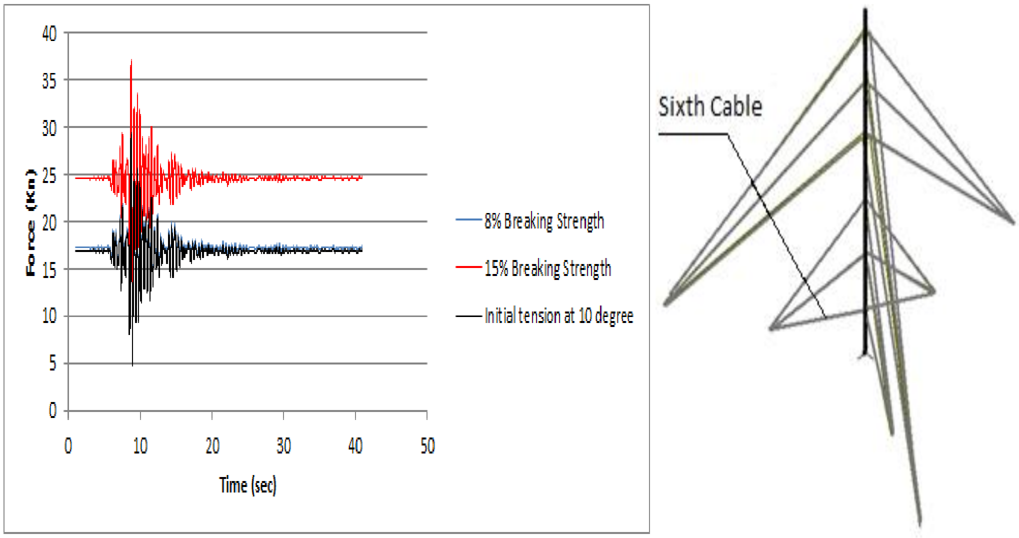

Figure A-26 *Tension in Cable #6 under Park field earthquake*

23.3	29.5	29.7	29.7	29.2	29.8
44.7	39.5	44.3	44.8	44.3	44.1
33.1	33.3	38.9	33.5	33.1	33.4
57.6	57.0	57.2	50.4	57.8	57.5
42.1	42.0	41.8	43.0	38.3	41.6
29.9	29.8	29.4	29.8	29.5	29.8

Figure A-27 *Maximum cable tensions (kN)for 8% of RBS under Parkfield earthquake*

32.4	29.6	29.0	29.7	29.8	29.8
44.4	56.4	43.5	44.3	44.5	44.5
33.3	33.2	61.3	33.2	33.3	33.4
57.4	57.2	55.8	72.6	57.5	57.6
41.9	41.8	41.4	41.5	51.7	42.1
29.7	29.7	29.5	29.6	29.8	37.2

Figure A-28 *Maximum cable tensions (kN) for 15% of RBS under Parkfield earthquake*

$$\begin{bmatrix} 0.78 & 0.99 & 1.00 & 1.01 & 0.98 & 1.00 \\ 1.13 & 1.00 & 1.00 & 1.01 & 1.00 & 0.99 \\ 0.99 & 1.00 & 1.01 & 1.00 & 0.99 & 1.00 \\ 1.00 & 0.99 & 0.99 & 1.01 & 1.00 & 1.00 \\ 0.99 & 0.99 & 1.00 & 1.03 & 1.00 & 0.99 \\ 1.00 & 1.00 & 0.99 & 1.00 & 0.99 & 1.00 \end{bmatrix}$$

Figure A-29 $T_{max\ ij}$: Normalized maximum dynamic cable tensions (kN) for 8% of RBS under Parkfield records

$$\begin{bmatrix} 1.08 & 0.99 & 0.98 & 1.01 & 1.00 & 1.00 \\ 1.13 & 1.43 & 0.98 & 1.00 & 1.00 & 1.00 \\ 1.00 & 1.00 & 1.59 & 0.99 & 0.99 & 1.00 \\ 1.00 & 0.99 & 0.97 & 1.45 & 0.99 & 1.00 \\ 0.99 & 0.99 & 0.99 & 1.38 & 1.35 & 1.00 \\ 1.00 & 1.00 & 0.99 & 1.94 & 1.00 & 1.25 \end{bmatrix}$$

Figure A-30 $T_{max\ ij}$: Normalized maximum dynamic cable tensions (kN) for 15% of RBS under Parkfield records

Cable No.	Initial tension (kN)		Nominal peak tension (kN)	DAF 8%	DAF1 5%	Nominal	8%/Nominal	15%/Nominal
	Static	% RBS						
1	20.2	8.08	29.4	1.56	1.32	1.46	1.07	0.91
2	30.0	10.22	44.0	1.44	1.23	1.47	0.98	0.84
3	21.0	10.13	32.9	2.07	1.55	1.57	1.32	0.99
4	30.6	8.86	56.7	2.47	1.94	1.85	1.33	1.05
5	19.1	9.21	41.5	1.73	1.51	2.17	0.80	0.70
6	16.9	10.32	29.4	1.51	1.51	1.74	0.87	0.87

Table A-1 Peak dynamic cable under Parkfield record for tension variations in Cable #1

2.2 Montreal earthquake (1732)

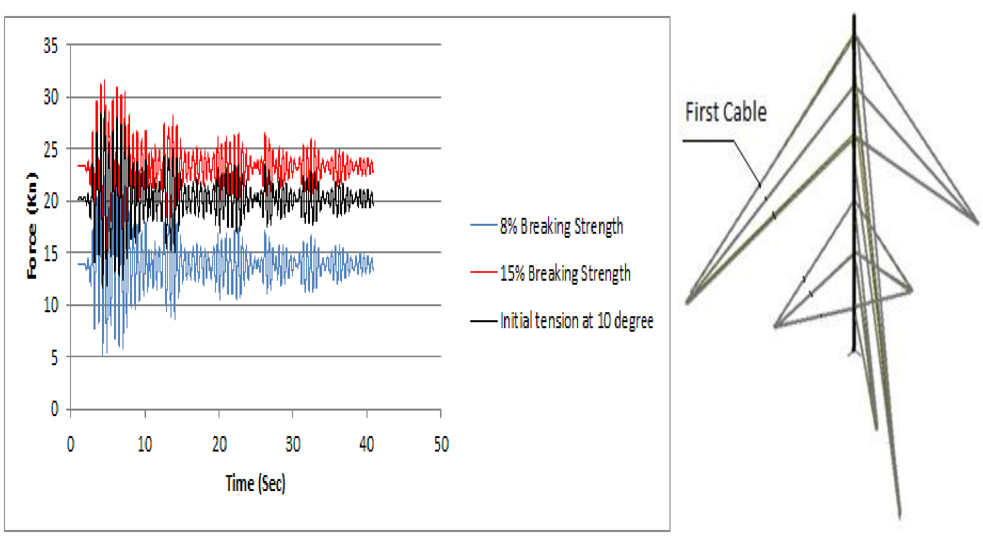

Figure A-31 Cable tension in Cable #1 under Montreal earthquake

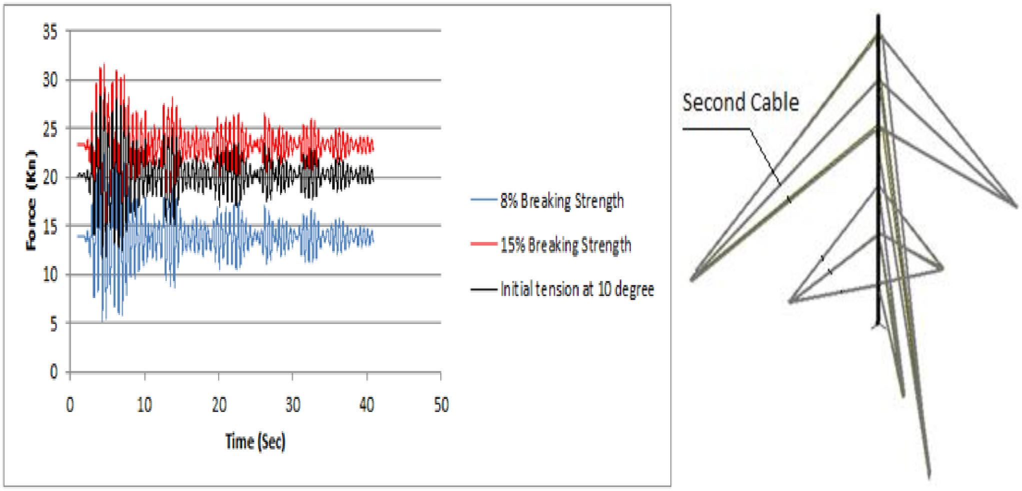

Figure A-32 *Cable tension in Cable #2 under Montreal earthquake*

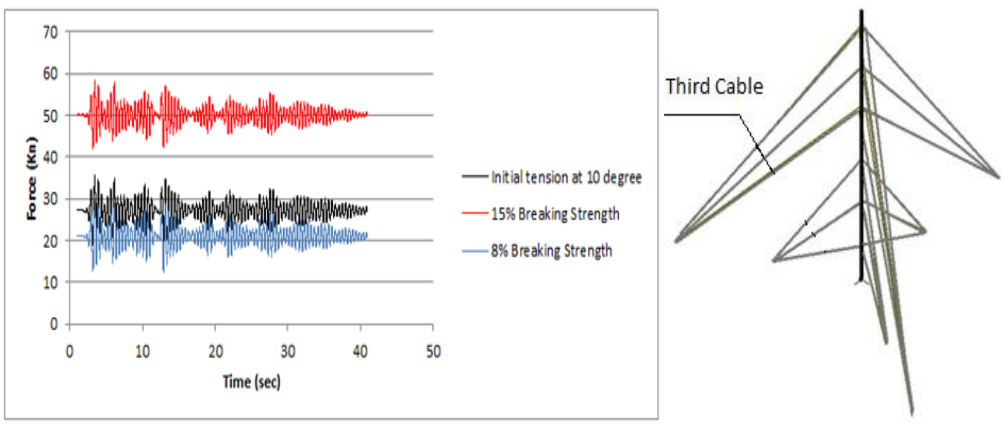

Figure A-33 *Cable tension in Cable #3 under Montreal earthquake*

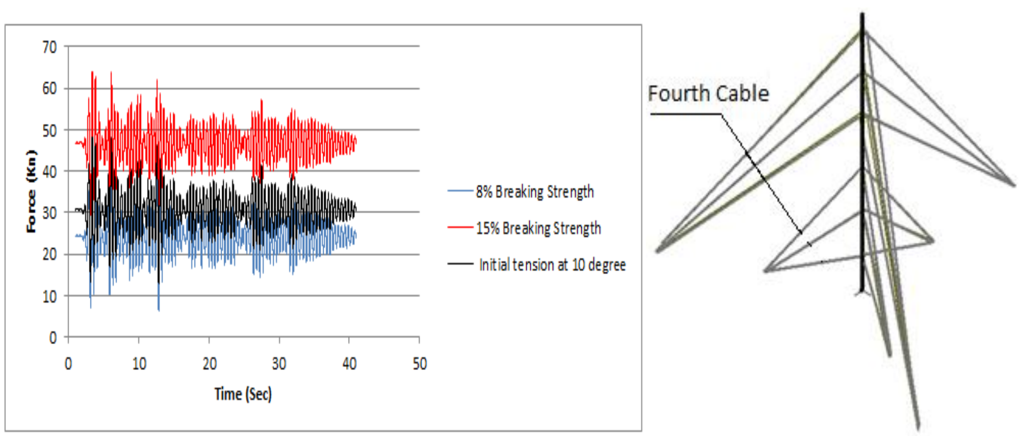

Figure A-34 *Cable tension in Cable #4 under Montreal earthquake*

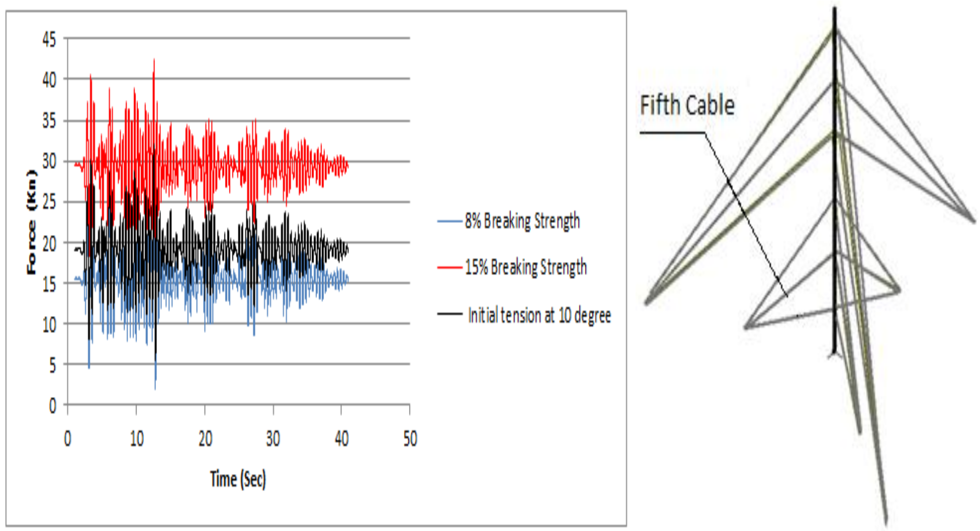

Figure A-35 Cable tension in Cable #5 under Montreal earthquake

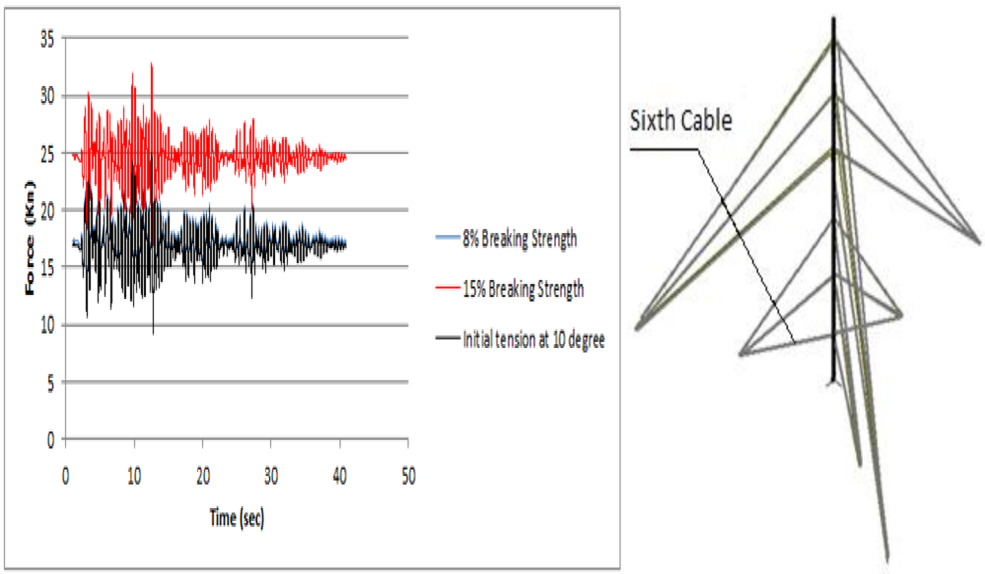

Figure A-36 Cable tension in Cable #6 under Montreal earthquake

22.5	29.1	28.9	29.1	29.0	29.0
44.8	39.4	44.2	44.6	44.1	44.1
30.1	30.0	35.6	30.1	30.1	30.1
49.1	48.4	48.5	41.9	48.5	48.2
32.8	32.6	32.4	32.6	28.4	32.5
25.3	25.5	25.4	25.4	25.4	25.4

Figure A-37 Maximum cable tensions (kN) for 8% of RBS under Montreal earthquake

31.6	28.8	28.5	28.9	29.0	29.0
44.2	56.1	43.3	44.3	44.3	44.4
29.9	29.8	58.3	30.0	30.1	30.1
48.6	48.5	47.7	64.0	48.9	48.9
32.4	32.4	32.1	32.2	42.4	32.5
25.4	25.4	25.3	25.3	25.5	32.8

Figure A-38 Maximum cable tensions (kN) for 15% of RBS under Montreal earthquake

1.00	1.00	1.00	1.00	1.00	1.00
1.00	1.00	1.00	1.00	0.99	0.99
1.00	1.00	1.00	0.99	1.00	1.00
0.99	0.99	0.98	0.98	0.99	0.99
1.00	0.99	0.99	0.99	1.00	1.00
0.99	1.00	0.99	1.00	1.00	1.00

Figure A-39 $T_{max\ ij}$: Normalized maximum dynamic cable tensions (kN) for 8% of RBS under Montreal records

$$\begin{bmatrix} 1.40 & 0.99 & 0.99 & 1.00 & 1.00 & 1.00 \\ 0.99 & 1.42 & 0.98 & 0.99 & 1.00 & 1.00 \\ 0.99 & 0.99 & 1.64 & 0.98 & 1.00 & 1.00 \\ 0.98 & 0.99 & 0.96 & 1.50 & 0.80 & 1.00 \\ 0.99 & 0.98 & 0.98 & 0.98 & 1.49 & 1.00 \\ 1.00 & 1.00 & 0.99 & 0.99 & 1.00 & 1.29 \end{bmatrix}$$

Figure A-40 $T_{max\ ij}$*: Normalized maximum dynamic cable tensions (kN) for 15% of RBS under Montreal records*

Cable No.	**Initial tension (kN)**		**Nominal peak tension (kN)**	**DAF 8%**	**DAF1 5%**	**Nominal**	**8%/Nominal**	**15%/Nominal**
	Static	**% RBS**						
1	20.2	8.08	28.60	1.62	1.36	1.42	1.14	0.96
2	30.0	10.22	43.90	1.55	1.32	1.46	1.06	0.90
3	21.0	10.13	29.60	1.31	1.17	1.41	0.93	0.83
4	30.6	8.86	48.10	1.72	1.37	1.57	1.10	0.87
5	19.1	9.21	32.10	1.83	1.44	1.68	1.09	0.86
6	16.9	10.32	25.10	1.48	1.33	1.49	0.99	0.90

Table A-2 Peak dynamic cable under Montreal record for tension variations in Cable #1

2.3 Taft earthquake (1952)

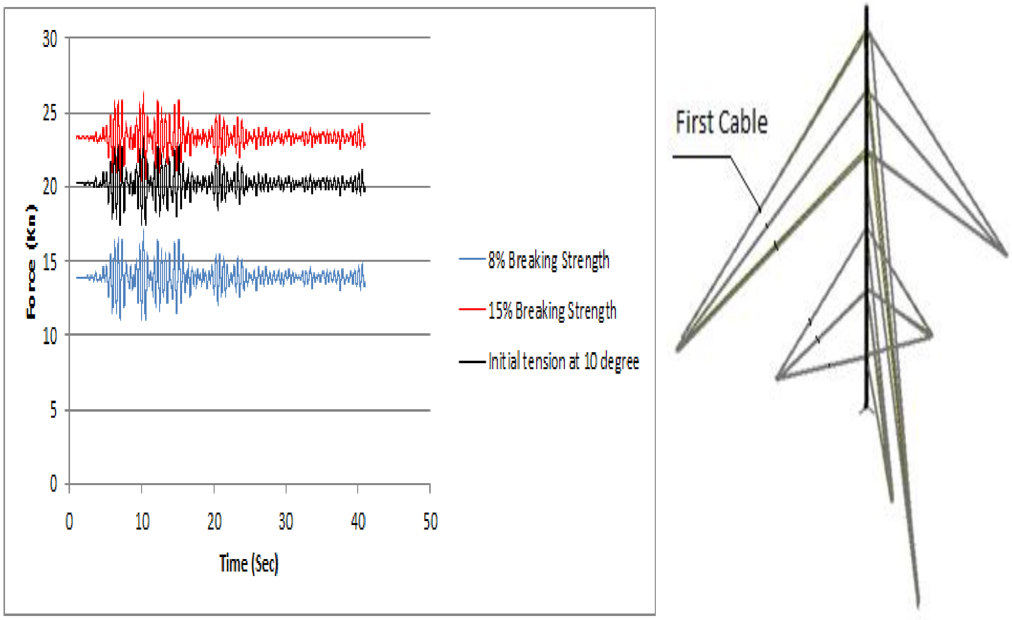

Figure A-41 Cable tension in Cable #1 under Taft earthquake

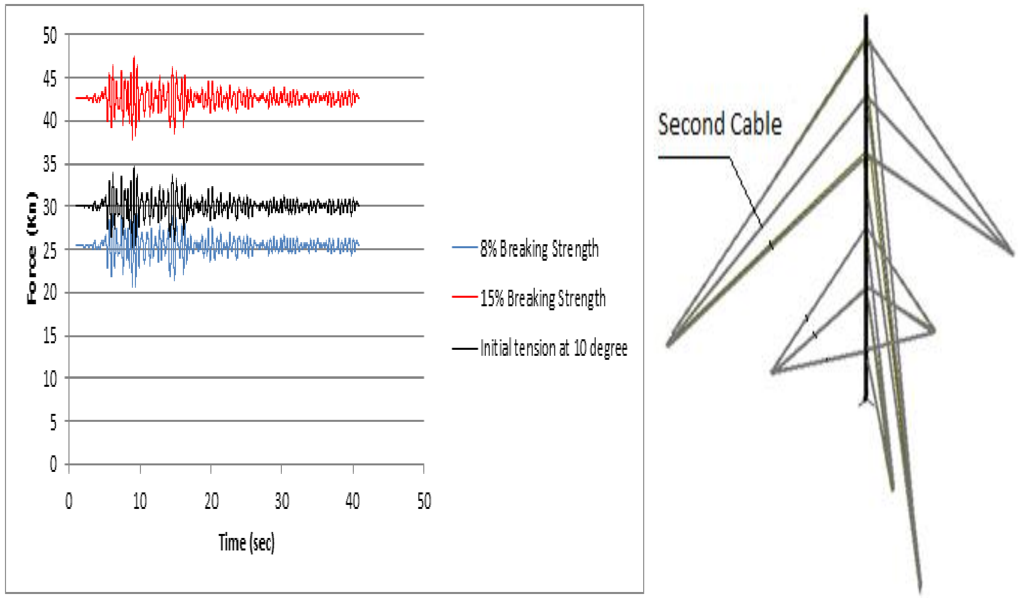

Figure A-42 Cable tension in Cable #2 under Taft earthquake

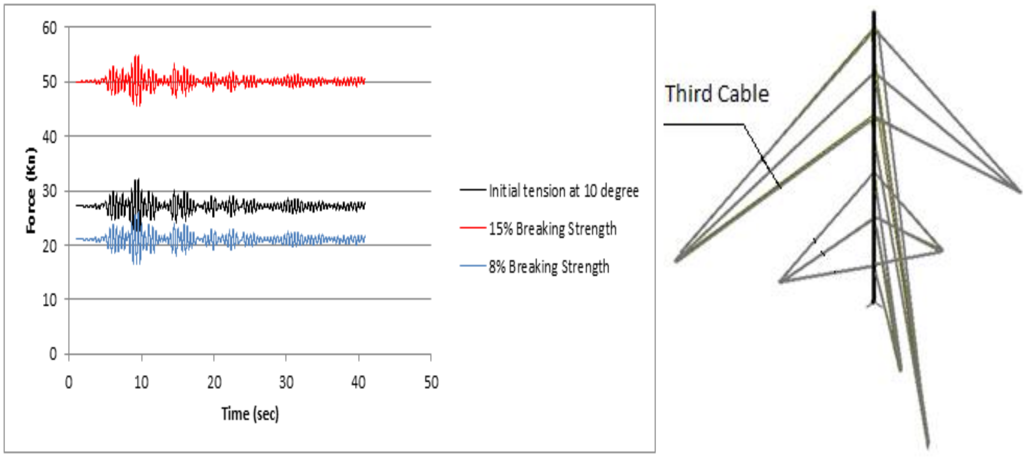

Figure A-43 Cable tension in Cable #3 under Taft earthquake

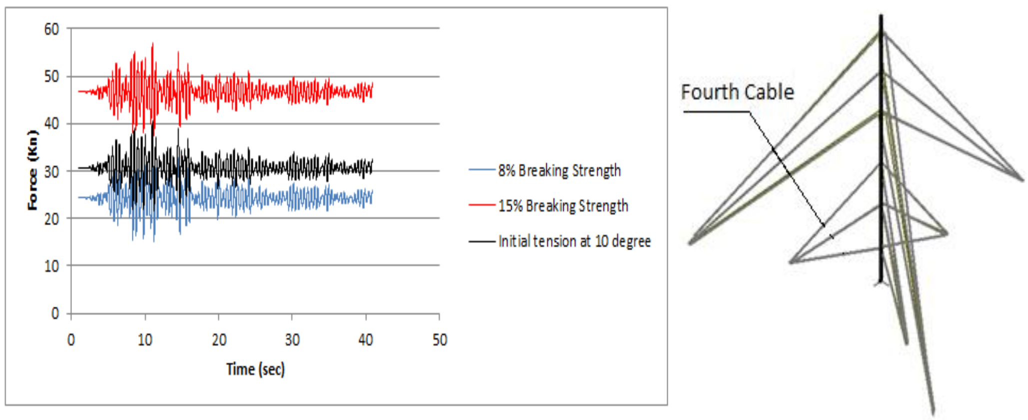

Figure A-44 Cable tension in Cable #4 under Taft earthquake

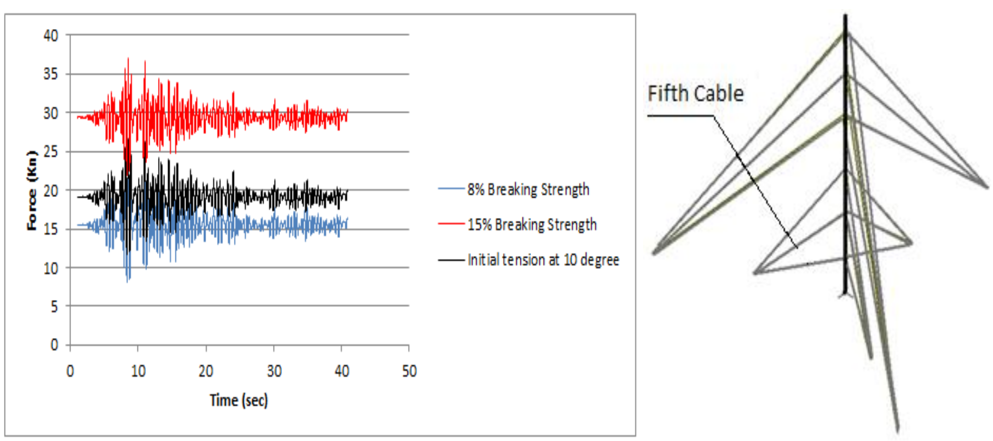

Figure A-45 Cable tension in Cable #5under Taft earthquake

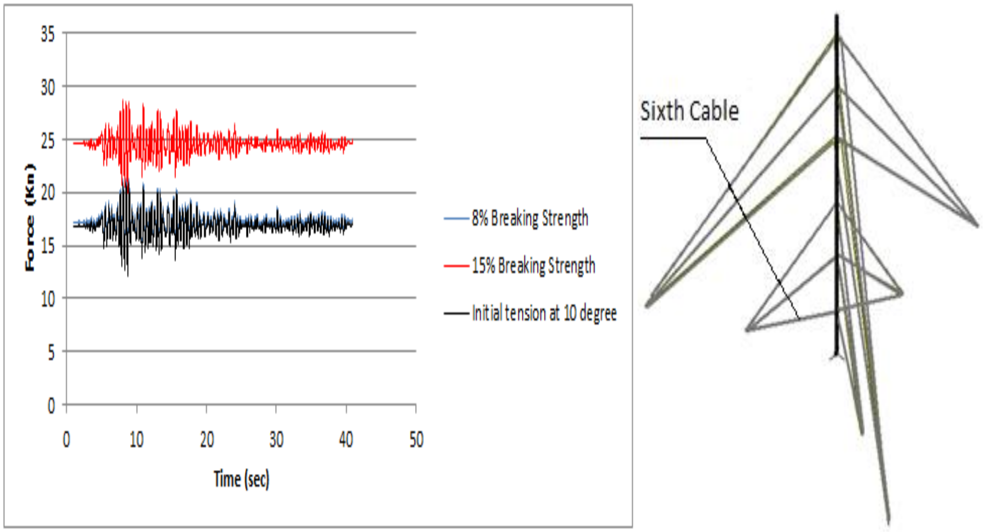

Figure A-46 *Cable tension in Cable #6 under Taft earthquake*

17.2	23.2	23.5	23.3	23.2	23.5
35.0	30.1	35.1	35.3	35.3	35.3
26.5	26.1	32.1	26.2	26.2	26.3
41.1	41.5	41.0	34.4	41.4	41.4
27.1	27.2	27.1	27.0	23.0	27
21.3	21.3	21.3	21.3	21.3	21.3

Figure A-47 *Maximum cable tensions (kN) for 8% of RBS under Taft earthquake*

26.4	23.6	23.4	23.7	23.8	23.8
35.1	47.4	34.5	35.1	35.2	35.3
26.4	26.3	54.9	26.5	26.6	26.6
41.3	41.1	39.5	56.8	41.4	41.4
27.1	27.1	26.8	27.0	37.0	27.2
21.3	21.3	21.2	21.3	21.3	28.7

Figure A-48 *Maximum cable tensions (kN) for 15% of RBS under Taft earthquake*

1.00	0.97	0.99	0.98	0.97	0.99
0.99	1.00	1.00	1.00	1.00	1.00
1.00	0.98	1.00	0.97	0.99	0.99
0.99	1.00	0.99	1.01	1.00	1.00
1.00	0.99	1.00	1.00	1.00	1.00
1.00	1.00	1.00	1.00	1.00	1.00

Figure A-49 $T_{max\ ij}$: Normalized maximum dynamic cable tensions (kN) for 8% of RBS under Taft records

1.53	0.99	9.81	1.00	1.00	1.00
0.99	1.57	0.98	0.99	1.00	1.00
1.00	0.99	1.72	0.98	1.00	1.00
0.99	0.99	0.95	1.67	1.00	1.00
1.00	0.99	0.99	1.00	1.61	1.00
1.00	1.00	1.00	1.00	1.00	1.35

Figure A-50 $T_{max\ ij}$: Normalized maximum dynamic cable tensions (kN) for 15% of RBS under Taft records

Cable No.	Initial tension (kN)		Nominal peak tension (kN)	DAF 8%	DAF 15%	Nominal	8%/Nominal	15%/Nominal
	Static	% RBS						
1	20.2	8.08	23.40	1.24	1.13	1.16	1.07	0.98
2	30.0	10.22	34.70	1.19	1.11	1.16	1.02	0.96
3	21.0	10.13	26.10	1.18	1.10	1.24	0.95	0.88
4	30.6	8.86	40.70	1.42	1.22	1.33	1.06	0.91
5	19.1	9.21	26.70	1.48	1.26	1.40	1.06	0.90
6	16.9	10.32	21.00	1.24	1.17	1.24	1.00	0.94

Table A-3 Peak dynamic cable under Taft record for tension variations in Cable #1